1991

Application of surface-enhanced resonance Raman spectroscopy to chlorophyll and chlorophyll derivatives

Lana Lynn Thomas
Iowa State University

Order Number 9126260

Application of surface-enhanced resonance Raman spectroscopy to chlorophyll and chlorophyll derivatives

Thomas, Lana Lynn, Ph.D.

Iowa State University, 1991

U·M·I
300 N. Zeeb Rd.
Ann Arbor, MI 48106

Application of surface-enhanced resonance Raman spectroscopy to chlorophyll and chlorophyll derivatives

by

Lana Lynn Thomas

A Dissertation Submitted to the
Graduate Faculty in Partial Fulfillment of the
Requirements for the Degree of
DOCTOR OF PHILOSOPHY

Department: Chemistry
Major: Analytical Chemistry

Approved:

Signature was redacted for privacy.

In Charge of Major Work

Signature was redacted for privacy.

For the Major Department

Signature was redacted for privacy.

For the Graduate College

Iowa State University
Ames, Iowa

1991

TABLE OF CONTENTS

TO NADO AND MY NEPHEWS

ABSTRACT

Chlorophylls and chlorophyll derivatives are fundamental components of green plants and are directly involved in light trapping and electron transfer during photosynthesis. In Chapters 1-3 surface-enhanced resonance Raman spectroscopy (SERRS) has been employed to obtain Raman vibrational spectra for chlorophyll *a*, pheophytin *a*, and chlorophyll *b* adsorbed on a roughened silver electrode and excited from within the Soret band to the lowest energy transition in the red at 77K. Cooling to liquid nitrogen temperature was found to improve the spectral quality by minimizing sample heating and photooxidation. Most significantly, the fluorescence accompanying red excitation was quenched at the roughened Ag surface at low temperature and this resulted in richly detailed SERRS spectra. Distinctive SERRS spectra were obtained for each excitation wavelength. Selective excitation within the various electronic transitions can thus be utilized to verify assignments of the vibrational modes of the chlorophylls and pheophytin *a* and to monitor their interactions and photochemical behavior in biomimetic systems and *in vivo*.

Metal electrodes are preferable for SERRS studies of photosynthetic pigments because the electrogenerated species can be created and monitored with minimal sample manipulation and chemical interference. Although the roughened silver electrode provides intense Raman spectra for the neutral

photosynthetic pigments, its oxidation potential is too low for SERRS studies of electron transfer reactions involving chlorophyll a *in vitro* and/or *in vivo* within the light harvesting and reaction center complexes of green plants. Roughened gold provides surface enhancement with red excitation. While this is a narrower spectral enhancement range than for silver, Au can provide information on the RR spectrum coupled to the lowest π-π^* transitions, about which little is known because of fluorescence problems. In addition, Au has a broader electrochemical range that is well suited for all the photosynthetic pigments. Thus, in Chapter 4 a roughened gold electrode was investigated as a SERRS substrate for chloropyll a, pheophytin a, and chlorophyll b with red excitation at 77K. Distinct spectra of each of the photosynthetic pigments were obtained from the roughened Au electrode demonstrating that it is a viable SERRS substrate. Also, Au provides a means to monitor electron transfer in photosynthetic systems by excitation within the lowest electronic transition.

GENERAL INTRODUCTION

Photosynthesis is the conversion of light into chemical energy in bacteria and green plants. In green plants, this process can be represented by the following chemical equation:

$$6CO_2 + 6H_2O \xrightarrow[\text{chlorophyll}]{\text{light}} 6(CH_2O) + 6O_2$$

The unraveling of the active components and mechanisms of photosynthesis has been an area of intense interest. Chlorophyll *a*, pheophytin *a*, and chlorophyll *b* are major chromophoric constituents in the photosynthesis process of green plants.

Photosynthesis occurs within the thylakoid membranes of chloroplasts found in green plants. Inside the thylakoid membrane are two structurally independent protein complexes Photosystem I (PS I) and Photosystem II (PS II). Within each photosystem light energy is trapped and transferred to the reaction center by the proximal and distal antenna complexes. The reaction center (RC) contains specialized chlorophylls and other molecules that act as electron donors and electron acceptors, respectively. Below is a general overview of how the chlorophylls and pheophytin *a* function within PS I and PS II. Several recent reviews provide a more detailed account of these photosystems.[1-5]

Much more is known about PS II due to its mechanistic similarity with the well characterized bacterial RC. Light

harvesting in PS II is accomplished through the proximal and distal antenna complexes. The proximal antenna complex is tightly bound to the RC and contains chlorophyll a. The distal antenna complex has two parts, the light harvesting complex (LHC II) and the accessory chlorophyll proteins (ACP II); both contain chlorophyll a and chlorophyll b. The exact function of the antenna complexes is not completely understood. It has been proposed that the proximal antenna may function in binding or regulating the electron transport components due to its proximity to the RC. The LHC II complex is believed to enable the organism to extend its light absorption to other wavelength regions. The role of ACP II is unclear. Suggestions for its function include coupling to the proximal antenna and the RC or as a linker to the LHC II proteins. Also, it may be involved in dissipating any excess radiation energy the RC can not accomodate. Within RC II, it is accepted that chlorophyll a is the primary electron donor molecule that is activated by a quantum of light and pheophytin a is the primary electron acceptor.

Like PS II, light harvesting in PS I is accomplished through antenna complexes containing chlorophyll a and chlorophyll b. The proximal antenna complex is tightly bound to RC I and contains chlorophyll a. The distal antenna complex includes LHC I and ACP I which both contain chlorophyll a and b. The primary electron donor for PS I is

generally assumed to be a chlorophyll a dimer. A specialized chlorophyll a molecule is indicated as the primary electron acceptor. However, research is currently underway to confirm the identity of the primary electron donor and acceptor for RC I.

In order to understand the structure and function of these complexes within their respective photosystems, a method is needed to monitor the constituents and events of photosynthesis in vitro and in vivo. Raman spectroscopy is a viable method for this task. While Raman spectroscopy is complimentary to Infrared (IR) spectroscopy it also offers several advantages. Not only can Raman be used on all types of samples (solids, crystals, gases, liquids, etc.), it is especially suited to study aqueous samples. Biological samples contain water which absorbs strongly in the infrared, but does not produce strong Raman scattering. Also, low frequency modes can readily be measured in Raman spectroscopy whereas most modern IR equipment does not readily measure spectra below 400 cm^{-1}.

One disadvantage of Raman spectroscopy is its low sensitivity. Nevertheless, this problem can be solved if the molecule of interest contains a chromophore. If a laser frequency is used that is within an electronic absorption band the Raman signal is greatly enhanced. This process is known as resonance Raman (RR) scattering. RR spectroscopy provides

a sensitive and selective probe of chromophore structure. Molecules can be selectively monitored by utilizing an excitation wavelength that produces a RR spectrum for that particular molecule.

Another disadvantage of Raman and RR spectroscopy is that fluorescence often overwhelms the Raman scattering from biological materials. Surface-enhanced Raman (SERS) or surface-enhanced resonance Raman (SERRS) spectroscopy involves the adsorption of molecules on a SERS active metal. SERRS has been demonstrated to be an effective solution to the fluorescence problem[6-8] and has been used to determine vibrational information for a large number of biologically significant molecules.[9-11]

Silver, gold and copper are the most commonly used SERS substrates. These metal surfaces can be prepared as thin metal films vapor deposited on inert supports, as colloids through chemical reduction, and as electrodes using an oxidation-reduction cycle to roughen the surface. The mechanism of SERRS (SERS) is not completely understood. Although many publications exist that attempt to explain the theoretical basis for surface enhancement it is generally accepted that there are two major classes of enhancement mechanisms. Electromagnetic enhancement mechanisms attribute the SERS effect to increased local electric fields at the metal surface. The increased field strength is due to

excitation of collective oscillations of the conduction electrons (surface plasmons) at the metal surface.[12-14] Molecular or chemical mechanisms attribute the enhanced scattering to the formation of new excited states via charge transfer (adatom) or to the formation of a molecule-metal complex.[15,16]

In present studies, roughened silver and gold electrodes were used as SERRS substrates for two reasons. First, the roughened Ag electrode produced the best SERRS spectra for the chlorophylls and pheophytin a with the chosen excitation wavelengths. The reason for chlorophyll or pheophytin adsorption at these surfaces is not known. While little is known about the nature of the roughened electrode surface, recent studies report the presence of metal salts on the surface of the electrochemically roughened metal surface. Evans et al.[17] assigned the Raman band at 240 cm^{-1}, detected on a Ag electrode that had been roughened with 0.1 M KCl as the electrolyte, to the Ag-Cl stretch. This is in agreement with surface Ag-halide stretches reported by other SERS studies.[18-21] Gao and Weaver,[22] using a gold electrode roughened in the presence of 0.1 M KCl reported a band, assigned as the Au-Cl stretch, at ca. 265 cm^{-1}. Upon addition of 10 mM or more of bromide or iodide anion the 265 cm^{-1} band disappeared and bands appeared at 185 and 120 cm^{-1}, the Au-Br and Au-I stretches, respectively. Similarly, Holze,[23] using gold electrodes

roughened in the presence of 0.1 M KCl and 0.1 M K_2SO_4, assigned the Raman bands at 265 and 270 cm^{-1} to the Au-Cl and Au-SO_4 stretches, respectively. Preliminary data recorded in this study are in agreement with these findings. Thus, the metal salt on the roughened electrode surface may assist the adsorption of biological molecules.

Second, metal electrodes are well suited for SERRS electrochemical studies of photosynthetic pigments. Ag and Au electrodes provide the electrochemical range needed to perform studies on the chlorophylls and pheophytin a radical ions. Preliminary results by Heald[24] report a SERRS spectrum of the pheophytin a radical anion using a Ag electrode and 406.7 nm excitation. In the future, it is desirable to perform electrochemical studies on the individual components in vitro and eventually on whole RCs. Our previous studies of reaction centers[25] and chromatophore preparations[26] have already demonstrated that SERRS studies of designated membrane components are feasible. Some fluorescence will remain when using SERRS with red excitation to study photosynthetic preparations since the fluorescence quenching falls off exponentially with distance from the surface.[27,28] However, the Raman spectra for those molecules close to the surface should be above the fluorescence. The following chapters are the first steps to realizing this future goal.

Explanation of Dissertation Format. This dissertation follows an alternate format. The form of Sections 1-4 comply

with the guidelines established by the Journal of the American Chemical Society for manuscripts to be submitted. Section 1 is a paper that was published in the Journal of the American Chemical Society in December, 1990. The second and third authors of this paper are Jae-Ho Kim and Therese M. Cotton, respectively. Sections 2, 3, and 4 will be submitted to the Journal of the American Chemical Society with each Section as an individual paper. Therese M. Cotton will be second author on each of these manuscripts.

REFERENCES

1. Glazer, A. N.; Melis, A. Ann. Rev. Plant Physiol. **1987**, 38, 11-45.
2. Mathis, P.; Rutherford, A. W. In New Comprehensive Biochemistry, Photosynthesis; Amesz, J., Ed.; Elsevier: Amsterdam, 1987; Vol. 15, pp. 63-96.
3. Thompson, L. K.; Miller, A. F.; de Paula, J. C.; Brudwig, G. W. Israel Journal of Chemistry, **1988**, 28, 121-128.
4. Lagoutte, B.; Mathis, P. Photochem. Photobiol. **1989**, 49, 833-844.
5. Hansson, Ö; Wydrzynski, T. Photosyn. Res. **1990**, 23, 131-162.
6. Cotton, T. M.; Schultz, S. G.; Van Duyne, R. P. J. Am. Chem. Soc. **1980**, 102, 7960-7962.
7. Weitz, D. A.; Garoff, S.; Gersten, J. I.; Nitzan, A. J. Phys. Chem. **1983**, 78, 5324-5338.
8. Hildebrandt, P.; Spiro, T. G. J. Phys. Chem. **1988**, 92, 3355-3360.
9. Cotton, T. M. In Spectroscopy of Surfaces; Clark, R. J. H., Hester, R. E., Eds.; John Wiley & Sons: New York, 1988; Vol. 16, pp. 91-153.
10. Koglin, E.; Sequaris, J. -M.; In Topics in Current Chemistry; Springer-Verlag: Berlin, 1986; Vol. 134, pp. 1-53.
11. Nabiev, I.; Efremov, R. G.; Chumanov, G. D. Sov. Phys.

Usp. **1988**, 31, 241-262.

12. Gersten, J. I.; Nitzan, A. J. Chem. Phys. **1980**, 73, 3023-3037,
13. Kerker, M.; Wang, D. S.; Chew, H. Appl. Opt. **1980**, 19, 4159-4174.
14. Ferrell, T. L. Phys. Rev. B: Condense. Matter **1982**, 25, 2930-2932.
15. Furtak, T. E. J. Electroanal. Chem. Interfacial Electrochem. **1983**, 150, 375.
16. Otto, A. In Light Scattering in Solids; Cardona, M., Gunthrodt, G., Eds.; Springer-Verlag: Berlin, 1984; Vol. IV, pp. 289-461.
17. Evans, J. F.; Albrecht, M. G.; Ullevig, D. M.; Hexter, R. M. J. Electroanal. Chem. **1980**, 106, 209-234.
18. Wetzel, H.; Gerischer, H.; Pettinger, B. Chem. Phys. Lett. **1981**, 78, 392-397.
19. Fleischman, M.; Hendra, R. J.; Hill, I. R.; Pemble, M. E. J. Electroanal. Chem. **1981**, 117, 243-255.
20. Owen, J. F.; Chen, T. T.; Chang, R. K.; Laube, B. L. Surf. Sci. **1983**, 125, 679-698.
21. Weaver, M. J.; Hupp, J. T.; Barz, F.; Gordon, J. G.; Philpott, M. R. J. Electroanal. Chem. **1984**, 160, 321-333.
22. Gao, P.; Weaver, M. J. J. Phys. Chem. **1986**, 90, 4057-4063.
23. Holze, R. Surf. Sci. **1988**, 202, L612-L620.
24. Heald, R. L. Resonance Raman and Electrochemical

Investigations of Primary Electron-Transfer Species in Photosynthesis; Ph.D. thesis, University of Nebraska, Lincoln, NE, 1989.

25. (a) Cotton, T. M.; Van Duyne, R. P. FEBS Lett. **1982**, 147, 81-84. (b) Picorel, R.; Holt, R. E.; Heald, R.; Cotton, T. M.; Seibert, M. J. Am. Chem. Soc. In Press.

26. (a) Picorel, R.; Holt, R. E.; Cotton, T. M.; Seibert, M. In Progress in Photosynthesis Research; Biggins, J., Ed.; Martinus Nijhoff Publishers: The Netherlands, 1987; pp. 1.4 423-426; (b) Picorel, R.; Holt, R. E.; Cotton, T. M.; Seibert, M. J. Biol. Chem. **1988**, 263, 4374-4380; (c) Seibert, M.; Cotton, T. M.; Metz, J. G. Biochim. Biophys. Acta **1988**, 934, 235-246; (d) Picorel, R.; Lu, T.; Holt, R. E.; Cotton, T. M.; Seibert, M. Biochemistry **1990**, 29, 707-712.

27. Kuhn, H.; Mobius, D. Agnew Chem. Internat. Edit. **1971**, 10, 9.

28. Chance, R. R.; Prock, A.; Silbey, R. Adv. Chem. Phys., **1975**, 37, 1.

SECTION 1. A COMPARATIVE STUDY OF RESONANCE RAMAN AND SURFACE-ENHANCED RESONANCE RAMAN CHLOROPHYLL *a* SPECTRA USING SORET AND RED EXCITATION

ABSTRACT

Surface-enhanced resonance Raman scattering (SERRS) spectra are reported for chlorophyll *a* adsorbed on a silver electrode at 298 and 77 K using 406.7, 457.9, 514.5, and 647.1 nm excitation. Submerging the electrode in degassed water at 298 K was found to improve the spectral quality by minimizing sample heating and photooxidation. Spectral intensities and peak resolutions were greater at all excitation wavelengths at liquid nitrogen temperature. Most significantly, roughened silver at the low temperature, quenched the fluorescence accompanying red excitation and minimized sample photooxidation, resulting in richly detailed SERRS spectra of chlorophyll *a*. The close correspondence between chlorophyll *a* resonance Raman (RR) and SERRS spectra suggests that an electromagnetic mechanism is the major source of the surface enhancement, rather than a chemical mechanism (e.g., a charge-transfer complex between chlorophyll *a* and the metal). The spectral similarities, together with the presence of the MgN_4 vibration band in the SERRS spectra, also provides evidence that structural alterations (e.g., cleavage of ring V or loss of Mg) do not occur in chlorophyll *a* after adsorption at the electrode surface. A distinctive SERRS spectrum was obtained for each excitation wavelength. Selective excitation within the various electronic transitions can thus be utilized to verify assignments of the vibrational modes of

chlorophyll *a* and to monitor its interactions and photochemical behavior in biomimetic systems.

INTRODUCTION

Chlorophyll a (Chl a) plays an essential role in the conversion of sunlight into chemical energy in green plants and blue green algae. Chlorophylls are metallochlorins (dihydrogen-reduced metalloporphyrins) found in photosynthetic membranes. The obligatory presence of metallochlorins in lieu of metalloporphyrins in photosynthetic and certain other biological systems is not understood. However, in an attempt to elucidate the structural and photochemical behavior of these compounds, resonance Raman (RR) spectroscopy has been utilized as a probe of the vibrational and electronic structure of metalloporphyrins[1-4] and, more recently, metallochlorins and chlorophylls.[5-12] The latter species result from reduction of the $C_b=C_b$ bond of Ring IV of the porphyrin macrocycle. This destroys the in-plane degeneracy and has a profound effect on the electronic absorption spectrum. The typical B and Q electronic transitions of symmetrical porphyrins are split into x and y components. In addition, the Q transition gains considerable intensity relative to that observed in porphyrins.

The differences in the chlorin electronic properties are reflected in their RR spectra, which are strongly affected by excitation conditions. Resonance Raman excitation within the strongly allowed B transition results in enhancement of symmetric, in-plane modes arising primarily from Franck-Condon type scattering[9a,10a,10d,10e,11,13a,b], although a small contribution

from non-Condon mechanisms has been estimated recently[14]. Excitation within the Q_x band produces enhancement via vibronic coupling between this state and the intense B state(s). Excitation within the Q_{y0} transition has been accomplished in only a few instances by using various subterfuges to avoid or reduce the intense fluorescence from this state.[7b,7c,12,14] For example, Mattioli et al.[14] have recently obtained resonance excitation profiles for two modes in Ni Pheo *a* within the Q_y 0,0 and 0,1 region of the absorption spectrum. Their results indicate significant [ca. 40%] non-Condon activity within this excitation region as a result of vibronic coupling to the one or more of the B states. Thus, the RR scattering mechanisms within this transition appear to be much more complex than in the case of porphyrins of higher symmetry.

Several investigations have focused on Raman spectroscopy of isolated chlorophyll pigments as a first step in understanding their role in the photosynthetic membrane.[10a,b,9,11,15] RR band assignments have been suggested for a number of chlorophylls.[10] The objective of the RR investigations of chlorophyll *a* has been to define the effect of axial coordination[16] on the RR (as well as IR) spectra,[9a] to identify bands that are both ligation- and metal-sensitive,[9,15] and to determine the effects of isotopic substitution on the spectrum in an effort to assign bands to specific vibrations of the macrocycle.[17] Both RR[11] and FTIR difference spectroscopy[18] have

also been used to characterize the Chl a cation radical vibrational spectrum.

In spite of the considerable data available, a complete and unambiguous assignment of the chlorophyll a vibrational spectrum has not yet appeared. This is partly due to limitations imposed by the high fluorescence produced at many of the laser excitation wavelengths used to obtain RR spectra of chlorophylls. The use of metal-substituted chlorins and chlorophylls does allow observation of fluorescence-free RR spectra. However, the metal has a significant perturbing effect on the vibrational spectrum as well as on the properties of the chlorophyll (e.g., ligation, aggregation, etc.). Another approach for surmounting the fluorescence problem is the use of CARS spectroscopy. Höxtermann et al.[19] reported resonance CARS spectra of Chl a excited with 694.3 nm. However, this technique is experimentally demanding and a more straightforward method is needed to determine the RR spectrum of chlorophylls using excitation into the lowest energy $^1\pi$-π^* states.

Surface-enhanced Raman scattering (SERS) spectroscopy offers considerable promise for obtaining a complete excitation spectrum of the chlorophylls. This technique has been demonstrated as an effective method for obtaining spectra of highly fluorescent molecules. The enhancement effect can increase Raman scattering intensity by 10^3-10^6 fold and adsorption of molecules on the SERS-active metal surface

results in fluorescence quenching.[12,20,21] In addition, the coupling of RR enhancement with surface enhancement (surface-enhanced resonance Raman scattering (SERRS)) results in an increase in scattering intensity by a factor of 10^3 to 10^5 over that observed under resonance or surface conditions alone.[12,21] Many publications have appeared in which attempts were made to determine the theoretical basis for surface enhancement. It is generally accepted that there are two major classes of enhancement mechanisms. Electromagnetic mechanisms attribute the SERS enhancement to increased local electric fields at the metal surface. The increased field strength is due to excitation of the collective oscillations of the conduction electrons (surface plasmons) at the metal surface.[22-24] Molecular or chemical mechanisms attribute the enhanced scattering to the formation of new excited states via charge-transfer (adatom) or to the formation of a molecule-metal complex.[25,26]

In spite of an incomplete understanding of the mechanism, SERS (SERRS) has been used to determine vibrational information from a large number of biologically significant molecules.[27-29] There have also been a number of studies pertaining to the chlorophylls or chlorophyll derivatives. Uphaus et al.[30] obtained SERRS spectra with 457.9 nm excitation for Chl _a_, bacteriochlorophyll _a_, and bacteriopheophytin _a_ monolayers on silver islands films. Andersson et al.[31] reported a Qy-excited SERRS spectrum of Chl _a_ multilayers on a silver film. Recently, SERRS was applied to the elucidation of the Raman

spectrum of copper chlorophyllin a, a chlorin derivative, which was adsorbed on colloidal silver or gold and excited within the blue and red regions of the electronic absorption spectrum.[12]

Previous SERRS studies of Chl a have demonstrated that it is possible to obtain spectra under various conditions. The present study is concerned with a detailed comparison between the RR and SERRS spectra of Chl a obtained under various conditions of excitation. The use of SERRS provides detailed and highly resolved spectra of Chl a adsorbed on a roughened silver electrode. The similarity between the RR and SERRS spectra supports an electromagnetic mechanism as the dominant mode of enhancement at the silver surface and also demonstrates that structural alteration of chlorophyll a does not occur as a result of adsorption on the electrode surface. Each excitation wavelength produces a distinctive spectrum, indicating dramatic changes in mode enhancements. These intensity changes provide insights regarding the structural changes accompanying electronic excitation. The SERRS data also provide additional criteria for band assignments and suggest the mode of interaction of Chl a with the surface. Because the purpose of this study is to compare the RR and SERRS spectra of Chl a, a detailed discussion of each band assignment will not be given here. Rather, the analysis will be limited to those bands which are most affected by the interaction of Chl a with the silver surface.

EXPERIMENTAL SECTION

Chlorophyll a preparation. Chl a (Figure 1-1.) was isolated from spinach according to an established procedure.[32] Prior to use, the Chl a was purified by isocratic semi-preparative reverse phase high performance liquid chromatography (rp HPLC) on a Phenomenex C18 guard column and Phenomenex 10 μm C18 25 cm x 10 mm i.d. column. The mobile phase was acetonitrile/methanol 3:1 (v/v) with a flow rate of 5 ml/min. All solvents were Omnisolv HPLC grade and were degassed prior to use by vacuum filtration. The HPLC equipment consists of a Model 2350 ISCO high pressure pump, Model 2360 ISCO gradient programer, and a Model V4 ISCO absorbance detector set at 445 nm. One ml of a Chl a solution in the mobile phase was injected into the system and the central portion of the Chl a peak was collected. The concentration of the eluent was typically ca. 2×10^{-4} M based on its electronic absorption spectrum.

For RR experiments the purified Chl a solutions were placed in 5 mm o.d. Pyrex tubes, vacuum degassed using three freeze-pump-thaw cycles, and sealed under vacuum. For SERRS experiments the roughened electrode was immersed in the chosen chlorophyll fraction separated by HPLC. The Chl a was adsorbed onto the electrochemically roughened electrode by allowing the electrode to remain in the purified Chl a solution (2×10^{-4} M) for 10 minutes in the dark. The Chl a concentration on the electrode surface, approximately

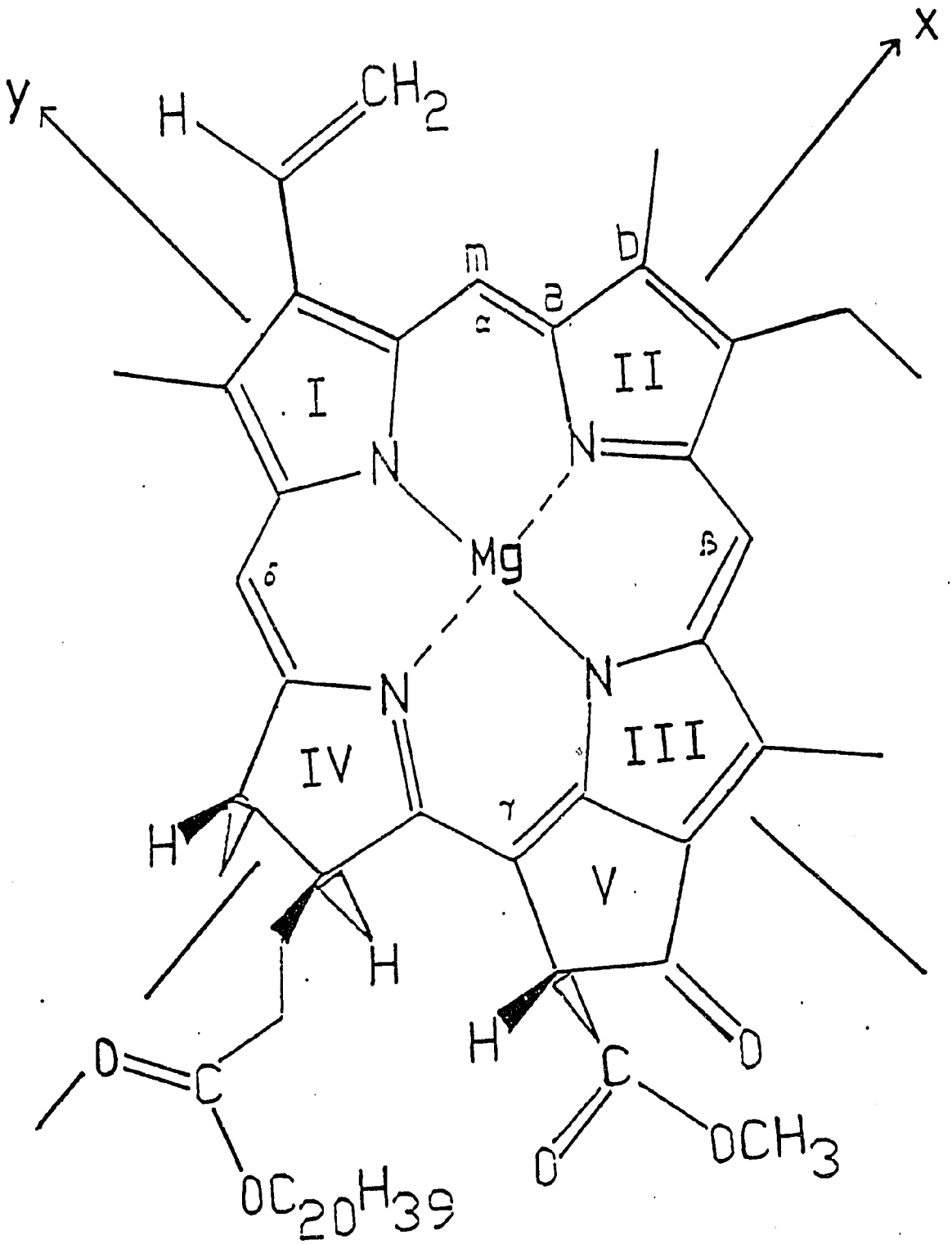

Figure 1-1. Structure of Chl a.

monolayer level (1×10^{-10} mol Chl *a* / cm^2), was estimated by sonicating the electrode in CH_2Cl_2 and recording a fluorescence spectrum of the resulting solution. The electrode surface area was determined electrochemically to be 0.28 cm^2.

The purity of the Chl *a* was monitored and confirmed before and after the Raman experiments by analytical rp HPLC and UV/VIS spectroscopy. A Phenomenex Ultrex 3 μm C18 7.5 cm x 4.6 mm i.d. column was used for the chromatography. Electronic absorption spectra were measured using a 1 cm pathlength cuvette and a Shimadzu J-260 UV/VIS spectrophotometer.

Electrode preparation. A silver electrode was used as the SERRS substrate. It was constructed by sealing a flattened silver wire into a glass tube with Torr seal. The exposed surface was rectangular with dimensions approximately 4 x 7 mm. The electrode was polished using successively finer grades of alumina (5.0, 0.3, 0.05 μm). The electrode was rinsed and sonicated between polishing steps. Following the polishing procedure the electrode was cleaned by cathodization at -2.0 V for 1 minute and roughened by using an oxidation-reduction cycle (ORC) consisting of a double potential step from an initial potential of -550 mV to +550 mV and back to -550 mV in 0.1 M Na_2SO_4 solution. The total charge passed during the oxidation step was equivalent to 25 mC/cm^2. A SSCE (saturated sodium calomel electrode) was used as the reference electrode and a Pt wire served as the auxiliary electrode.

Resonance Raman and SERRS spectroscopy. Laser excitation of the Raman and surface Raman scattering was provided by a Coherent Innova 90 Ar^+ laser (457.9 and 514.5 nm) or a Coherent Innova 100 Kr^+ laser (406.7 and 647.1 nm). The laser power was 25 mW for all the spectra reported here. Raman scattered light was collected in a backscattering geometry.

SERRS spectra obtained with 647.1 nm excitation were recorded using a Spex Triplemate spectrometer coupled to a Princeton Applied Research Corp. (PARC) Model 1421-R-1024HD intensified SiPD detector cooled to -40 C. The spectra were collected and processed with an OMA-3 (PARC) optical multichannel analyzer. RR and SERRS spectra obtained by excitation at the other wavelengths were recorded using a Model 1420 (PARC) intensified SiPD detector. These spectra were collected and processed with an OMA-2 (PARC) optical multichannel analyzer. The reported spectra are composites of 16 scans, with 5 s and 1 s integration periods per scan for the RR and SERRS spectra, respectively.

SERRS spectra of the adsorbed Chl _a_ at room temperature (298 K) were obtained by transferring the electrode to a quartz Dewar flask containing degassed HPLC grade water. The Dewar flask was constructed with a transparent body to allow direct acquisition of a SERRS spectrum during electrode immersion in water. Low temperature (77 K) SERRS spectra of the adsorbed Chl _a_ were obtained by transferring the electrode to the quartz Dewar flask containing liquid nitrogen.

RESULTS

Electronic Absorption Spectroscopy. The electronic absorption spectrum of Chl *a*, together with several assigned transitions, is shown in Figure 1-2. The splitting is much greater between the Q_x and the Q_y transitions than between the B_x and B_y bands. This was originally observed in metallochlorins.[33,13a] In the Soret region of the spectrum, the B_x transition is strongest and occurs at 431 nm. The B_y transition is present as a blue shoulder at ca. 413 nm. In the green to red region of the spectrum, the four maxima at 663, 618, 580, and 535 nm are assigned as vibronic bands belonging to the Q_y and Q_x transitions. Until recently these bands were assigned as $Q_y(0,0)$, $Q_y(1,0)$, $(Q_x(0,0) + Q_y(2,0))$, and $Q_x(1,0)$ respectively.[34-36] There is still agreement that the 663 nm band is the $Q_y(0,0)$. However, according to the linear dichroism and fluorescence polarization studies of Fragata et al.[37] the 618, 580, and 535 nm vibronic bands belong to $Q_x(0,0)$, $(Q_y(1,0) + Q_x(1,0))$ and $(Q_x(0,0) + Q_y(2,0))$, respectively. The Q_x contribution to the 535 nm band is twice that of Q_y and, therefore, can still be considered to arise predominantly from an x-polarized electronic transition.

Raman Spectroscopy. The excitation wavelengths used for obtaining RR and SERRS spectra are given in the figure legends and indicated in Figure 1-2. Table 1-1 lists the major RR and SERRS (298 and 77 K) bands and their vibrational assignments. These assignments are based primarily on the recent normal

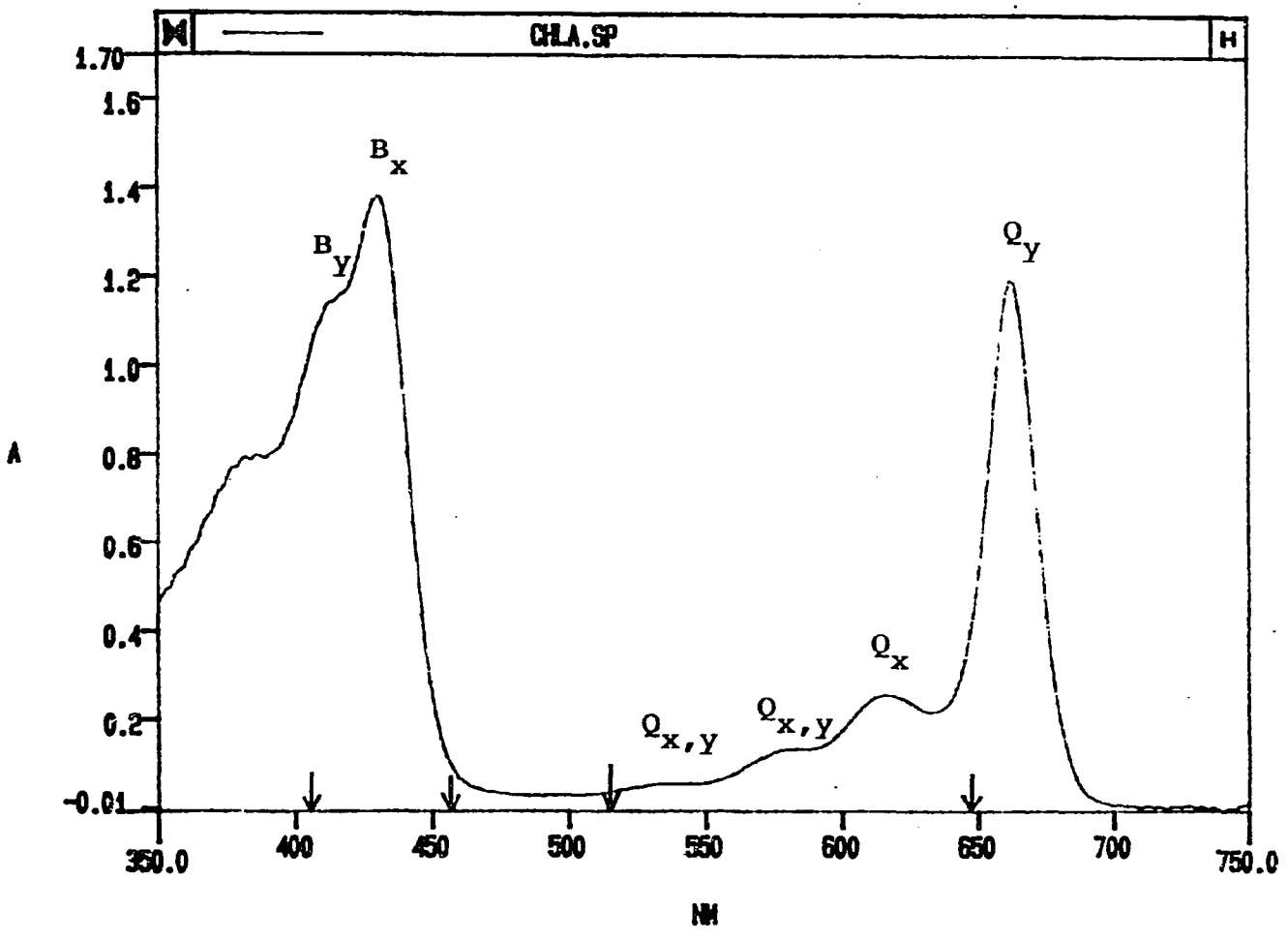

Figure 1-2. Absorption spectrum of Chl a in ACN/MeOH (3:1 v/v).

Table 1-1. Chl a RR and SERRS Frequencies (cm^{-1})

RR		SERRS[a]				
406.7[b]	457.9[b]	406.7[b]	457.9[b]	514.5[b]	647.1[b]	assignment[c]
1684		1677 1684				$\nu(C_9=O)$
1599	1599	1604 1606	1611 1610	1608 1610	 1602	$\nu C_aC_m(\alpha,\beta)$
1548	1548	1550 1553	1556 1555	1554 1557	 1538	νC_aC_b(III); νC_bC_b(I)
	1520	1535 1535	1528 1529	1528 1530		νC_bC_b(I); νC_aC_b(III)
1488		1490 1494	 1490	1493 1496	 1490	$\nu C_aC_m(\delta)$; νC_aC_b(I)
1433	1433	1429 1437	1433 1437	1444 1437	 1429	$\nu C_aC_m(\gamma,\delta)$; νC_aC_b(I-III)
			1385 1385	1390 1389	 1385	νC_aC_b(II); $\nu C_aC_m(\alpha,\delta)$
1379	1376	1377 1379	1377 1377	1376 1376		νC_aN(IV); νC_aC_b(I,III)
1344	1343	1350 1357	1348 1351	1346 1346	 1350	νC_aN(IV); νC_aN(I,III)
		1329 1329	1330 1330	1327 1328	1321 1327	νC_aN(I); $\delta C_mH(\delta)$

[a]Top frequency is at 298K and bottom frequency is at 77K.
[b]Excitation wavelength in nm.
[c]Assignments based on those reported by Lutz[10a], Hildebrandt and Spiro[12], and Boldt et al.[13a] Mode descriptions are ν=stretch, δ=in-plane deformation, and γ=out-of-plane deformation. C_a, C_b, C_m and the characters in parentheses refer to the macrocycle positions shown in Figure 1-1.

Table 1-1. continued

RR		SERRS[a]				
406.7[b]	457.9[b]	406.7[b]	457.9[b]	514.5[b]	647.1[b]	assignment[c]
1285	1290	1286	1287	1286	1285	$\delta C_mH(\alpha,\beta)$;
		1288	1287	1288	1282	υC_aN(II,IV)
1221		1221		1231	1221	γC_bH(IV);
		1227		1231	1218	$\delta C_mH(\delta)$
	1210		1209	1216		γC_bH(IV);
			1208	1210		$\nu C_mH(\delta)$
1182	1182	1181	1184	1184	1180	υC_mC_{10}(IV);
		1186	1186	1186	1185	νC_bH(IV)
1147	1150	1141	1146	1153	1139	νC_aN(II);
		1144	1146	1159	1143	νC_aNC_a(I)
	1042		1045			νC_aN(III)
		1050	1042	1046	1050	
986	988	987	984	982	981	δC_mC_aN(III);
		986	987	985	986	νC_9C_{10}(V)
914		914	918	918	911	δC_aC_bS
		914	914	920	919	
791	796	794	795	795		δC_aC_bS
		793	794	796	798	
751		751			743	δC_aC_bS
		752	743	748	748	

Table 1-1. continued

RR		SERRS[a]				
406.7[b]	457.9[b]	406.7[b]	457.9[b]	514.5[b]	647.1[b]	assignment[c]
	717	707 717	709 717	728		
686	698	698 696	 703	695 700	694	
			577 577		 569	
	513		498 519		 519	
			464 467			
			344 344			
316	314		 320			
253			265 274			
			213			
			184			

mode analysis by Boldt et al.[13a]

RR spectra obtained with excitation in the B absorption band are shown in Figure 1-3. The spectra resulting from 406.7 nm excitation are in resonance with the B_y transition. Figure 1-3b and 1-4b show spectra of Chl a obtained with 457.9 nm excitation, or in resonance with the B_x transition. The RR spectra are similar to those reported previously and are consistent with Franck-Condon activity of in-plane ring modes in resonance with the strongly allowed B transitions.[9a,10a,d,e,11] A comparison of the two spectra indicates strong bands at 1548cm^{-1} (νC_aC_b (III); νC_bC_b (I)) at both excitation wavelengths. The 406.7 nm excited spectrum includes bands at 1684 (νC_9=O), 1599 (νC_aC_m (α,β)), 1488 (νC_aC_m (δ); νC_aC_b(I)), and 1221 cm^{-1} (γC_bH (IV); δC_mH (δ)); these bands are weak or absent in the 457.9 nm excited spectrum. This is reasonable considering that 406.7 nm light produces electronic excitation along the y-axis of Chl a (Figure 1-1.); the C_9=O bond and ring I and ring III C_aC_b bonds lie parallel, or nearly so, to this axis. Modes containing bonds that are parallel to the electronic transition dipole moment and that are distorted in the excited state are expected to undergo the strongest enhancement. This does not explain the weak enhancement of the νC_aC_m (α,β,δ) bands with 457.9 nm excitation, however. Previously, Lutz[10a] reported a medium intensity 1599 cm^{-1} band and a very weak 1488 cm^{-1} band using 441.6 nm excitation.

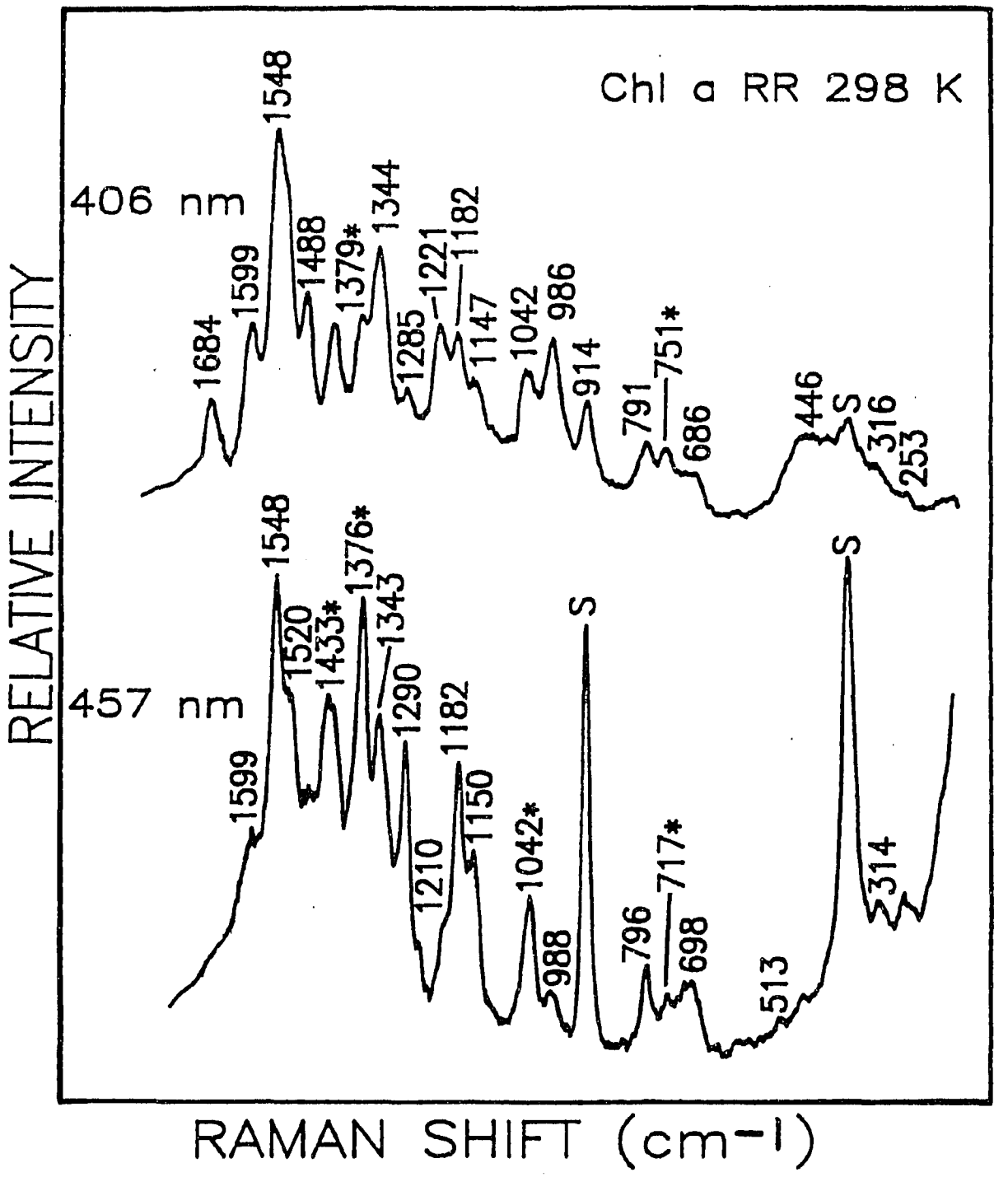

Figure 1-3. RR of Chl a in ACN/MeOH (3:1 v/v).

Perhaps 457.9 nm is too far removed from the B_x maximum for resonance enhancement of these modes. In contrast, bands at 1290 ($\delta C_mH(\alpha,\beta)$; νC_aN (II,IV)), 1182 (νC_mC_{10}; γC_bH (IV)), and 1150 cm^{-1} (νC_aN (II); δC_aNC_a (I)) are more intense in the 457.9 nm excited spectrum as compared to their intensities in the 406.7 nm excited spectrum. This also appears acceptable because rings II and IV are aligned along the x-axis and modes associated with these rings should be enhanced using laser lines close to the B_x transition. While both the B_x and B_y show strong enhancement of the C_aC_b and C_bC_b modes it appears the 457.9 nm portion of the B_x enhances pyrrole modes associated with the inner bonds of the macrocycle (νC_aN) and the B_y enhances pyrrole modes associated with the periphery of the macrocycle (νC_aC_m). The appearance of the MgN_4 bands with 457.9 nm excitation is also supportive of this inner selectivity. Within the 750-1100 cm^{-1} region, the spectra obtained at the two excitation wavelengths have more similarities than spectra in the high frequency region. Some differences exist in the 400-750 cm^{-1} region, but this region has not been previously assigned and will not be discussed here.

Attempts to obtain Raman spectra with 514.5 nm and 568.2 nm excitation were unsuccessful using the solution concentrations employed here (2×10^{-4} M). These lines are not in resonance with the B bands and the Q_x transition is very weak. Fluorescence obscured the RR spectrum at the 647.1 nm excitation.

Figure 1-4 shows Chl a SERRS spectra obtained at room temperature (298 K) excited within the B and Q bands. The electrode was submerged in degassed water during spectral acquisition and this appears to stabilize Chl a by dissipating sample heating and reducing photooxidation. Thus, the SERRS signals did not degrade during the time required to accumulate 16 scans. SERRS spectra of Chl a with excitation in the B and Q bands at 77 K are shown in Figures 1-5.

DISCUSSION

Comparison of the RR vs. SERRS spectra. The use of B band excitation allows direct comparison of RR (Figure 1-3) and SERRS (Figure 1-4) spectra. As can be seen the SERRS spectra are clearly surface-enhanced and display sharper, better resolved peaks in spite of the fact that the absolute amount of Chl a present in the laser beam is ca. 10^7 lower than in the RR experiments. The RR spectra contain solvent bands, as indicated with an "S". The bands marked with an asterisk have contributions from both the solvent and Chl a. In contrast, intense SERRS spectra are observed with only very weak contribution from the solvent. This is a consequence of the much stronger interaction between Chl a and the Ag surface as compared to the solvent-Ag surface interaction, as well as to the additional resonance contribution to the Chl a surface spectrum. Overall, more peaks are observed in the low frequency SERRS spectra as compared to the low frequency RR spectra, especially using 457.9 nm excitation.

A similar, though not identical, intensity pattern is also noted on comparing the RR (Figure 1-3) and SERRS spectra (Figure 1-4). The similarity of the RR and SERRS frequencies is indicative of an electromagnetic enhancement mechanism.[22-24,26,38] Chemical enhancement mechanisms result in frequency shifts as well as relative intensity changes in the SERRS spectra as compared to the RR spectra.[38]

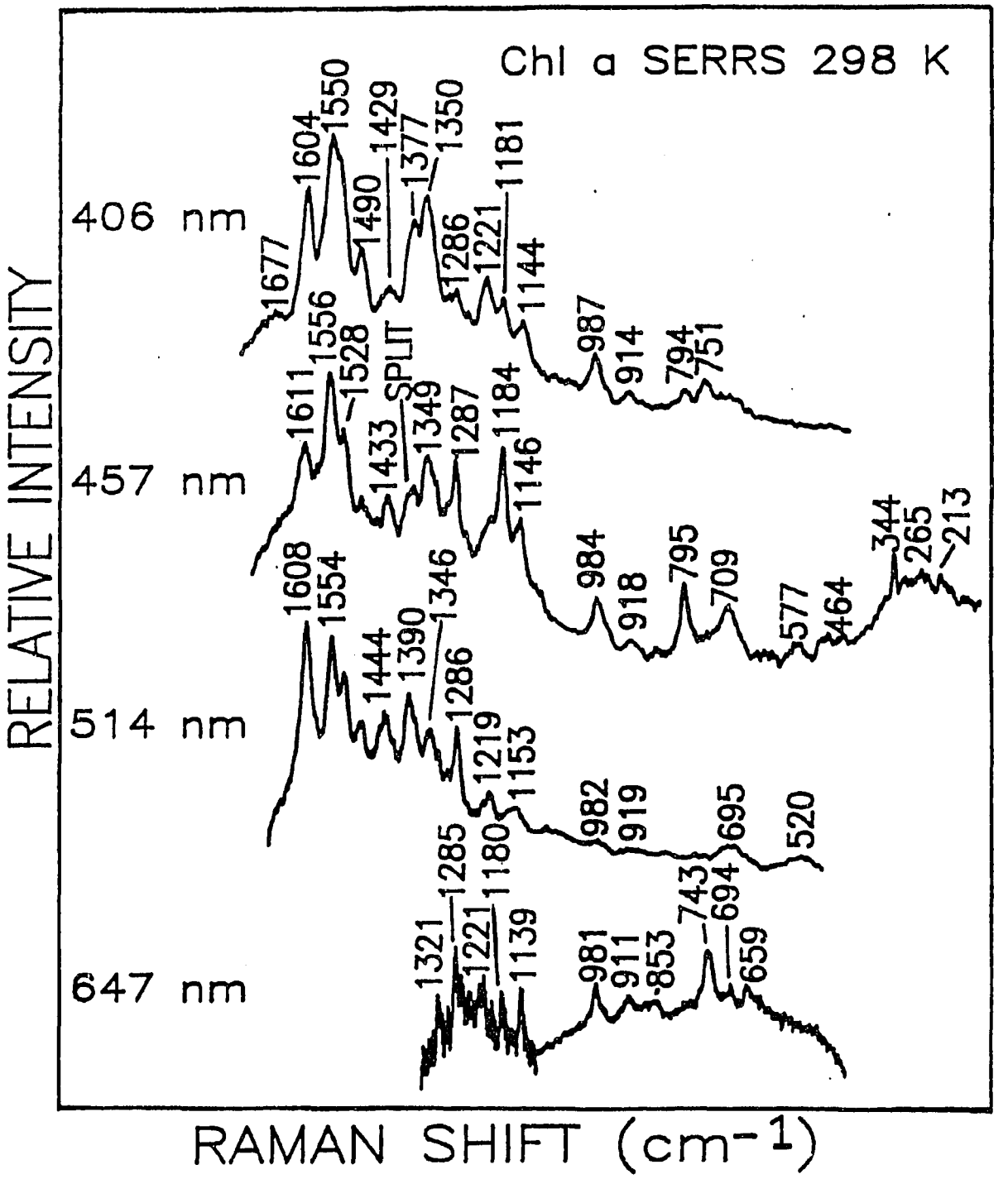

Figure 1-4. SERRS of Chl a at 298 K.

Also, the presence of peaks at 344 and 213 cm^{-1} (MgN_4 vibrations) indicate Chl *a* does not undergo detectable structural alterations upon adsorption.

Some differences do exist in frequencies and relative intensities of the bands, however. There are at least two possible origins for these differences. First, environmental effects may change the coordination state of Chl *a*. The solution spectra were recorded in acetonitrile/methanol (3:1) and the frequencies of coordination-sensitive bands are near those characteristic of six-coordinate Chl *a*.[9a] The surface spectra, on the other hand, are closer to five-coordinate Chl *a*. Thus, a change in coordination may result following emersion of the electrode from the adsorbing solution. Second, relative intensity differences may reflect the orientation of the macrocycle at the metal surface. Electromagnetic enhancement theory attributes the relationship between band intensities and molecular orientation to the coupling of the electric field at the electrode surface with the polarizability tensors of the adsorbed molecule. Bonds that have polarizability tensors perpendicular to the electrode surface are preferentially enhanced.[39,40]

In order to predict the orientation of the Chl *a* on the surface, it is necessary to consider the nature of the forces involved in the adsorbate/surface interaction. There are two types: polar forces involving the interaction of the porphyrin macrocycle with the surface, and nonpolar forces arising

from the phytol tails. Assuming that the Ag surface is hydrophilic, Chl a would be expected to interact through a polar functionality. There are several possibilities including the keto and ester groups on rings V and IV. Another possibility is that the vinyl moiety on ring I could interact with the surface through the formation of a pi-complex with Ag. Consideration of the van der Waal's interactions between the phytol tails suggests that surface-adsorbed structures producing maximal contact between the hydrophobic tails of adsorbed Chl's should be favored. As a result of the balance of these two forces, the adsorption of Chl a is expected to resemble that of other amphiphilic species[41] and result in a self-assembled monolayer structure.

An examination of the SERRS bands undergoing the greatest changes in frequency and/or intensity can provide evidence for a particular orientation of Chl a at the surface. Table 1-2 lists such bands as observed for B_x and B_y excitation. Only the high frequency region is considered because differences between the SERRS and RR spectra were greatest here. From an analysis of the data shown in Table 1-2, it is doubtful that the chlorophyll macrocycle lies parallel to the plane of the Ag surface for three reasons. First, if Chl a were to adsorb flat on the Ag surface, the polarizability tensors involving stretching vibrations of the pyrrole rings would lie parallel to the surface and these modes should not be strongly enhanced. Yet, inspection of Table 1-2 shows that these ring modes

Table 1-2. Comparison of RR and SERRS bands (406.7 and 457.9 nm) of Chl a.

RR	Δ cm^{-1}		Δ Intensity	Assignment[a]
	406.7nm	457.9nm		
1599	+7	+11	>	$\upsilon C_aC_m(\alpha,\beta)$
1548	+5	+8	>	$\upsilon C_aC_b(III)$; $\upsilon C_bC_b(I)$
1520	b	+9	>	$\upsilon C_bC_b(I)$; $\upsilon C_aC_b(III)$
1488	+6	b	>>	$\upsilon C_aC_m(\delta)$; $\upsilon C_aC_b(I)$
1385	b	b	>	$\upsilon C_aC_b(II)$;$\upsilon C_aC_m(\alpha,\delta)$
1379	0	split	c	$\upsilon C_aN(IV)$;$\upsilon C_aC_b(I,III)$
1344	+13	+8,split	c	$\upsilon C_aN(I,III)$;$\upsilon C_aN(IV)$
1330	b	b	>	$\upsilon C_aN(I)$;$\delta C_mH(\delta)$
1290	+3	-3	0	$\delta C_mH(\alpha,\beta)$;$\upsilon C_aN(II,IV)$
1221	+6	b	0	$\gamma C_bH(IV)$;$\delta C_mH(\delta)$
1210	b	-2	0	$\gamma C_bH(IV)$;$\delta C_mH(\delta)$
1182	+4	+4	0	$\upsilon C_mC_{10}(V)$;$\gamma C_bH(IV)$
1147	-3	-4	0	$\upsilon C_aN(II)$;$\delta C_aNC_a(I)$

[a]See Table 1-1. and Figure 1-1. for references, abbreviations, and mode descriptions.
[b]Peak does not appear in RR spectrum.
[c]A portion of the frequency shift and decrease in intensity is due to the decrease in contribution by the solvent.

Δ cm^{-1} and Δ Intensity = (SERRS(77K) value) - (RR value).

(1599, 1548, 1520, 1343, 1330 cm^{-1}) are precisely the ones that experience the greatest change at the surface. Second, the out-of-plane modes in the low frequency region should be enhanced with parallel orientation. However, the low frequency SERRS spectra are not strongly enhanced relative to the RR spectra. Third, a parallel orientation of the macrocyclic plane is not possible because of steric hindrance by the substituents on ring IV and V.

Based upon previous spectral monolayer studies of monolayers of Chl a and other surface-active porphyrins, it is highly probably that the Chl a macrocycle is adsorbed at some angle to the Ag surface. Schick et al.[41], in a RR study of monolayer assemblies of Zn(II), Cu(II), and Co(II) substituted H_2TOOP [5,10,15,20-tetrakis[4-(1-octyloxy)phenyl]-porphyrins] on glass slides, determined that the porphyrin planes were tilted at an angle of ca. 40°; the planes were 4-5 Å apart, and canted at an angle of approximately 47° with respect to one another.

Considering next the likely site of molecule-surface interaction, it is expected that if Chl a adsorption occurred through any of the substituents on rings IV or V, the carbonyl vibrations (ester or ketone) should be observed in the SERRS spectra. Enhancement of these modes is to be expected because of proximity of the oxygen functionalities to the surface and also because a component of the polarizability tensor would lie perpendicular to the surface. However, a significant

enhancement of the C=O modes is not observed in the SERRS spectra and it is concluded that these groups are not strongly interacting with the surface. A shift and broadening of the C-9 keto group from 1684 (Figure 1-3) to 1677 cm^{-1} (Figure 1-4) is observed in the 406.7 nm spectrum, which may reflect a weak interaction of this group with the surface.

Soriaga and Hubbard[42] have reported that aromatic molecules adsorb on smooth platinum electrodes reorient to form structures occupying a minimal surface area. This suggests that adsorption of Chl a at only one ring contact is favored over a structure requiring contact of two rings with the surface. Another feature of the interaction of only a single ring with the surface is that this arrangement would favor maximum contact between the phytyl tails, i.e., the projection of the macrocycle at the surface is minimal, providing closest packing of the tails.

Although an edge-on orientation of the Chl a macrocycle is clearly supported by the SERRS spectra, it is premature to speculate as to which edge is nearest the surface. It is conceivable that there are a number of orientation that result from spontaneous adsorption. Langmuir-Blodgett techniques will be used in future SERRS studies of the chlorophylls in an effort to control orientation.

In Figure 1-4, the SERRS spectra of Chl a at 298 K with 514.5 and 647.1 nm excitation are also shown. Resonance Raman spectra could not be obtained at these excita-

tion wavelengths. Using 514.5 nm excitation, the RR scattering was very weak at the solution concentration employed. Excitation at 647.1 nm resulted in intense fluorescence which obscured the RR spectrum. Overall, the SERRS technique provides several major advantages for spectroscopic studies of Chl a. These include extremely high sensitivity, fluorescence quenching and improved spectral resolution for all excitation wavelengths used in this study.

Nonetheless, the Ag surface did not completely quench fluorescence when 647.1 nm excitation was used (Figure 1-4) at 298 K. In fact, in the region 1300-1700 cm^{-1} (not shown) the Raman peaks were indiscernible from the background. The fluorescence was much weaker in the low frequency region of the spectrum, but the overall spectral intensity was not as great as that observed using B band excitation (Figure 1-4 406 and 457 nm excitation).

Surface-Enhanced Resonance Raman Scattering at 77 K. To minimize sample photodegradation and fluorescence, SERRS spectra were recorded at liquid nitrogen temperature (Figure 1-5). In general, spectra recorded at this temperature showed a dramatic suppression of broad-band emission, with narrower peaks, and frequency shifts when compared with SERRS spectra at room temperature. The spectral differences between SERRS at 298 and 77 K were greatest with 406.7 nm excitation. As can be seen from the figures, the C_9=O mode is much stronger and is up-shifted to 1684 cm^{-1} in the 77 K

spectrum. This shift may be indicative of a change in orientation of the macrocycle with respect to the surface, a change in the electronic properties of the molecule with temperature, a conformational change in the macrocycle, or some combination of these three possibilities.

Figure 1-5 displays SERRS spectra of Chl *a* at 77 K excited with various laser lines ranging from the violet to the red region of the electromagnetic spectrum. Changes in the spectra with excitation wavelength are more distinct than at 298 K. The excitation frequency dependent changes will be discussed below. Most significantly, at 77 K the fluorescence was quenched at the roughened Ag electrode and sample photooxidation was minimized, permitting acquisition of the entire spectrum. The remainder of the discussion will include only the SERRS results obtained at 77 K.

It is evident from Figure 1-5 that some bands that are strong at one excitation wavelength are not even observed at other excitation wavelengths. Differences in enhancement patterns are expected from a consideration of the differing enhancement mechanisms that are operative under B and Q excitation conditions, as described in the Introduction. The considerable variation in intensity patterns with changes in excitation wavelength was also noted in the RR studies of ClFe(III)pheophorbide by Andersson et al.[31] and in the SERRS studies of copper chlorophyllin using silver and gold colloid particles[12]. In the latter study it was concluded that the Ag

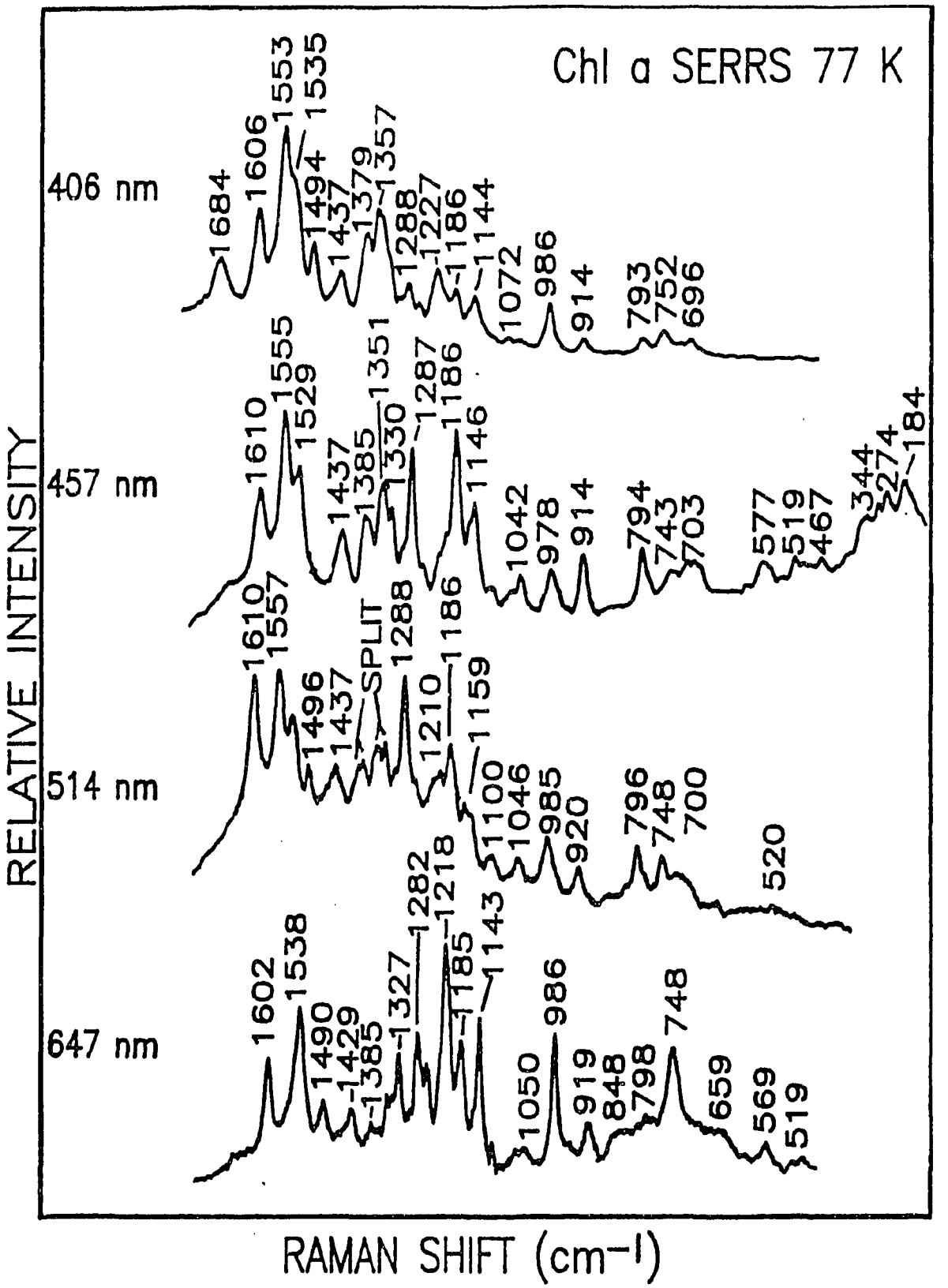

Figure 1-5. SERRS of Chl a at 77 K.

particles do not significantly perturb the copper chlorophyllin electronic states. Similarly, the data shown here also indicate that the Ag electrode surface does not significantly perturb the Chl *a* electronic states.

Excitation within the B_y absorption band using the 406.7 nm line produces a spectrum dominated by totally symmetric Franck-Condon-active modes aligned along the y-axis of the macrocycle. The spectrum obtained using 457.9 nm excitation is in resonance with the B_x absorption band and modes composed of bonds aligned along the x-axis of the macrocycle are preferentially enhanced.

A comparison of the 406.7 nm and 457.9 nm excited spectra shows that the 1494 cm^{-1} band in the former is absent and the 1535 cm^{-1} shoulder is clearly resolved and shifted to 1529 cm^{-1} band using 457.9 nm excitation. Also, as previously discussed in the context of the RR spectra, modes in the 1300-1100 cm^{-1} range are strongly enhanced with B_x but not with B_y excitation. The $\nu(C_aN)$ bands in the 1300-1400 cm^{-1} region are more highly resolved in the 457.9 nm spectrum. The orientation of the macrocycle relative to the surface results in differing enhancements for the $\nu(C_aN)$ of the various rings. The 1610 cm^{-1} band $\nu(C_aC_m)$ that appears in the 457.9 nm SERRS spectrum is assigned to CaCm (α,β) modes. The low frequency region of the B_x excited spectrum contains many more peaks than the B_y excited spectrum. The presence of the 344, 320, and 184 cm^{-1} (MgN_4 bands) in the 457.9 nm excited spectrum suggests this an

appropriate wavelength for selective monitoring of these modes in the study of photosynthetic reaction centers.

An examination of the 514.5 nm excited spectrum shows that it is very similar to that observed with 457.9 nm excitation. The 514.5 nm wavelength is in resonance with a weak absorption band which has a major contribution from the $Q_x(0,0)$ transition.[37] Thus, it is expected that these spectra should be similar because both electronic transitions lie parallel to the x-axis. Coupling between the B_x and Q_x transitions may additionally occur in the 514.5 nm spectrum. The 514.5 nm excited spectrum particularly resembles the 457.9 nm excited spectrum with regards to the splitting of the νC_aN modes and the presence of the 1528 cm^{-1} band. The 1385 cm^{-1} band of the latter spectrum is well-resolved from the other C_aN modes and is split into bands at 1389 and 1376 cm^{-1} in the 514.5 nm spectrum.

In addition, the B_x and Q_x excited spectra are similar in the low frequency region. However, the peaks at 1186 and 1146 cm^{-1} are much stronger in the B_x than in the Q_x excited spectrum and the MgN_4 vibrations are not enhanced in the latter.

Red excitation within the Q_{y0} absorption band produces a spectrum that has some features in common with all of the other spectra, but also presents some unique features. The region most enhanced is between 1250-1100 cm^{-1}, where the C-H bending vibrations are found. It has been proposed that the 1218 and 1185 cm^{-1} bands also contain contributions from out-

of-plane C_bH modes.[13a] The 1100-1300 cm^{-1} region of the spectrum resembles spectra reported recently for Ni Pheo a as obtained with Q_y excitation.[14] The close correspondence between the spectra of these compounds in this region is reasonable because these modes are not metal sensitive.[10a] As with 457.9 and 514.5 nm light the splitting of the $\nu(C_aN)$ modes occurs in the 1300-1400 cm^{-1} region. The low frequency region the Q_{y0} excited spectrum resembles the By excited spectrum in that both have a strong 986 cm^{-1} band (νC_9C_{10} (V); δC_mC_aN). In contrast with the other spectra, only the Q_{y0} excited spectrum displays the strong 748 cm^{-1} band (δC_aC_bEt).

The Q_{y0} band is intense and, as noted previously, excitation within this transition results in both Franck-Condon scattering as well as vibronic activity.[12,14] Vibrational modes aligned along the y-axis are expected to have the largest Franck-Condon overlap integrals. However, the bands enhanced with 406.7 nm (B_y) excitation are not the same as those enhanced with 647.1 nm (Q_{y0}) excitation. Among the wavelengths used in this study, only the 406.7 nm excited spectrum displays the peak assigned as $\nu(C_9=O)$ at 1684 cm^{-1}. Because the symmetric $C_9=O$ stretch is aligned along the y-axis it is expected that this vibration should also appear in the Q_y spectrum, but this is not observed. This implies that the Franck-Condon active modes are different for the B_y and Q_{y0}

transitions. Changes in the ground state configuration with respect to the excited state are not the same for B_y and Q_{y0} excitation.

CONCLUSIONS

The spectra presented in this paper are the first SERRS spectra of Chl *a* obtained with laser excitation wavelengths ranging from the violet to the red region of the electromagnetic spectrum. Distinct SERRS spectra were observed for each excitation wavelength and the enhancement pattern is typical of that reported previously for RR excitation of Chl *a* within the B electronic absorption bands, i.e., Franck Condon scattering is the major source of enhancement resulting from excitation within the B bands and vibronic coupling mechanisms are dominant for excitation within the Q_x absorption band. A comparison of the RR and SERRS spectra at two excitation wavelengths within the B transitions shows clearly that adsorption of Chl *a* does not cause a significant perturbation of these two electronic states. Only minor frequency shifts are observed in the surface as compared to solution spectra. Thus, surface-enhancement results primarily from an electromagnetic mechanism.

The intensity differences between the SERRS and RR spectra may reflect both environmental effects as well as orientation of the macrocycle with respect to the surface. Surface selection rules predicted by electromagnetic theory can be used to determine orientation. Future studies will include the characterization of Langmuir-Blodgett monolayers of Chl *a* at a metal surface. This technique will allow better experimental control over Chl *a* orientation.

The spectra obtained in resonance with Q_y are of particular importance. Previously, it has not been possible to observe RR scattering from Chl *a* using excitation wavelengths in resonance with this state because of intense fluorescence emission. The fluorescence-quenching advantage of SERRS makes it ideally suited for the objective of this study. A comparison of the SERRS spectrum of Chl *a* with the RR spectrum of Ni Pheo *a*[14] shows that the enhancement pattern is similar, especially in the 1200-1300 cm^{-1} region of the spectrum which is dominated by C-H bending modes and is relatively insensitive to the central metal ion. This fact, together with the similarity between the SERRS and RR spectra at the blue and green excitation wavelengths, lends further credence to the use of SERRS as a method of choice for observing vibrational spectra of Chl *a* when excited within the Q_y transition. The SERRS spectrum provides unique insights regarding the electronic properties of this state and this technique should be useful for obtaining resonance excitation profiles within the lowest energy transition.

Resonance Raman spectroscopy has been used extensively for the study of a variety of photosynthetic preparations,[43] as well as for characterizing the isolated chlorophylls. The goal of these studies has been to provide structural information regarding the organization of the chlorophylls within the photosynthetic membrane. Such information elucidates the mechanistic role of these important pigments in the photosyn-

thetic processes (i.e., light harvesting and electron transfer steps). The results presented herein suggest that SERRS offers a viable approach for the study of intact photosynthetic preparations. Our previous studies of reaction centers[44] and chromatophore preparations[45] have already demonstrated that SERRS studies of designated membrane components are feasible. In addition to the fluorescence quenching advantage, SERRS provides extremely high sensitivity, thereby minimizing the amount of material required for spectral analysis. The distance sensitivity can be used to obtain information concerning the spatial relationship of various components to the membrane surface. Finally, the ability to control the potential at an electrode surface suggests that SERRS may also be useful for determining spectra at fixed redox states of the reaction center.

ACKNOWLEDGEMENT

Ames laboratory is operated for the U.S. Department of Energy by Iowa State University under contract no. W-7405-Eng-82. This article was supported by the Division of Chemical Sciences, Office of Basic Energy Sciences.

REFERENCES

1. Johnson, B. B.; Peticolas, W. Annu. Rev. Phys. Chem. **1976**, 27, 465-491.
2. Spiro, T. G.; Stein, P. Annu. Rev. Phys. Chem. **1977**, 28, 501-521.
3. Felton, R. H.; Yu, N. -T. In The Porphyrins; Dolphin, D., Ed.; Academic Press: New York, 1978; Vol. II, pp 341-388.
4. Spiro, T. G. In Iron Porphyrins; Lever, A. B. P., Gray, H. B., Eds.; Addison-Wesley: Reading, MA, 1982; Part II, pp 89-152.
5. (a) Ozaki, Y.; Kitagawa, T.; Ogoshi, H. Inorg. Chem. **1979**, 18, 1772-1776. (b) Ozaki, Y.; Iriyama, K.; Ogoshi, H.; Ochiai, T.; Kitagawa, T. J. Phys. Chem. **1986**, 90, 6105-6112. (c) Ozaki, Y.; Iriyama, K.; Ogoshi, H.; Ochiai, T.; Kitagawa, T. J. Phys. Chem. **1986**, 90, 6113-6118.
6. Ching, Y.; Ondrias, M. R.; Rousseau, D. L.; Muhoberac, B. B.; Wharton, D. C. FEBS Lett. **1982**, 138, 239-244.
7. (a) Andersson, L. A.; Loehr, T. M.; Lim, A. R.; Mauk, A. G. J. Biol. Chem. **1984**, 259, 15340-15349. (b) Andersson, L. A.; Loehr, T. M.; Chang, C. K.; Mauk, A. G. J. Am. Chem. Soc. **1985**, 107, 182-191. (c) Andersson, L. A.; Loehr, T. M.; Sotiriou, C.; Wu, W.; Chang, C. K. J. Am. Chem. Soc. **1986**, 108, 2908-2916. (d) Andersson, L. A.; Sotiriou, C.; Chang, C. K.; Loehr, T. M. J. Am. Chem.

Soc. **1987**, 109, 258-264.

8. (a) Cotton, T. M.; Timkovich, R.; Cork, M. S. FEBS Lett. **1981**, 133, 39-44. (b) Cotton, T. M.; Van Duyne, R. P. J. Am. Chem. Soc. **1981**, 103, 6020-6026. (c) Cotton, T. M.; Parks, K. D.; Van Duyne, R. P. J. Am. Chem. Soc. **1980**, 102,6399-6407.

9. (a) Fujiwara, M.; Tasumi, M. J. Phys. Chem. **1986**, 90, 250-255. (b) Fujiwara, M.; Tasumi, M. J. Phys. Chem. **1986**, 90, 5646-5650.

10. (a) Lutz, M. In Advances in Infrared and Raman Spectroscopy; Clark, R. J. H., Hester, R. E., Eds.; John Wiley & Sons: New York, 1984; Vol. 11, pp 211-300. (b) Robert, B.; Lutz, M. Biochemistry **1986**, 25, 2303-2309. (c) Lutz, M.; Hoff, A. L.; Brehamet, L. Biochim. Biophys. Acta **1982**, 679, 331-341. (d) Lutz, M. J. Raman Spectrosc. **1974**, 2, 497-516. (e) Lutz, M.; Breton, J. Biochem. Biophys. Res. Commun. **1973**, 53, 413-418.

11. Heald, R. L.; Callahan, P. M.; Cotton, T. M. J. Phys. Chem. **1988**, 92, 4820-4824.

12. Hildebrandt, P.; Spiro, T. G. J. Phys. Chem. **1988**, 92, 3355-3360.

13. (a) Boldt, N. J.; Donohoe, R. J.; Birge, R. R.; Bocian, D. F. J. Am. Chem. Soc. **1987**, 109, 2284-2298; (b) Donohoe, R. J.; Atamian, M.; Bocian, D. F. J. Phys. Chem. **1989**, 93, 2244-2252.

14. Mattioli, T. A.; Haley, L. V.; Koningstein, J. A. Chem.

Phys. **1990**, 140, 317-329.

15. Fonda, H. N.; Babcock, G. T. In Progress in Photosynthesis Research; Biggens, J., Ed.; Martinus Nijhoff: Boston, 1987; Vol. I, pp 449-452.
16. Cotton, T. M.; Loach, P. A.; Katz, J. J.; Ballschmiter, K. Photochem. Photobiol. **1978**, 27, 735-749.
17. Lutz, M.; Kleo, J.; Gilet, R.; Henry, M.; Plus, R.; Leicknam, J. P. In Proceedings of the 2nd International Conference on Stable Isotopes; Klein, E. R., Klein, P. D., Eds.; U.S. Department of Commerce: Springfield, VA, 1975; pp 462-469.
18. Nabedryk, E.; Leonard, M.; Mantele, W.; Breton, J. Biochemistry **1990**, 29, 3242-3247.
19. Höxtermann, B.; Werncke, W.; Tscho, J. T.; Lau, A.; Hoffmann, P. Studia Biophys. **1986**, 115, 85-94.
20. Weitz, D. A.; Garoff, S.; Gersten, J. I.; Nitzan, A. J. Chem. Phys. **1983**, 78, 5324-5338.
21. Cotton, T. M.; Schultz, S. G.; Van Duyne, R. P. J. Am. Chem. Soc. **1980**, 102, 7960-7962.
22. Gersten, J. I.; Nitzan, A. J. Chem. Phys. **1980**, 73, 3023-3037.
23. Kerker, M.; Wang, D. S.; Chew, H. Appl. Opt. **1980**, 19, 4159-4174.
24. Ferrell, T. L. Phys. Rev. B: Condens. Matter; **1982**, 25, 2930-2932.

25. Furtak, T. E. J. Electroanal. Chem. Interfacial Electrochem. **1983**, 150, 375.

26. Otto, A. In Light Scattering in Solids; Cardona, M., Gunthrodt, G., Eds.; Springer-Verlag: Berlin, 1984; Vol.IV, pp 289-461.

27. Cotton, T. M. In Spectroscopy of Surfaces; Clark, R. J. H., Hester, R. E., Eds.; John Wiley & Sons: New York, 1988; Vol.16 pp. 91-153.

28. Koglin, E. ; Sequaris, J. -M. In Topics in Current Chemistry; Springer-Verlag: Berlin, 1986; Vol. 134, pp. 1-53.

29. Nabiev, I.; Efremov, R. G.; Chumanov, G. D. Sov. Phys. Usp. **1988**, 31, 241-262.

30. Uphaus, R. A.; Cotton, T. M.; Möbius, D. Thin Solid Films; **1986**, 132, 173-185.

31. Andersson, L. A.; Loehr, T. M.; Cotton, T. M.; Simpson, D. J.; Smith, K. M. Biochim. Biophys. Acta **1989**, 974, 163-179.

32. Strain, H. H.; Svec, W. A. In The Chlorophylls; Vernon, L. P., Seely, G. R., Eds.; Academic: New York, 1966; pp 21-66.

33. Weiss, C. In The Porphyrins; Dolphin, D., Ed.; Academic: New York, 1978; Vol. III, p. 216.

34. Weiss, C. J. Mol. Spectrosc. **1972**, 44, 37-80.

35. Petke, J. D.; Maggiora, G. M.; Shipman, L.; Christofferson, R. E. Photochem. Photobiol. **1979**, 30,

203-223.

36. Shipman, L. L.; Cotton, T. M.; Norris, J. R.; Katz, J. J. J. Am. Chem. Soc. **1976**, 98, 8222-8230.

37. Fragata, M.; Norden, B.; Kurucsev, T. Photochem. Photobiol. **1988**, 47, 133-143.

38. Otto, A. Appl. Surf. Sci. **1980**, 6, 309-355.

39. Van Duyne, R. P. In Chemical and Biochemical Applications of Lasers; Moore, C. B., ed.; Academic Press: New York, 1979; Vol. IV, p 101.

40. Moskovits, M. J. Chem. Phys. **1982**, 77, 4408-4416.

41. Schick, G. A.; Schreiman, I. C.; Wagner, R. W.; Lindsey, J. S.; Bocian, D. F. J. Am. Chem. Soc. **1989**, 111, 1344-1350.

42. Soriaga, M. P.; Hubbard, A. T. J. Am. Chem. Soc. **1982**, 104, 3937-3945.

43. Lutz, M.; Robert, B. In Spectroscopy of Biological Molecules; Alix, A. J.P., Bernard, L., Manfait, M., Eds.; Wiley: New York, 1985; pp. 310-318.

44. Cotton, T. M.; Van Duyne, R. P. FEBS Lett. **1982**, 147, 81-84.

45. (a) Picorel, R.; Holt, R. E.; Cotton, T. M. ; Seibert, M. In Progress in Photosynthesis Research; Biggins, J., Ed.; Martinus Nijhoff Publishers: The Netherlands, 1987; pp. 1.4 423-426; (b) Picorel, R.; Holt, R. E.; Cotton, T. M.; Seibert, M. J. Biol. Chem. **1988**, 263, 4374-4380; (c) Seibert, M.; Cotton, T. M.; Metz, J. G. Biochim.

Biophys. Acta 1988, 934, 235-246; (d) Picorel, R.; Lu, T.; Holt, R. E.; Cotton, T. M.; Seibert, M. Biochem. 1990, 29, 707-712.

SECTION 2. A SURFACE-ENHANCED RESONANCE RAMAN SCATTERING STUDY OF PHEOPHYTIN *a* ON A ROUGHENED SILVER ELECTRODE: EFFECTS OF EXCITATION FROM THE SORET THROUGH THE RED.

ABSTRACT

A roughened silver electrode was employed to record surface-enhanced resonance Raman scattering (SERRS) spectra for pheophytin a using 406.7, 457.9, 476.2, 514.5, 530.9, and 647.1 nm excitation. SERRS spectra were recorded at liquid nitrogen temperature to minimize sample photodegradation and fluorescence. The agreement between the pheophytin a resonance Raman (RR) and SERRS spectra not only indicates that the major source of the surface enhancement is due to an electromagnetic mechanism rather than a chemical mechanism, but also provides evidence that pheophytin a does not undergo any structural changes after adsorption at the electrode surface. Each excitation wavelength provides a distinctive SERRS spectrum. Adsorption of Pheo a on the roughened silver at low temperature reduced the fluorescence sufficiently to reveal a unique low frequency region with red excitation. Thus, SERRS, in combination with selective excitation within the various electronic transitions, can be utilized to monitor the photochemical and electrochemical behavior of pheophytin a *in vitro* and *in vivo* at an electrode surface.

INTRODUCTION

In green plants and blue-green algae photosynthesis converts sunlight into chemical energy via photoinduced charge separation and electron-transfer within photosystems I and II (PS I and PS II, respectively). Upon absorption of light photosynthesis begins with the photooxidation of the primary donor within the photosystem reaction center and ends with the fixation of carbon dioxide and the release of oxygen. A more detailed account of the photosynthetic processes within PS I[1] and PS II[2] has been reported recently.

Much more is known about PS II than PS I due to the similarity in structure and function of PS II to the well studied bacterial reaction center.[3] The primary charge separation occurs within the PS II reaction center with a specialized chlorophyll *a* molecule acting as the primary electron donor which transfers an electron to pheophytin *a*, the primary electron acceptor. Although many similarities exist between the PS II and the bacterial reaction center considerable additional information is needed to provide a detailed picture of the events responsible for photoinduced charge separation within the reaction center. The first step is to develop an understanding of the role of each separate constituent involved in the charge separation and electron-transfer events. This necessitates determining the consequences of electron transfer on the individual chlorophyll *a* (Chl *a*), pheophytin *a* (Pheo *a*), and their associated proteins.

Resonance Raman (RR) spectroscopy has proven to be a viable tool for studying the chlorophylls[4a,b,5-10] and pheophytins.[4a,c,6b] RR spectroscopy provides a vibrational "fingerprint" that identifies the molecule. Infrared (IR) studies also supply a vibrational spectrum but this method is plagued by strong water absorption in biological samples. Observation of low frequency modes below 400 cm^{-1} is also difficult with IR. Another advantage of RR is the selectivity gained by using an excitation wavelength that is within an electronic transition of the molecule. Thus, by selecting one wavelength of excitation over another it is possible to monitor a single type of molecule within the reaction center.

In spite of the selectivity and sensitivity that RR offers it is often troubled by fluorescence interference. Surface-enhanced resonance Raman spectroscopy (SERRS) has proven to be an effective technique for acquiring spectra of fluorescent molecules. Previous SERRS studies in the past of chlorophylls[11,12,14] and chlorophyll derivatives[11,12,13] have demonstrated that it is possible to obtain spectra using silver island films and silver sols as the substrates. Metal electrodes are preferable for SERRS studies of photosynthetic systems and pigments because electrogenerated species can be created and monitored with minimal sample manipulation and interference.

Ideally, one would like to monitor selectively Chl *a*, the primary electron donor, or Pheo *a*, the primary electron accep-

tor, within the PS II reaction center with the goal of identifying the transient species formed during photoexitation. To realize this goal the individual° SERRS spectra of Chl _a_ and Pheo _a_ must be recorded by selecting excitation wavelengths that correspond to electronic transitions in the electronic absorption spectrum of each molecule. This information would establish excitation wavelengths that enhance the spectrum of one molecule over the other. Recently, Thomas et al.[14] reported SERRS spectra of Chl _a_ on a roughened Ag electrode with excitation wavelengths ranging from the violet to the red regions of the electromagnetic spectrum. It is equally important to use SERRS to observe Chl _a_ and Pheo _a_ individually while controlling the potential at the electrode surface. RR and FTIR difference spectroscopy have been used to provide spectra of the Chl _a_ cation radical[7,15] and the Pheo _a_ anion radical[16-19], but the RR spectra are weak and the IR spectra provide no selectivity. The SERRS spectrum of Pheo _a_ and the Pheo _a_ anion radical have been reported by Heald[19] with 406.7 nm excitation on a roughened Ag electrode. Heald found the SERRS spectrum is much stronger than the RR spectrum and no structural alteration of Pheo _a_ occurred upon adsorption at the electrode surface. These results demonstrate the utility of SERRS for studing photosynthetic pigments and their electrochemical properties.

In the results reported here SERRS spectra of Pheo _a_ were obtained on a roughened Ag electrode at 77 K with various

excitation wavelengths. The agreement between the RR and SERRS spectra indicate that Pheo a interacts weakly with the electrode surface and that it is not structurally altered as a result of adsorption at the electrode surface. The intensity changes that occur in the SERRS spectrum with excitation wavelength indicate changes in mode enhancements and these provide insights regarding the structural changes in the molecule that accompany electronic excitation.

EXPERIMENTAL

Pheophytin a preparation. Pheo a (Figure 2-1) was prepared by acidification of chlorophyll a with HCl. Chlorophyll a was isolated from spinach extract according to an established procedure.[20] Chlorophyll a and Pheo a were purified by reverse phase high performance liquid chromatography (rp-HPLC).[14]

For RR experiments the purified Pheo a was dissolved in methylene chloride (ca. 1 mg/100μl). This solution was transferred to a 5mm o.d. Pyrex tube and the solution was evaporated with nitrogen gas. The Pheo a formed a thin film on the tube walls. The tube was sealed under vacuum. For SERRS experiments Pheo a was adsorbed onto an electrochemically roughened electrode [14] by dipping the electrode in the purified Pheo a solution (ca. 1 x 10^{-4} M in acetonitrile/methanol 3:1 v/v) for 20 minutes. All sample manipulation and experimental operations were performed in subdued light.

The purity of Pheo a was monitored and confirmed before and after the Raman experiments by analytical rp-HPLC[14] and UV/VIS spectroscopy. Electronic absorption spectra were measured using a 1 mm pathlength cuvette and a Perkin Elmer Lambda 6 UV/VIS spectrophotometer.

RR and SERRS spectroscopy. The instrumentation and experimental conditions for collecting, processing, and recording the Raman and surface Raman scattering has been

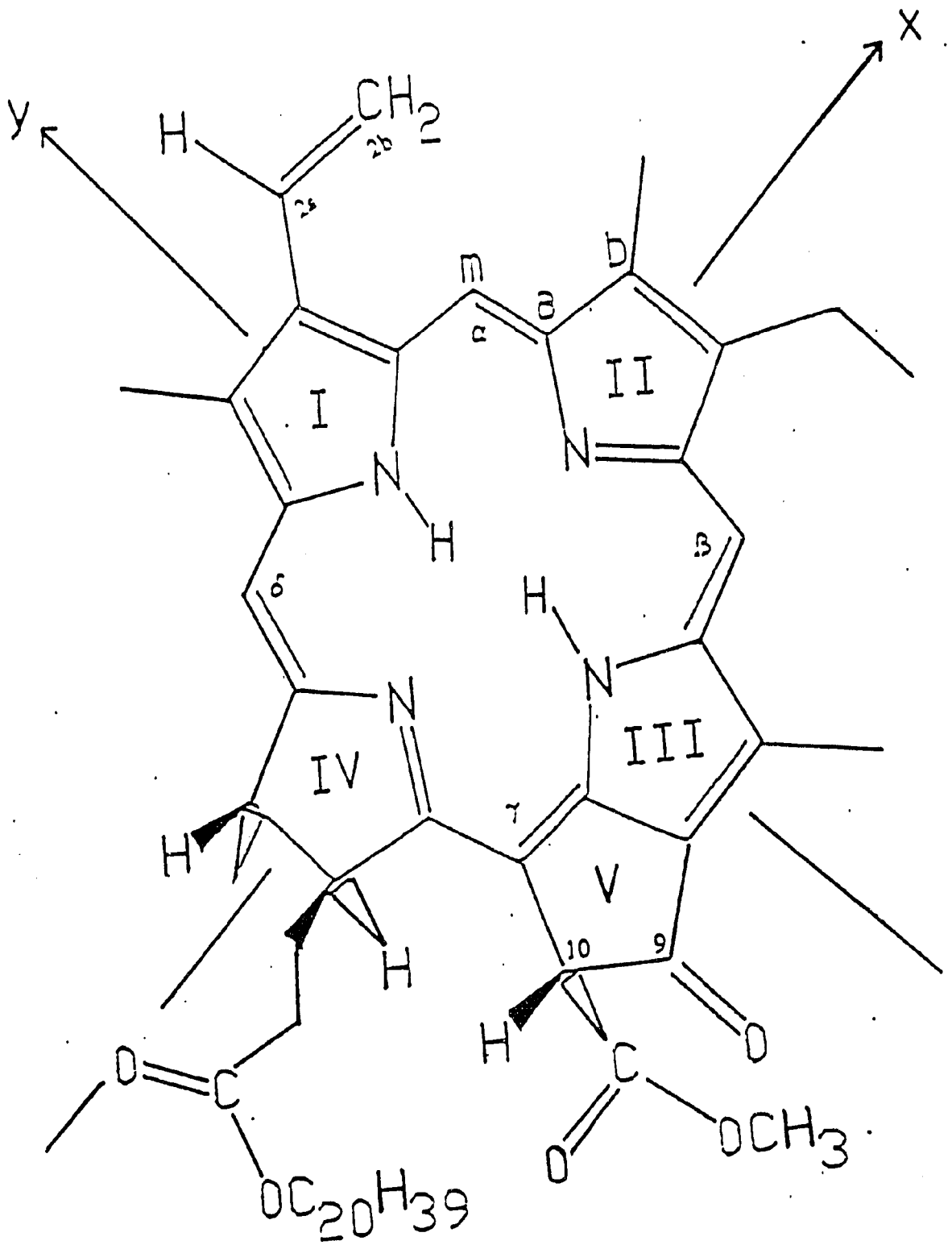

Figure 2-1. Structure of Pheo a.

described elsewhere.[14] The reported spectra are composites of 25 scans with 10 second and 1 second integration periods per scan for the RR and SERRS spectra, respectively at 406.7 and 457.9 nm excitation. At 514.5 nm excitation the SERRS data was obtained using a 5 second integration period per scan. Raman spectra obtained with excitation at 476.2 and 530.9 nm (provided by a Coherent Innova Kr^+ laser) are composites of 15 scans with 10 second and 3 second integration periods per scan for the RR and SERRS spectra, respectively. The SERRS spectrum recorded with 647.1 nm excitation is a composite of 15 scans with 5 second integration period per scan. The laser power was 25 and 10 mW for RR and SERRS samples, respectively.

RESULTS

Electronic Absorption Spectroscopy. Figure 2-2 shows the electronic absorption spectrum of Pheo a. The arrows indicate the excitation wavelengths used in the Raman experiments. The absorption spectrum agrees with those previously reported.[20,21] According to linear dichroism results, Fragata et al.[21] assign the maximum at 409 nm as the B transition with both X and Y contributions. At 395 nm the polarization is at 40 degrees and at 416 nm the polarization is at 50 degrees (angles are clockwise from X-axis of the molecular framework as represented in Figure 2-1). The bands at 470, 535 and 605 nm have major contribution from the $Q_{X(0,0)}$ transition. The $Q_{Y(0,0)}$ transition is assigned as a major contributor 506 and 665 nm bands. However, a small contribution from the $Q_{X(0,0)}$ transition is assigned at 660 nm. Thus, the band at 665 nm maximum is comprised of both the $Q_{X(0,0)}$ and $Q_{Y(0,0)}$ transitions.

Raman Spectroscopy. Figures 2-3 through 2-7 are RR (298 K) versus SERRS (77 K) spectra. The uncertainty of the assignments is ±5 cm^{-1}. The low frequency region is not shown due to the fact that the Raman spectrum from the glass sample tube obscured the Raman signal from Pheo a. The excitation wavelengths used in the Raman experiments are indicated in the figure legends. The spectra agree with those reported in the past and are consistent with Franck-Condon activity of in-plane ring modes in resonance with the strongly allowed B transition.[4a,6,19] Attempts to obtain a RR spectrum with red

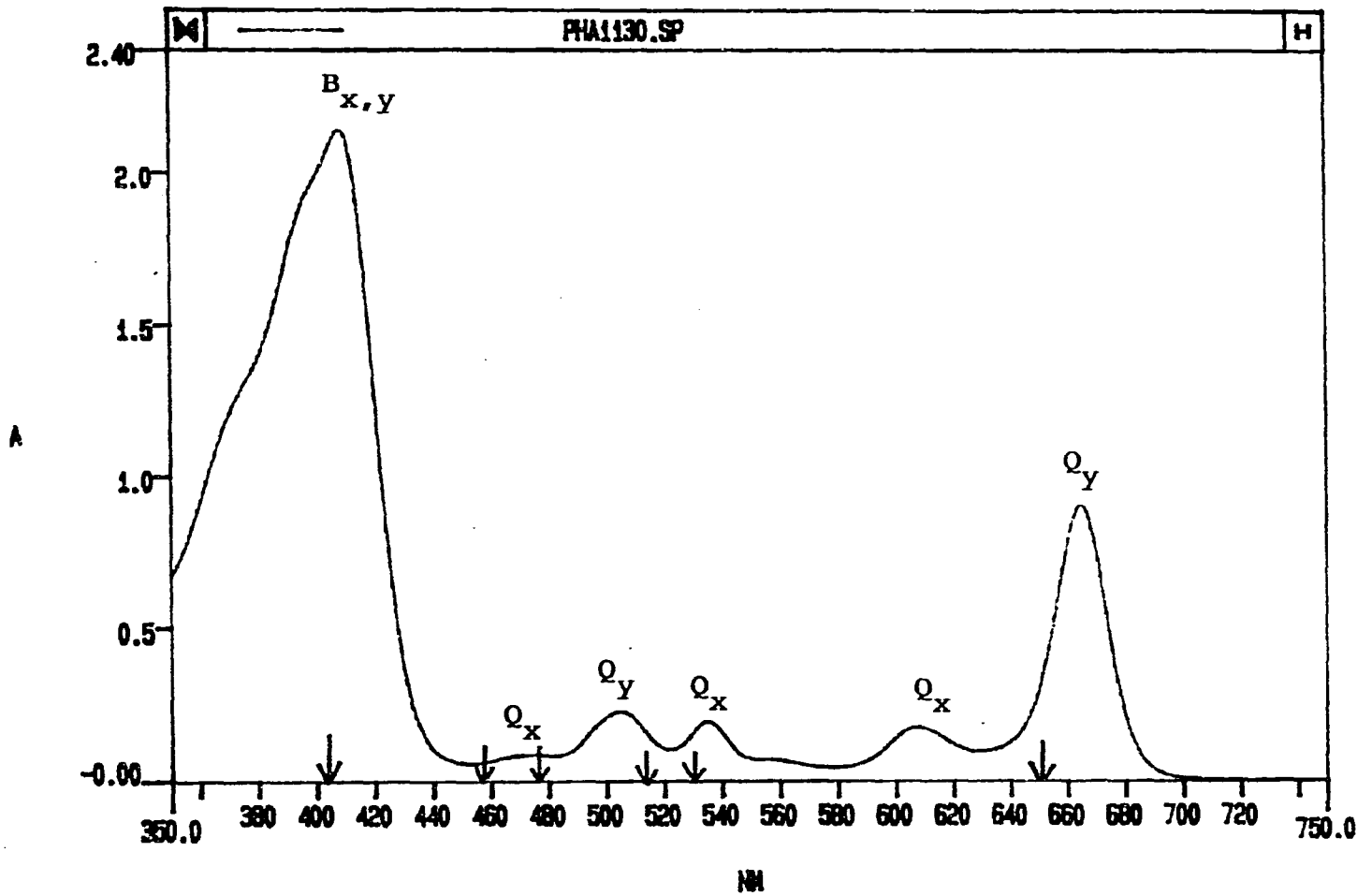

Figure 2-2. Absorption spectrum of Pheo a in ACN/MeOH (3:1 v/v).

excitation were unsuccessful due to fluorescence interference.

Figures 2-8 and 2-9 display the SERRS spectra obtained with excitation wavelengths from the violet to the red region of the electromagnetic spectrum. Most significantly, at 77 K the fluorescence was quenched at the roughened Ag electrode and sample photooxidation was minimized permitting acquisition of a SERRS spectrum with red excitation. A SERRS spectrum of Pheo a was attempted with 676.2 nm excitation but the Raman signal was too weak and the fluorescence overwhelmed the spectrum. It may be that at this excitation wavelength the resonance enhancement is minimal.

Table 2-1 lists the major SERRS bands and their vibrational assignments. Lutz[4a] found that the wavenumbers of the Raman-active modes for pheophytins are within ca. 10 cm^{-1} of the corresponding bands in the chlorophylls. Thus, the vibrational assignments are based primarily on the recent normal mode analysis by Boldt et al.[22]

Table 2-1. Average values of the Major SERRS (77K) Frequencies (cm^{-1}) for Pheo a using Soret through Red excitation.

cm^{-1}	Assignment[a]	cm^{-1b}
1694	$\upsilon C_9=O$	910
1620	$\upsilon C_aC_m(\alpha,\beta)$; $\upsilon C_{2a}=C_{2b}$ vinyl	900
1585	υC_aC_b(III); C_bC_b(I)	835
1558	υC_bC_b(I); υC_aC_b(III)	792
1502	υC_aC_b(I); $C_aC_m(\gamma)$	772
1448	$\upsilon C_aC_m(\gamma,\delta)$; υC_aC_b(I-III)	745
1408	υC_aC_b(II); $\upsilon C_aC_m(\alpha,\delta)$	730
1364		713
1352	υC_aN(IV); υC_aN(I,III)	677
1304	υC_aN(II); $\delta C_mH(\alpha)$; [b] δCH_2	618
1225	δC_bH(IV); $\delta C_mH(\delta)$	562
1160	υC_aN(IV);$\delta C_aC_mC_a(\alpha,\beta,\gamma,\delta)$	460
1131	υC_aC_b(IV);$\delta C_aC_mC_a(\alpha,\beta,\gamma)$	370
1123	υC_aC_b(IV); υC_bS	345
1037	υC_aN(III); υC_bS	250
982	υC_mC_aN(III); υC_9C_{10}(V)	

[a]Assigments based on those reported by Lutz[4a,22]. C_a, C_b, C_m and characters in parentheses refer to the macrocycle positions shown in Figure 2-1. Mode descriptions are υ=stretch and δ=in-plane deformation.
[b]No assignments have been reported for bands below 980 cm^{-1}.
[c]Vinyl scissors[23].

DISCUSSION

RR versus SERRS. 406.7 nm excitation (Figure 2-3). The bands in the 1490-550 cm^{-1} region have the same relative intensities in the RR and in SERRS spectra, but the bands are sharper and better resolved in the SERRS spectra. However, with the exception of the $\nu C_9{=}O$ at 1696 cm^{-1}, the 1700-1490 cm^{-1} frequency region contains several bands that are more intensite in the SERRS spectrum. In the SERRS spectrum the major band at 1587 cm^{-1} (νC_aC_b (III); νC_bC_b (I)) is much narrower with the 1617 cm^{-1} band (νC_aC_m (α, β)) and 1560 cm^{-1} band (νC_bC_b (I); νC_aC_b (III)), which are not resolved in the RR spectrum, appearing as distinct shoulders. Also, the intensity of the 1502 cm^{-1} band (νC_aC_b (I); νC_aC_m (γ)) increases threefold and the 1404 cm^{-1} band (νC_aC_b (II); νC_aC_m (α,δ) twofold in the SERRS spectrum.

457.9 nm excitation (Figure 2-4). As with 406.7 nm excitation, the most strongly enhanced region with 457.9 nm excitation is 1700-1490 cm^{-1}. While the 1692 cm^{-1} band ($\nu C_9{=}O$) remains the same, the 1583 cm^{-1} is narrower and the broad shoulder in the RR spectrum at 1619/1605 cm^{-1} is a distinct band at 1622 cm^{-1} in the SERRS spectrum. Also, no band is present at 1502 cm^{-1} in the RR spectrum, but one appears in the SERRS spectrum. Below 1490 cm^{-1} the relative intensities of all bands match between the RR and SERRS spectra.

476.2 nm excitation (Figure 2-5). With excitation further into the blue green the $\nu C_9{=}O$ band is very weak. As

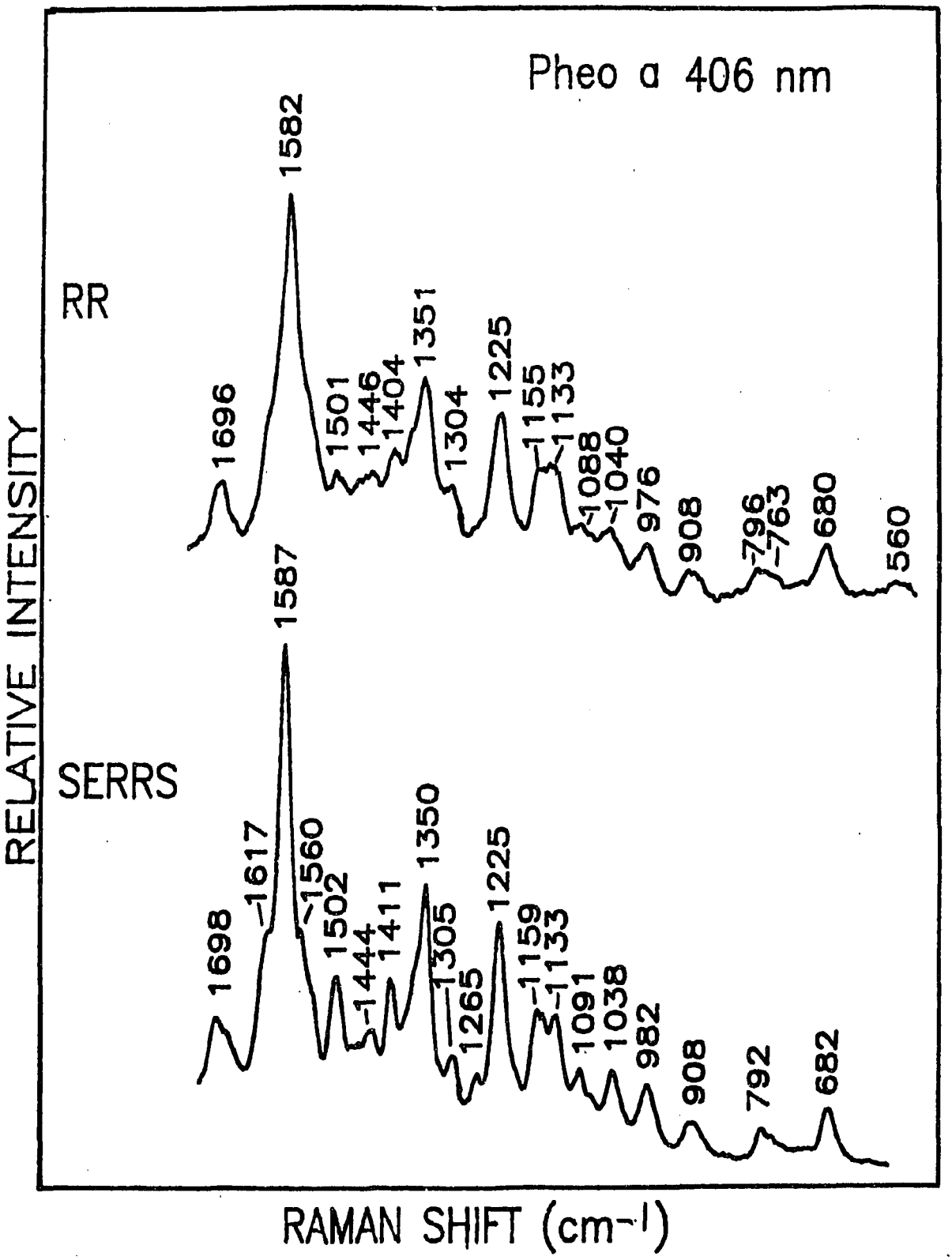

Figure 2-3. RR and SERRS of Pheo a at 406.7 nm excitation.

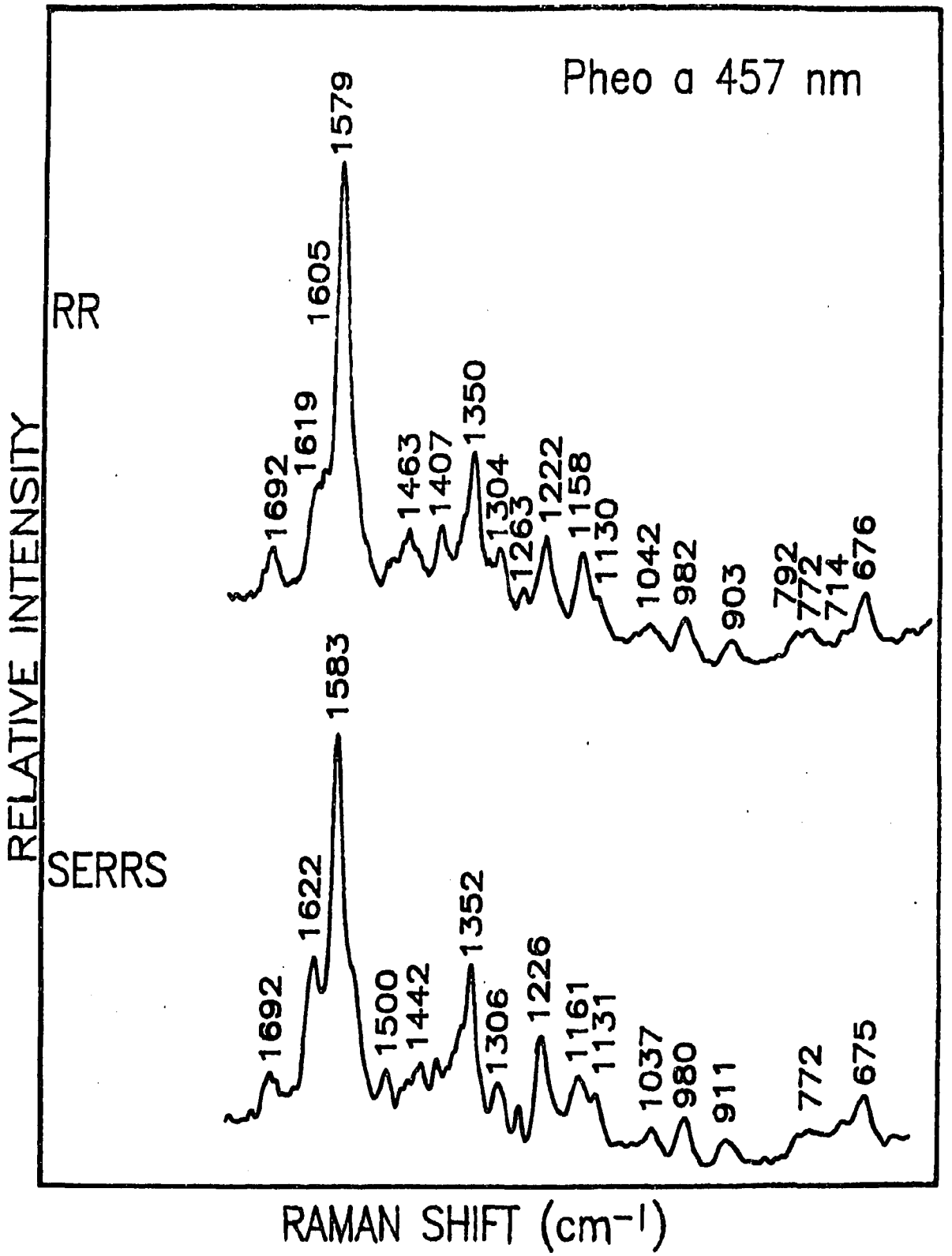

Figure 2-4. RR and SERRS of Pheo a at 457.9 nm excitation.

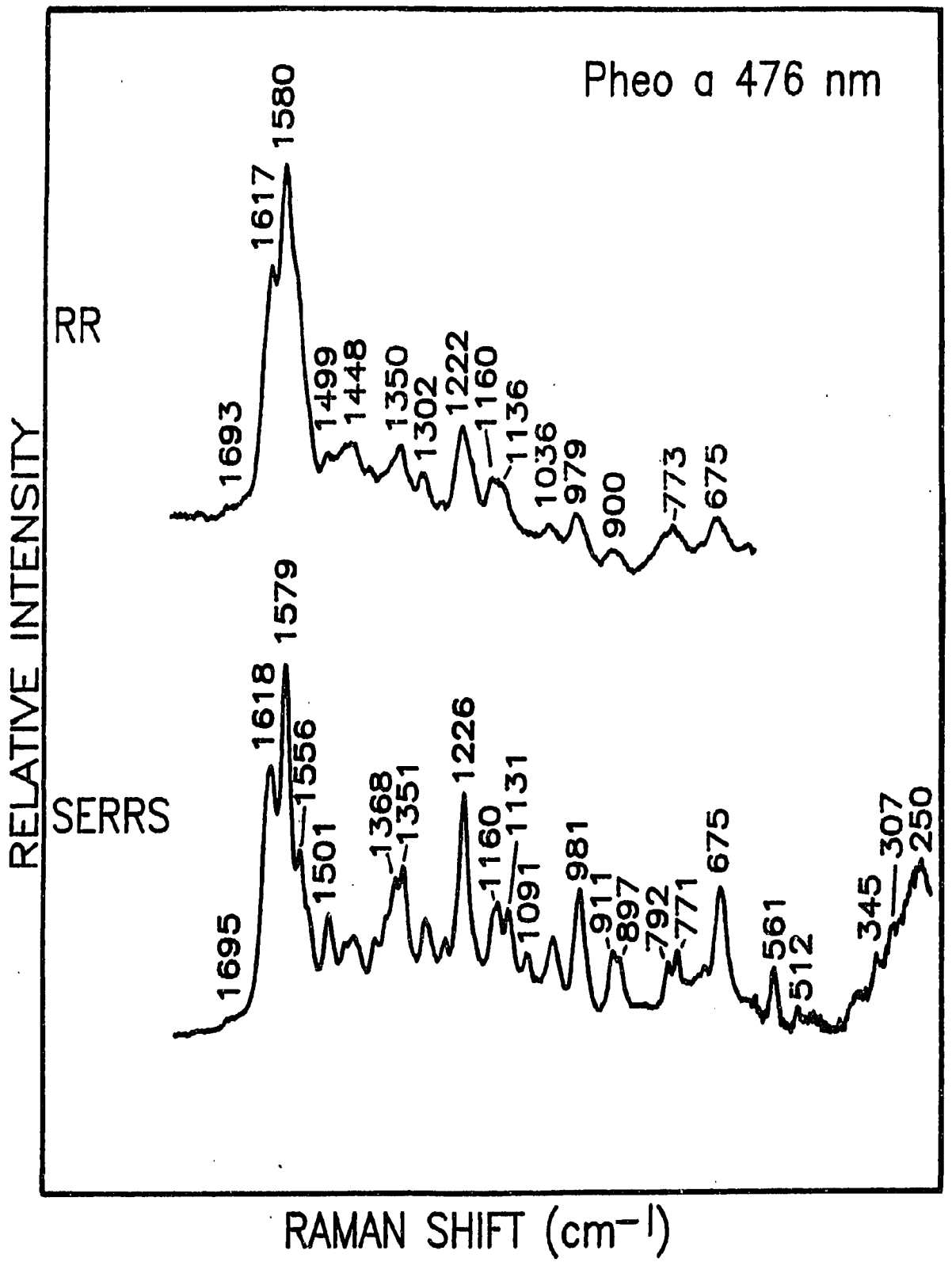

Figure 2-5. RR and SERRS of Pheo a at 476.2 nm excitation.

in the case of 457.9 nm excitation, the 1617 and 1502 cm^{-1} bands are more enhanced in the SERRS than in the RR spectrum. In contrast to 457.9 nm excitation, there is a definite peak on the shoulder of the 1579 cm^{-1} band at 1556 cm^{-1} in the SERRS spectrum. Also, the 1350 and 900 cm^{-1} bands in the RR spectrum split in the SERRS spectrum producing bands at 1368/1351 cm^{-1} and 911/897 cm^{-1}. Overall, all bands are much sharper in the SERRS spectrum than in the RR spectrum. In addition, excitation at 476.2 nm enhancess low frequency modes in the SERRS spectrum.

514.5 nm excitation (Figure 2-5). The most noticeable effect on changing from blue green to green excitation is the loss of the $\nu C_9=O$ vibration at ca. 1693 cm^{-1} in both the RR and SERRS spectra. As with Soret and blue excitation the 1585 and the 1612/1615 cm^{-1} bands sharpen with 514.5 nm excitation. However, unlike blue excitation, the 1556 cm^{-1} shoulder in the RR spectrum disappears in the SERRS spectrum. Also, in the RR spectrum the 1408 cm^{-1} band (υC_aC_b (II); υC_aC_m (α, δ)) is more intense than the 1353 cm^{-1} band (υC_aN (IV); υC_aN (I, III)), but the reverse is true in the SERRS spectrum. Futhermore, spectra obtained with 514.5 nm excitation differ substantially from those obtained with blue excitation in that in the 1490-500 cm^{-1} region the SERRS spectrum has many peaks that increase in intensity as compared to their RR counterparts. The bands at 1408, 1303, and 1224 cm^{-1} are strongest in the RR spectrum. However, in the SERRS spectrum the bands at 1358, 1223, and

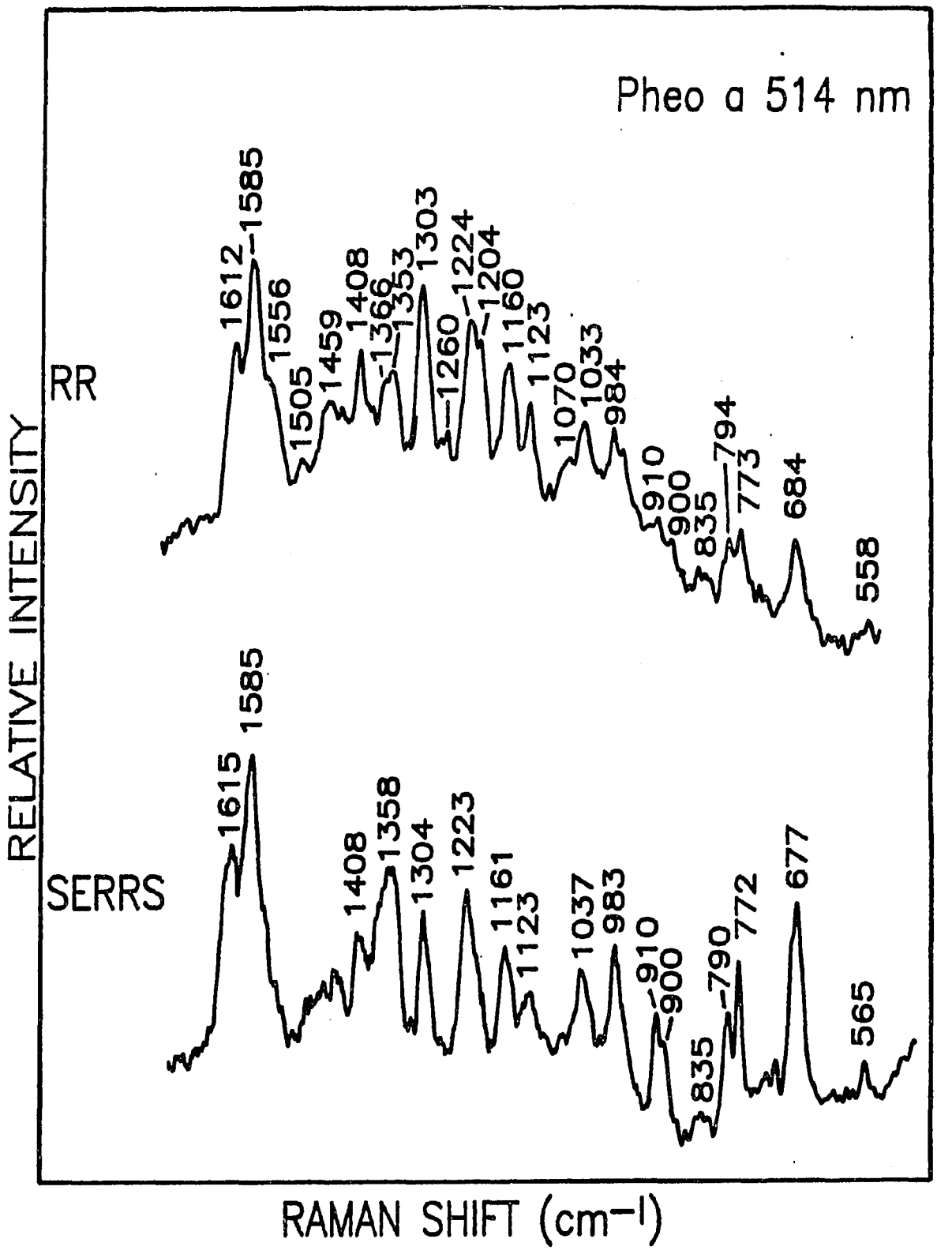

Figure 2-6. RR and SERRS of Pheo a at 514.5 nm excitation.

677 cm^{-1} are the strongest with all having approximately the same relative intensity. These bands correspond to pyrrole stretching and deformation modes.

530.9 nm excitation (Figure 2-6). As with 514.5 nm excitation, no carbonyl band is present at ca. 1693 cm^{-1} in either the RR or the SERRS spectrum. Several relative intensity changes can be seen on comparing the RR and SERRS, with the most obvious differences occurring in the 1620 to 1450 cm^{-1} region. In the RR spectrum the 1619 and 1557 cm^{-1} bands are shoulders on the dominant 1585 cm^{-1} band. However, in the SERRS spectrum, the 1621 cm^{-1} is now dominant and more intense than the 1587 cm^{-1} band and the 1557 cm^{-1} band is almost equal in intensity to the 1587 cm^{-1} band. The 1502 cm^{-1} band has tripled in intensity in the SERRS spectrum. These bands correspond to the C_aC_b, C_bC_b, and C_aC_m modes of the macrocycle. In the region below 1450 cm^{-1} the RR and SERRS spectra are similar except for the band at 1408 cm^{-1} which loses intensity in the SERRS spectrum. Excitation at 530.9 nm provides considerable detail in the low frequency region in the SERRS spectrum.

Overall, a similar intensity pattern can be seen on comparing the RR and SERRS spectra with excitation at 406.7 and 457.9 nm. The SERRS spectra are clearly surface-enhanced and display sharper, better resolved peaks although only ca. a monolayer of Pheo a is present at the electrode surface. The similarity between the RR and the SERRS spectra is indicative

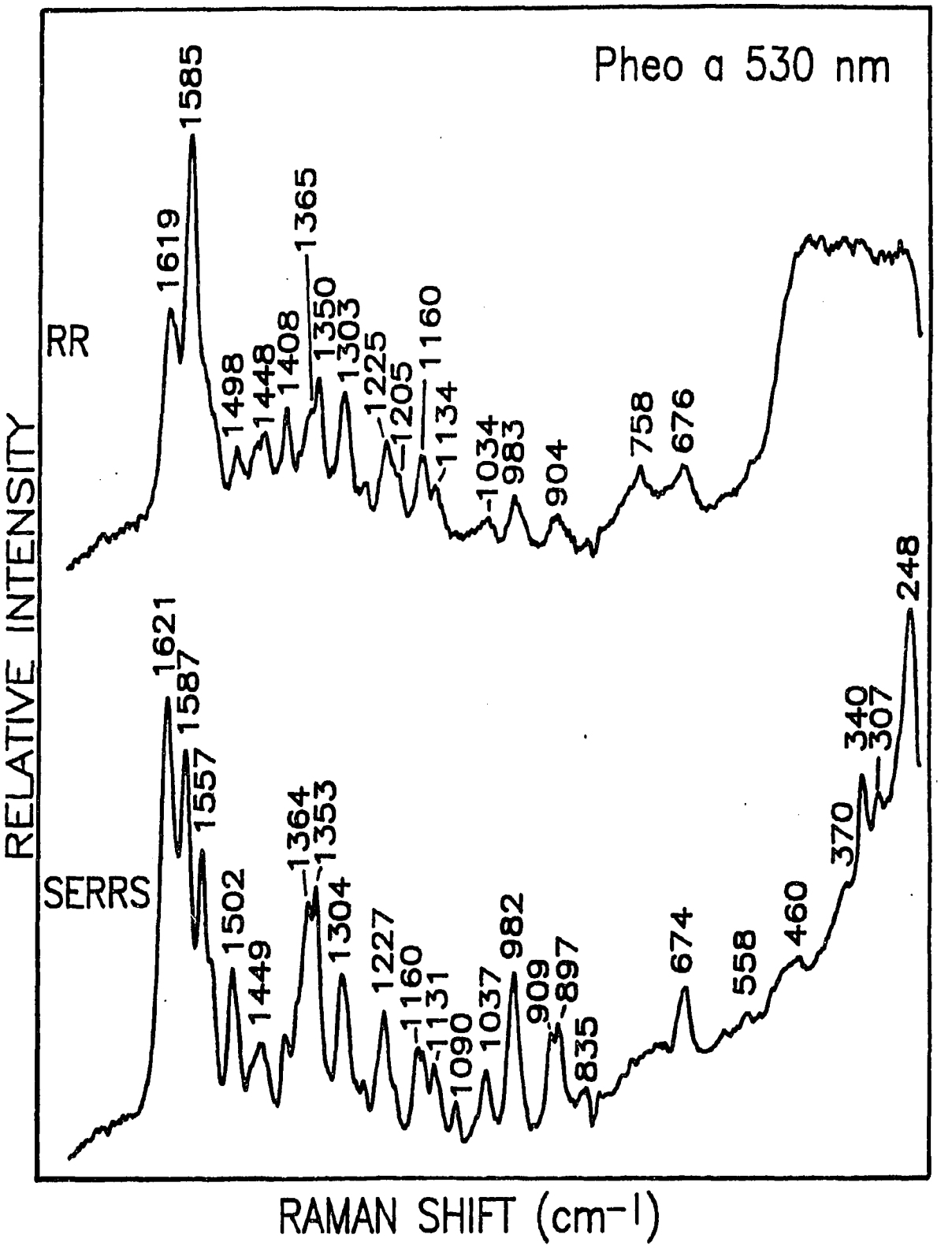

Figure 2-7. RR and SERRS of Pheo a at 530.9 nm excitation.

of an electromagnetic enhancement mechanism.[24-27] Chemical enhancement mechanisms result in significant frequency shifts as well as changes in the relative intensity pattern in the SERRS spectrum as compared to the RR spectrum.[28] The 1620-1500 cm^{-1} region is the most strongly enhanced. This region is characterized by in plane skeletal modes involving C_aC_m, C_aC_b, and C_bC_b vibrations which corresponds to the macrocycle oriented edgewise as was found with Chl _a_.[14] In contrast, the SERRS spectra at excitation wavelengths greater than 457.9 nm, while similar to the RR spectra, have intensity increases for bands at ca. 1620 (υC_aC_m (α, β); $\upsilon C_{2a}=C_{2b}$ vinyl), 1556 (υC_bC_b (I); υC_aC_b (III)), 1502-(υC_aC_b (I); υC_aC_m (γ)), and 1350 cm^{-1} (υC_aN (IV); υC_aN (I, III)). Intensity changes can be correlated with the orientation of bonds with respect to the electrode surface. Surface selection rules predicted by electromagnetic theory determine bonds that have polarizability tensors perpendicular to the electrode surface are preferentially enhanced.[29,30] If Pheo _a_ adsorbs flat at the Ag surface, the polarizability tensors involving stretching vibrations of the pyrrole rings (C_aC_b, C_bC_b, C_aC_m, C_aN) would lie parallel to the surface and these modes should not be strongly enhanced. However, these ring modes (ca. 1620, 1556, 1502, 1350 cm^{-1}) are precisely the ones that experience the greatest enhancement in the SERRS spectra. Thus, these intensity increases can be due to the macrocycle having an edgewise orientation at the electrode surface.

SERRS. Figure 2-8 and 2-9 show SERRS spectra of Pheo a at 77 K excited with various lines ranging from the violet to the red region of the electromagnetic spectrum. A comparison of the SERRS spectra obtained at various excitation wavelengths shows that each spectrum has a distinctive 1700-1500 cm^{-1} region as described in the previous section.

Differences in enhancement patterns are expected from a consideration of the different electronic transitions that are operative under B and Q excitation conditions. A variation in intensity patterns with changes in excitation wavelength was noted in the RR studies of ClFE(III) pheophorbide by Andersson et al.[12] This was also the case in the SERRS studies of copper chlorophyllin on silver and gold colloids by Hildebrandt et al.[13] and in the SERRS studies of chlorophyll a on a roughened silver electrode by Thomas et al.[14] As in both of the SERRS studies cited above, the results of the Pheo a data indicate that the silver surface does not significantly perturb the electronic state of the molecule.

In SERRS spectra obtained with 406.7 through 530.9nm excitation the disappearance of the carbonyl band (ca. 1696 cm^{-1}) is one of the most obvious changes. Another change to be noted is that the band at ca. 1620 cm^{-1} increases in intensity and is the strongest band with 530 nm excitation. Lutz[4a] reported a band that contained a 1625 cm^{-1} component when the RR spectrum of Pheo a was excited with 540 nm light. From linear dichroism spectra of oriented Pheo a, Breton et al.[31]

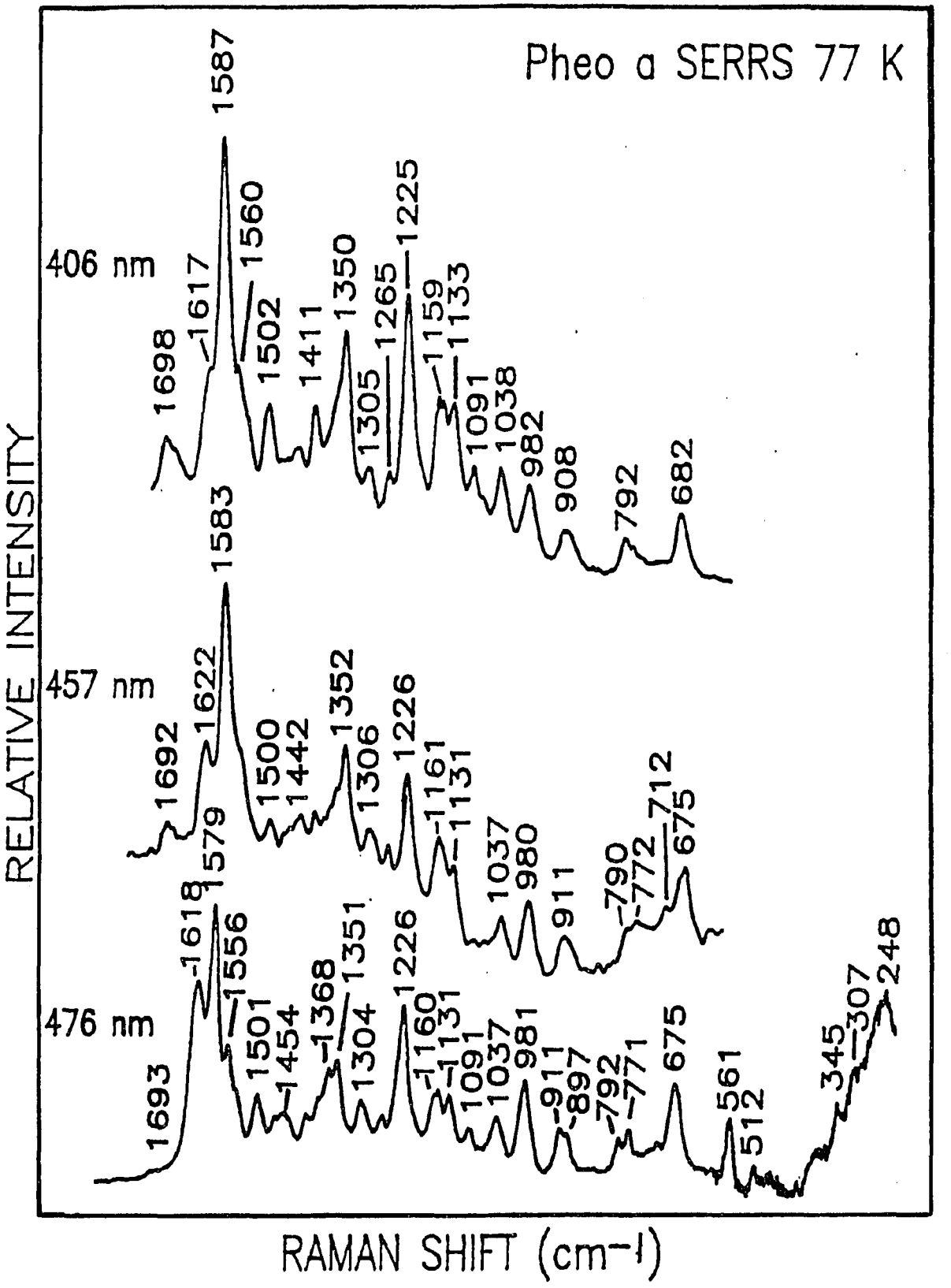

Figure 2-8. SERRS of Pheo a at 77 K.

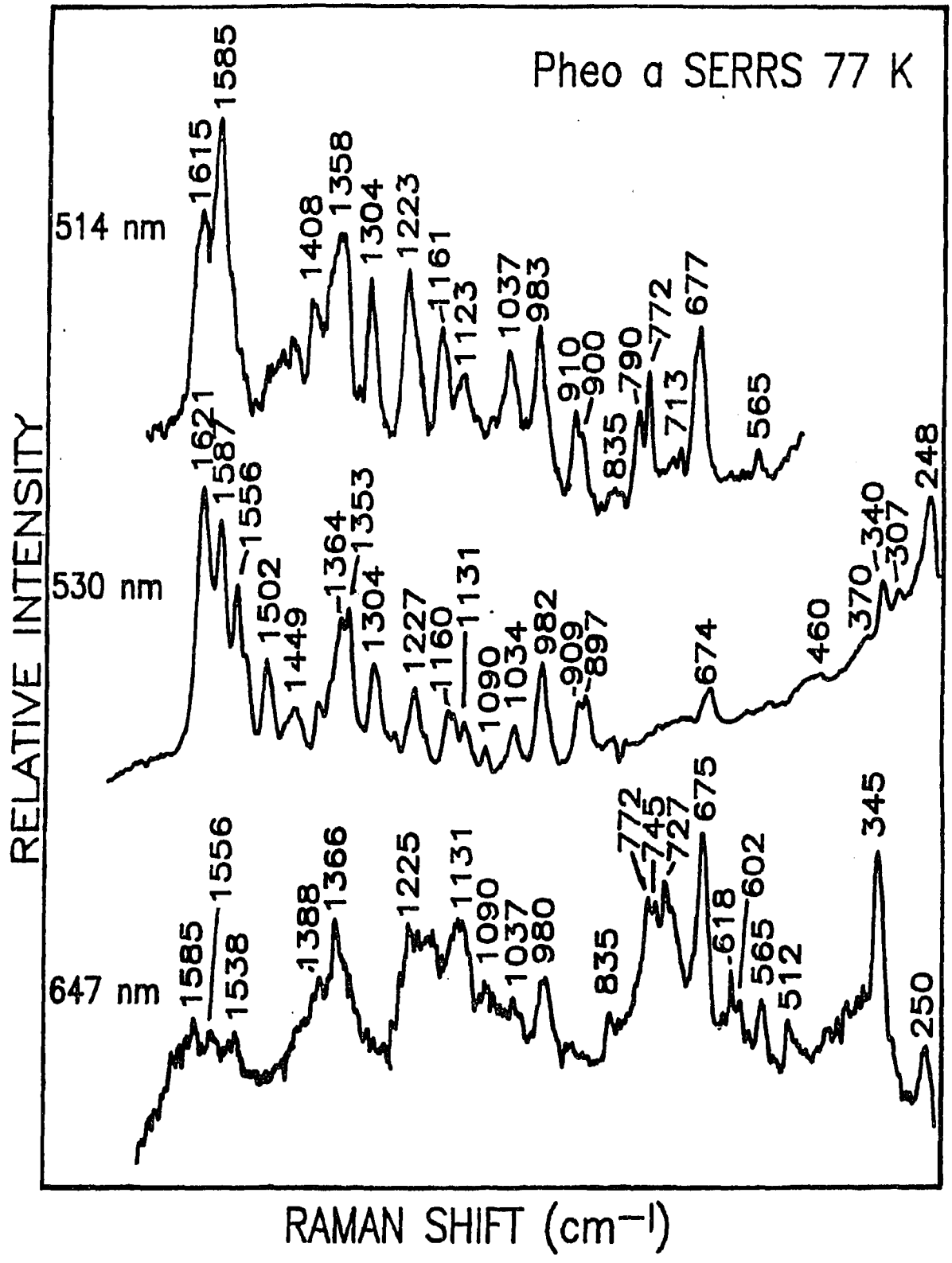

Figure 2-9. SERRS of Pheo a at 77 K.

proposed that the 540 nm electronic band of Pheo a should be polarized out of the phorbin plane forming an angle between 30 and 90 degrees. Based on the fact that the vinyl group of Pheo a is in an out-of-plane orientation[32,33] and the above information, Lutz[4a] proposed that the 1625 cm^{-1} band may involve $\nu C=C$ (vinyl) stretching. Because excitation with 530 nm is within the 540 nm electronic band, the increase in intensity of the 1621 cm^{-1} band may be due to a contribution from the vinyl stretching mode. Additional support for this interpretation is obtained from a consideration of the 1304 cm^{-1} band which also increases in intensity with green excitation and has contributions from δCH_2(vinyl scissors).[22,23] Also, as the excitation wavelength is increased the 1556 (except with 514.5 nm excitation), 1350, and 1304 cm^{-1} bands increase in intensity. In general, excitation with 406, 457, 476, 514 and 530 nm enhances the 1700-1300 cm^{-1} region, excitation with 514 and 530 nm enhances the 1450-650 cm^{-1} region, and excitation with 476, 530, and 647.1 nm enhances the 650-200 cm^{-1} region of the Pheo a Raman spectrum. In the SERRS studies of Chl a on a roughened Ag electrode by Thomas et al.[14] each SERRS spectrum of Chl a excited from the violet to the red region of the electromagnetic spectrum gave a very distinct spectrum in the 1620-1500 cm^{-1} region. The $\nu C_9=O$ band only appeared with 406 nm excitation (at 1684 cm^{-1}). However, unlike Pheo a, Chl a also produces a distinct spectrum at each excitation wavelength for the 1400-1100 cm^{-1} region. This

region involves primarily C_aN modes (I-IV). It appears that the Mg at the center of the macrocycle contributes to the differentiation of the x versus y polarized C_aN stretching modes. Although the Mg is replaced by two hydrogens, the bands found in the 1400-1100 cm^{-1} region of the Pheo a SERRS spectrum change very little with excitation wavelength. This indicates that the x and y polarized C_aN vibrations are more equivalent for Pheo a.

Most important is the information to be gained from the spectrum with red excitation. This is the first report of a Raman spectrum for Pheo a excited within its lowest π-π^* state. With red excitation more of the low frequency region is revealed with bands at 618/602, 512, 345, and 250 cm^{-1}. While some of these bands appear in the SERRS spectra with excitation at 476 and 530 nm, the SERRS intensity pattern is different with red excitation than at those excitation wavelengths. Many of these bands have not been assigned, but are shown to be sensitive to C_aC_b substitution and/or are associated with C_aN vibrations.[4a,22] The absence of the carbonyl band at ca.1696 cm^{-1} is also noteworthy, but the high frequency region is dwarfed by fluorescence interference. Therefore, the bands at 1585, 1556, and 1538, which are stronger at other excitation wavelengths, occur as equivalent weak bands with 647 nm excitation. However, in the SERRS studies of Chl a by Thomas et al.[14] fluorescence was minimal and this region was not as strongly enhanced as the 1200-500

cm^{-1} region either. Thus, the pyrrole macrocyle modes are not as strongly enhanced with 647 nm excitation as with the other excitation wavelengths.

Spectra obtained with excitation at 457, 476, and 530 nm all are strongly coupled to the $Q_{x(0,0)}$ transition and thus, similar intensity patterns are expected for these excitation wavelengths. This is found to be true for 476 and 530 nm excitation. Similarly, although the 665 nm band in the Pheo a absorption spectrum is assigned to both the $Q_{x(0,0)}$ and $Q_{y(0,0)}$ transitions, excitation at 647 nm appears to involve coupling with the $Q_{x(0,0)}$ transition because the low frequency region obtained is similar to that obtained with 476 and 530 nm excitation. Perhaps 457 nm excitation involves coupling between the B and Q transitions. It is located in between the $B_{x,y}$ band at 409 nm and the $Q_{x(0,0)}$ band at 470 nm in the absorption spectrum. In fact, regions the SERRS spectrum obtained with 457 nm excitation resembles both the SERRS spectra taken with 406 and 476 nm excitation.

CONCLUSIONS

This paper is the first to report SERRS spectra of Pheo a recorded with violet, blue, green, and red excitation wavelengths. Each SERRS spectrum is distinctive and the enhancement patterns are consistent with those previously reported for RR excitation of Pheo a in the 406-540 nm range. The agreement between the RR and SERRS spectra indicates that adsorption of Pheo a does not significantly perturb the electronic states in this region of the spectrum. As a result, the surface enhancement is due primarily to an electromagnetic mechanism.

Of particular importance, the SERRS spectrum obtained in resonance with the 665 nm Q transition furnishes unique insights regarding the electronic properties of this state. Fluorescence emission has prevented the acquisition of a RR spectrum of Pheo a by excitation in resonance with this transition. SERRS should be valuable for obtaining resonance excitation profiles within this lowest energy transition. In addition, Pheo a has strong bands at 675 and 345 cm^{-1} which are not found in the Chl a SERRS spectrum at 647 nm excitation. Also, Chl a has distinctive bands at 918 and 748 cm^{-1} which do not appear in the Pheo a SERRS spectrum. Thus, Pheo a is distinguishable from Chl a using SERRS at 647 nm excitation.

The results presented here are provide evidence that it may be possible to monitor photosynthetic pigments within intact reaction centers and light harvesting complexes with

red excitation. Previous SERRS studies of reaction centers[34] and chromatophore preparations[35] have shown the applicability of SERRS for studying designated membrane components. Although RR spectroscopy has been used extensively to study a variety of photosynthetic preparations,[19,36] the information gained in this study combined with the results of our SERRS study of Chl *a*[14] on a roughened Ag electrode provides a basis for selectively probing these pigments within an intact reaction center at defined electrode potentials. It is anticipated that the information gained by these planned SERRS studies will provide structural information about the organization of the pigments within the photosynthetic membrane and also functional information about their role in the photosynthetic process.

ACKNOWLEDGEMENTS

Ames laboratory is operated for the U.S. Department of Energy by Iowa State University under contract no. W-7405-Eng-82. This article was supported by the Division of Chemical Sciences, Office of Basic Energy Sciences.

REFERENCES

1. Lagoutte, B.; Mathis, P. Photochem. Photobiol. **1989**, 49, 833-844.
2. Hansson, Ö.; Wydrzynski, T. Photosyn. Res. **1990**, 23, 131-162.
3. Michel, H.; Deisenhofer, J. Biochemistry **1988**, 27, 1-7.
4. (a) Lutz, M. In Advances in Infrared and Raman Spectroscopy; Clark, R. J. H., Hester, R. E., Eds.; John Wiley and Sons: New York, 1984; Vol. 11, pp. 211-300. (b) Lutz, M.; Kleo, J.; Gilet, R.; Henry, M.; Plus, R.; Leicknam, J. P. In Proceedings of the 2nd International Conference on Stable Isotopes; Klein, E. R., Klein, P. D., Eds.; U.S. Department of Commerce: Springfield, VA, 1975; pp. 462-469. (c) Lutz, M. J. Raman Spectrosc. **1974**, 2, 497-516.
5. Robert, B.; Lutz, M. Biochemistry **1986**, 25, 2303-2309.
6. (a) Fujiwara, M.; Tasumi, M. J. Phys. Chem. **1986**, 90, 250-255. (b) Fujiwara, M.; Tasumi, M. J. Phys. Chem., **1986**, 90, 5646-5650.
7. Heald, R. L.; Callahan, P. M.; Cotton, T. M. J. Phys. Chem. **1988**, 92, 4820-4824.
8. Fonda, H. N.; Babcock, G. T. In Progress in Photosynthesis Research; Biggens, J., Ed.; Martinus Nijhoff: Boston, 1987; Vol. I, pp. 449-452.
9. Cotton, T. M.; Loach, P. A.; Katz, J. J.; Ballschmitter, K. Photochem. Photobiol. **1978**, 27, 735-749.

10. Lutz, M.; Robert, B. In Biological Applications of Raman Spectroscopy; Spiro, T. G., Ed.; John Wiley and Sons, Inc.: New York, 1988; Vol. 3, pp. 347-411.

11. Uphaus, R. A.; Cotton, T. M.; Möbius, D. Thin Solid Films **1986**, 132, 173-185.

12. Andersson, L. A.; Loehr, T. M.; Cotton, T. M.; Simpson, D. J.; Smith, K. M. Biochim. Biophys. Acta **1989**, 974, 163-179.

13. Hildebrandt, P.; Spiro, T. G. J. Phys. Chem. **1988**, 92,3355-3360.

14. Thomas, L. L.; Kim, J.-H.; Cotton, T. M. J. Am. Chem. Soc. **1990**, 112, 3978-3986.

15. Nabedryk, E.; Leonard, M.; Mäntele, W.; Breton, J. Biochemistry **1990**, 29, 3242-3247.

16. Fujita, I.; Davis, M. S.; Fajer, J. J. Am. Chem. Soc. **1978**, 100, 6280-6282

17. Nabedryd, E.; Andrianambinitsoa, S.; Mäntele, W.; Breton, J. In The Photosynthetic Bacterial Reaction Center; Breton, J., Vermeglio, A., Eds.; Plenum: New York, 1988; pp. 237-ff.

18. Möenne-Loccoz, P.; Robert, B.; Lutz, M. Biochemistry **1989**, 28, 3641-3645.

19. Heald, R. L. Resonance Raman and Electrochemical investigations of Primary Electron-Transfer Species in Photosynthesis; Ph.D. thesis, University of Nebraska, Lincoln, NE, 1989.

20. Strain, H. H.; Svec, W. A. In The Chlorophylls; Vernon, L. P., Seely, G. R., Eds.; Academic: New York, 1966; pp. 21-66.

21. Fragata, M.; Nordén, B.; Kurucsiv, T. Phochem. Photobiol. **1988**, 47, 133-143.

22. Boldt, N. J.; Donohoe, R. J.; Birge, R. R.; Bocian, D. F. J. Am. Chem. Soc. **1987**, 109, 2284-2298.

23. Choi, S; Spiro, T. G.; Langry, K. C.; Smith, K. M. J. Am. Chem. Soc. **1982**, 104, 4337-4344.

24. Gersten, J. I.; Nitzan, A. J. Chem. Phys. **1980**, 73, 3023-3037.

25. Kerker, M.; Wang, D. S.; Chew, H. Applied Optics **1980**, 19, 4159-4174.

26. Ferrell, T. L. Phys. Rev. B: Condens. Matter **1982**, 25, 2930-2932.

27. Otto, A. In Light Scattering in Solids; Cardona, M., Gunthrodt, G., Eds.; Springer-Verlag: Berlin, 1984; Vol. IV, pp. 289-461.

28. Otto, A. Appl. Surf. Sci. **1980**, 6, 309-355.

29. Van Duyne, R. P. In Chemical and Biochemical Applications of Lasers; Moore, C. B., Ed.; Academic Press: New York, 1979; Vol. IV, p. 101.

30. Moskovits, M. J. Chem. Phys. **1982**, 77, 4408-4416.

31. Breton, J.; Michel-Villaz, M.; Paillotin, G. In Proc. 2nd Int. Congress on Photosynthesis Research; Forti, G., Avron, M., Melandri, A., Eds.; Dr. W. Junk N. V.: The

Hague, 1972; p. 349.

32. Chow, H. C.; Serlin, R.; Strouse, C. E. J. Am. Chem. Soc. **1975**, 97, 7230.

33. Serlin, R.; Chow, H. C.; Strouse, C. E. J. Am. Chem. Soc. **1975**, 97, 7237.

34. Cotton, T. M.; Van Duyne, R. P. FEBS Lett. **1982**, 147, 81-84.

35. (a) Picorel, R.; Holt, R. E.; Cotton, T. M.; Seibert, M. In Progress in Photosynthesis Research; Biggens, J., Ed.; Martinus Nijhoff Publishers: The Netherlands, 1987; pp. 1.4 423-426; (b) Picorel, R.; Holt, R. E.; Cotton, T. M.; Seibert, M. J. Biol. Chem. **1988**, 263, 4374-4380; (c) Seibert, M.; Cotton, T. M.; Metz, J. G. Biochim. Biophys. Acta **1988**, 934, 235-246; (d) Picorel, R.; Lu, T.; Holt, R. E.; Cotton, T. M.; Seibert, M. Biochemistry **1990**, 29, 707-712.

36. Lutz, M.; Robert, B. In Spectroscopy of Biological Molecules; Alix, A. J. P., Bernard, L., Manfait, M., Eds.; Wiley: New York, 1985; pp. 310-318.

SECTION 3. A SURFACE-ENHANCED RESONANCE RAMAN SCATTERING STUDY OF CHLOROPHYLL b ON A SILVER ELECTRODE WITH EXCITATION FROM THE VIOLET TO RED REGION OF THE ELECTROMAGNETIC SPECTRUM.

ABSTRACT

Surface-enhanced resonance Raman scattering (SERRS) spectra are presented for chlorophyll b adsorbed on a roughened silver electrode with 406.7, 457.9, 514.5, 568.2, 647.1 and 676.2 nm excitation. Each excitation wavelength produced a distinctive SERRS spectrum. Liquid nitrogen temperatures were used to minimize sample photodegradation and fluorescence. As a result, the SERRS spectra, while similar to the resonance Raman (RR) spectra, are more intense with greater peak resolution. The agreement between the RR and SERRS spectra imply that an electromagnetic mechanism is the major source of the surface enhancement and that chlorophyll b does not undergo structural alteration upon adsorption at the electrode surface. Also, the roughened electrode at low temperature produced detailed low frequency vibrations at 457.9 and 514.5 nm excitation. Furthermore, the SERRS spectra obtained with 647.1 and 676.2 nm excitation are the first reported for chlorophyll b excited within the lowest $^1\pi$-π^* electronic state. Selective excitation within the various electronic transitions can be utilized to verify the structural and functional properties of chlorophyll b within the light harvesting complexes of green plants and algae.

INTRODUCTION

The first step of photosynthesis is the harvesting or trapping of light energy within photosystems I and II (PS I and PS II) of green plants and algae. The light-harvesting complexes contain photosynthetic pigments which allow these complexes to use a larger fraction of the visible spectrum. Light-harvesting complexes (LHC), pigment-protein complexes that surround the reaction center, absorb light and transfer this energy to the primary electron donor within the reaction center complex of the photosystem. Light-harvesting complexes for PS I and PS II in green plants and algae are not as well characterized as those associated with the well studied bacterial reacion center. However, it is known that LHCs contain chlorophyll a, chlorophyll b, and a small amount of carotenoids. Both LHC I and LHC II contain two distinct chlorophyll a/b protein entities within PS I and PS II, respectively.[1,2,3] PS II is comprised of more chlorophyll b than PS I.

The primary function of these pigments within the LHC units appears to be to enhance the absorption of visible light. This is accomplished two ways. The first is via the overlap of the absorption spectra of the individual pigments which provide effective light for photosynthesis in two regions, 400-550 nm and 650-680 nm.[3,4] The second path which provides maximal visible light absorption is through sensitized fluorescence. The phenomenon of sensitized fluorescence involves the interaction of two molecules, the donor and

acceptor, that may be physically separate. When the molecules are illuminated with a wavelength of light that only the donor pigment absorbs, it will emit light which corresponds to the fluorescence spectrum of the acceptor pigment. The energy of the fluorescent state of the donor molecule overlaps with the absorption band of the acceptor molecule and thus, the energy of excitation of the donor molecule is transferred by resonance to the acceptor molecule. Thus, the fluorescence emission wavelength of the donor is in resonance with an absorption band of the acceptor. Energy transfer is always from the other excited chloroplast pigments to chlorophyll a due to chlorophyll a having its fluorescence at the longest wavelength.[4]

Dissipating excess radiation that the reaction center cannot handle is another possible function of the light-harvesting comlexes. When the primary electron acceptor is already reduced, no electrons can be transferred from the specialized reaction center chlorophyll to the acceptor. This chlorophyll loses its energy via heat or fluorescence. Fluorescence of the reaction center can be seen as an overflow mechanism for energy adsorbed by the light harvesting pigments from sunlight. All photosynthetic organisms emit a low level of fluorescence under normal conditions because electron transfer away from the primary electron acceptor is slower than the excitation of the reaction center chlorophyll.[4]

In Chlorella (algae) it was shown that the transfer of

excitation from chlorophyll b to chlorophyll a is 100% efficient while from carotenoids to chlorophyll a it is only 40%. The structural arrangement of these pigments within the membrane dictate the efficiency of energy transfer by this type of inductive resonance. The closer the pigments are the more efficient the energy transfer.[4] In subpicosecond fluorescence upconversion studies by Eads et al.[5] the rate of chlorophyll b to chlorophyll a electronic energy transfer in situ within the LHC pigment proteins of Chlamydomonas reinhardtii mutant C2 was reported at 0.5 ± 0.2 ps. To account for this transfer rate chlorophyll b must be strongly coupled to several chlorophyll a molecules which lowers the energy state of chlorophyll b and allows better overlap with chlorophyll a. Another possibility is that the donor chlorophyll b molecule has a large number of chlorophyll a molecules located within 12 Å of it.

Raman spectroscopy offers a method for studying the structure and interaction of chlorophyll b within LHC I and LHC II. Although normal Raman lacks sensitivity, this can be overcome by using a wavelength of excitation that is within an electronic transition of chlorophyll b. This technique is known as resonance Raman (RR) and also offers selectivity as well as sensitivity. Previous RR studies of chlorophyll b include selective Raman enhancement of chlorophyll b within spinach chloroplasts[6], excitation studies 441.6-514.5 nm[7] with vibrational assignments[8], the effects of isotopic substitu-

tion[9], and the effect of axial coordination on the Raman spectrum[10]. While RR is both sensitive and selective, it is often limited by fluoescence interference from biological samples. A RR spectrum excited within the Q_{y0} transition of chlorophyll b has not been obtained due to intense fluorescence from this state. This problem can be surmounted by using surface-enhanced resonance Raman spectroscopy (SERRS) which has proven to be an effective method for acquiring spectra of highly fluorescent molecules.[11,12,13] SERS (SERRS) has been used to determine vibrational information from a large number of biologically significant molecules.[14,15,16] There have also been a number of studies pertaining to the chlorophyll or chlorophyll derivatives. Uphaus et al.[17] obtained SERRS spectra of chlorophyll a, bacteriochlorophyll a, and bacteriopheophytin a monolayers on silver island films with 457.9 nm excitation. Andersson et al.[18] reported a Q_y excited SERRS spectrum of chlorophyll a multilayers on a silver film. Silver and gold colloids were used to determine the SERRS spectrum of copper chlorophyllin a, a chlorin derivative, excited within the blue and red regions of the electronic absorption spectrum.[11] Recently, Thomas et al.[19] reported SERRS spectra of chlorophyll a using a roughened silver electrode and violet to red excitation.

The spectra presented in this paper are the first SERRS spectra of chlorophyll b. This report is concerned with a detailed comparison between the RR and SERRS spectra of chlo-

rophyll b (Chl b) obtained under various excitation conditions. The agreement between the RR and SERRS spectra indicate an electromagnetic mechanism as the major source of enhancement at the silver surface and also suggests that Chl b does not undergo structural alteration upon adsorption at the electrode surface. The distinctive spectra at each excitation wavelength denote dramatic changes in mode enhancements. SERRS furnishes detailed and highly resolved spectra of Chl b. These intensity changes supply insights regarding the structural changes accompanying electronic excitation.

EXPERIMENTAL

Chlorophyll b preparation. Chl b (Figure 3-1.) was separated from spinach extract[20] by reversed phase high performance liquid chromatography[19] (rp-HPLC). For RR experiments the mobile phase was evaporated from the Chl b fraction. Then the purified Chl b was dissolved in methylene chloride (ca. 1 mg/100 μl) and transferred to a 5 mm o.d. Pyrex tube. The solution was evaporated with nitrogen gas to make a thin film on the tube walls and sealed under vacuum. For SERRS experiments Chl b was adsorbed at an electrochemically roughened electrode surface[19] by dipping the electrode in the purified Chl b solution (ca. 1 X 10^{-4} M in acetonitrile/methanol 3:1 v/v) for 20 minutes. All sample manipulation and experimental operations were performed in subdued light.

The purity of Chl b was monitored and confirmed before and after the Raman experiments by analytical rp-HPLC[19] and UV/VIS spectroscopy. Electronic absorption spectra were measured using a one mm pathlength cuvette and a Perkin Elmer Lambda 6 UV/VIS spectrophotometer.

RR and SERRS spectroscopy. The intstrumentation and experimental conditions for collecting, processing, and recording the Raman and surface Raman scattering has been described previously.[19] The spectra presented are composites of 25 scans with 10 second and 1 second integration periods per scan for the RR and SERRS spectra, respectively. The SERRS spectrum recorded with 568.2, 647.1 and 676.2 nm excitation

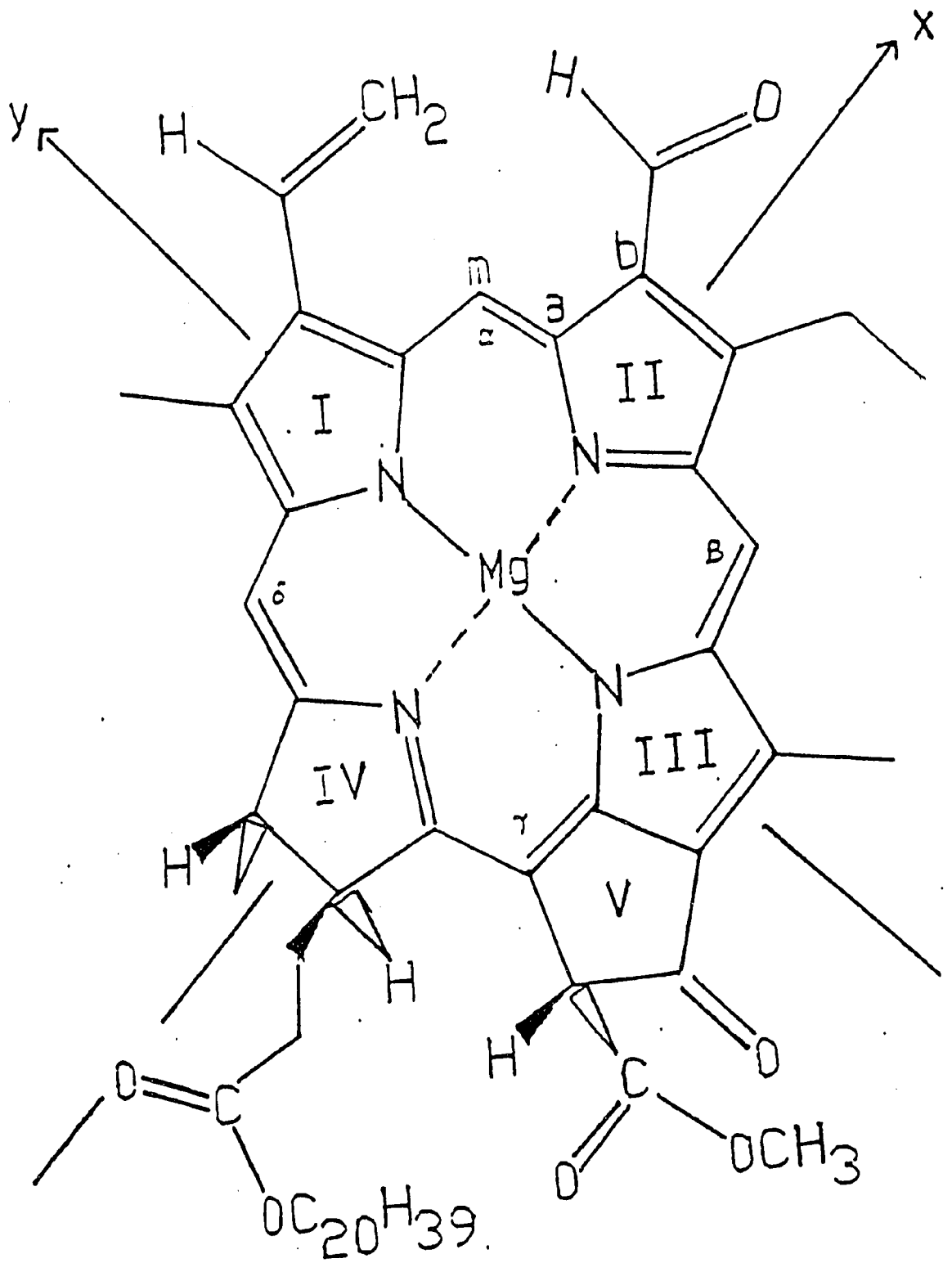

Figure 3-1. Structure of Chl b.

are composites of 15 scans with 5 second integration per scan. The laser power was 25 and 10 mW for RR and SERRS samples, respectively.

RESULTS

Electronic Absorption Spectroscopy. The electronic absorption spectrum of chlorophyll b (Chl b) is shown in Figure 3-2. The arrows in Figure 3-2 indicate the excitation wavelengths used in the Raman experiments. The absorption spectrum is in agreement with those previously reported.[4b,20b] The x and y polarized components of the Soret band overlap more in Chl b than in chlorophyll a (Chl a). The same is true for the x and y polarized components of the Q transition for Chl b. Thus, the maxima and minima of the fluorescence polarization data are less distinct and assignment of the individual x and y components for the B and Q electronic transitions is difficult.[4b] Even so, the fluorescent polarization data indicate that 430 and 590 nm bands contain the $B_{x(0,0)}$ and $Q_{x(0,0)}$ transitions, respectively. In contrast, the bands at 453 and 647 nm are contain major contributions from the $B_{y(0,0)}$ and $Q_{y(0,0)}$ transitions, respectively.

Raman Spectroscopy. Figures 3-3 through 3-6 compare the RR and SERRS of Chl b. The excitation wavelengths used in the Raman experiments are given in the figure legends and are indicated by arrows in the absorption spectrum (Figure 3-2). Frequency assignment uncertainty is ±5 cm^{-1}. Low frequency modes were difficult to obtain because of interference from the glass Raman signals produced by the capillary tube and dewar. The RR spectra correspond with those previously reported with excitation wavelengths between 420 and 515 nm.[7]

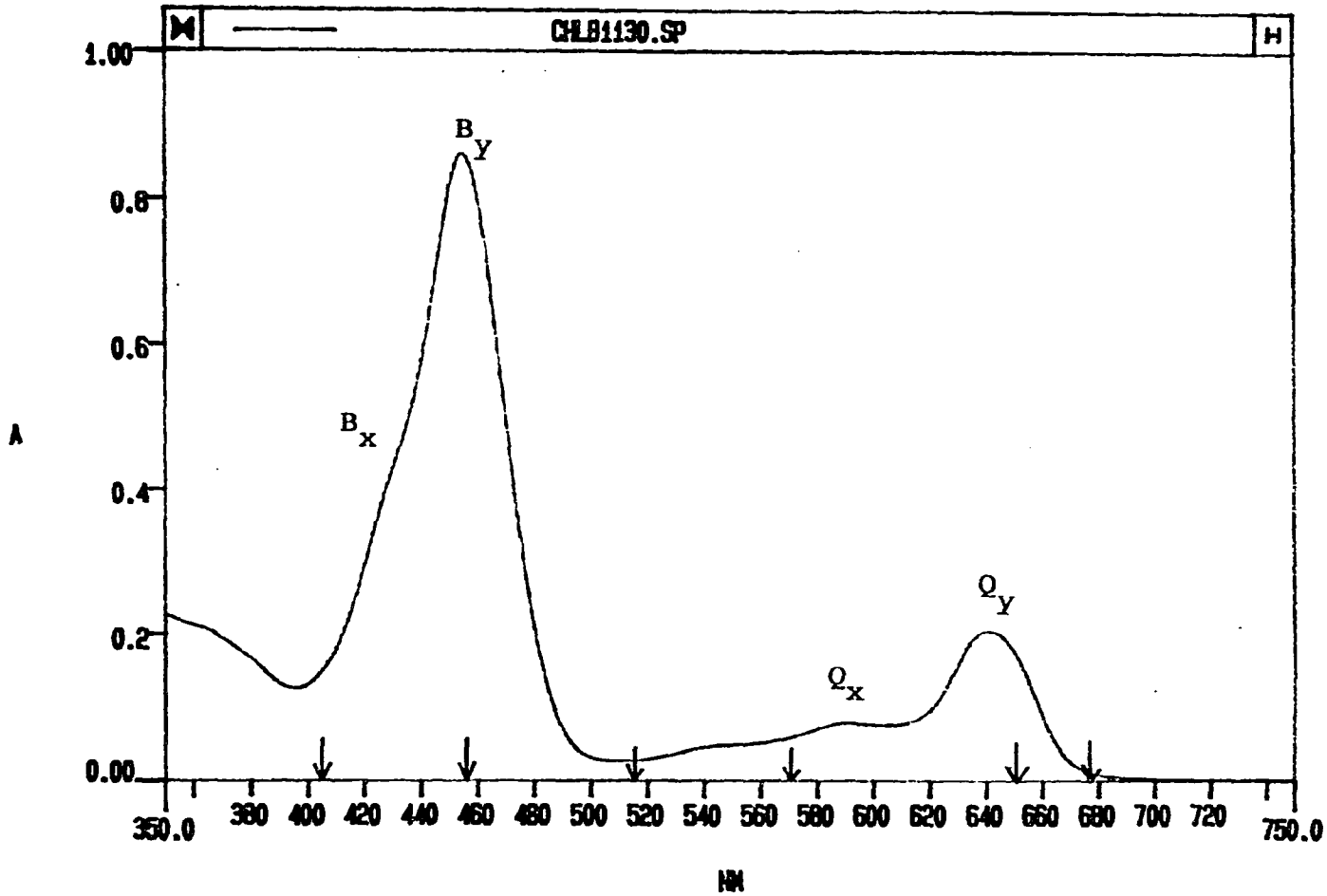

Figure 3-2. Absorption spectrum of Chl b in ACN/MeOH (3:1 v/v).

Attempts to attain RR spectra with red excitation (647.1 and 676.2 nm) were futile due to overwhelming fluorescence.

Figures 3-7 and 3-8 show the SERRS spectra of Chl b at liquid nitrogen temperature under various excitation conditions. The SERRS spectrum with 676.2 nm excitation was weak. However, with 647.1 nm excitation, the roughened Ag surface provided sufficient fluorescence quenching and the low temperature minimized the photooxidation of Chl b and resulted in a distinct, well resolved SERRS spectrum.

Table 3-1 lists the major SERRS bands of Chl b and their vibrational assignments. The assignments are based on those suggested by Lutz and Robert[8] and Boldt et al.[21]

Table 3-1. Average values for the Major SERRS (77K) bands for Chl b using Soret through red excitation.

cm^{-1}	Assignment[a]	cm^{-1}	Assignment[a]
1758	υC_{10a}-OMe	1070	
1692	$\nu C_9=O$	1045	
1662	$\nu C_3=O$	1002	νC_aN(III);δC_mC_aN(I)
1638	bound $\nu C_3=O$	985	δC_mC_aN(III);νC_9C_{10}
1617	νC_aC_m;νC_bC_b;νC_mH[b]	946	
1603		922	νCN;νCNC;νC_aC_b
1567	νC_aC_b(III);νC_bC_b(I)	838	
1522	νC_bC_b(I);νC_aC_b(III)	792	
1483	υCC	756	
1438	$\nu C_aC_m(\gamma,\delta)$;$\nu C_aC_b$I-III	745	
1428		720	
1394	νC_aC_b(II);$\upsilon C_aC_m(\alpha,\delta)$	703	
1349	νC_aN(IV);νC_aN(I,III)	620	
1323	νC_aN(I);$\delta C_mH(\delta)$	575	
1290	$\delta C_mH(\alpha,\beta)$;$\nu C_aN$(II,IV)	478	
1269	$\delta C_mH(\alpha,\beta)$	443	$\delta C_9=O$;δCNC
1228	γC_bH(IV);$\delta C_mH(\delta)$	403	
1214		378	
1189	νC_mC_{10}(V);γC_bH(IV)	347	MgN_4
1152	νC_aN(IV);$\delta C_aC_mC_a(\alpha$-$\delta)$	315/300	MgN_4
1123	νC_aC_b(IV);νC_bS	256	

[a]Assignments based on those reported by Lutz and Robert[8] and Boldt et al.[21] C_a, C_b, C_m refer to the macrocycle positions shown in Figure 3-1. Mode descriptions are υ=stretch and δ=in-plane deformation.

[b]This band is assigned as a bound $\upsilon C_3=O$ vibration in aggregated samples.[6]

DISCUSSION

RR versus SERRS. 406.7 nm excitation (Figure 3-3). When comparing the RR versus SERRS spectra both similarities and differences are obvious. The 1450-700 cm^{-1} region is similar in the RR and SERRS spectra. However, broad bands in the RR spectrum at 1286 and 703 cm^{-1} are sharper and better resolved in the SERRS spectrum.

In the 1700-1450 cm^{-1} region differences occur between the RR and SERRS spectra with greater intensity for the bands at ca. 1664 (νC_3=O), 1569 (νC_aC_b (III);$\nu C_bC_{b\,(I)}$), and 1480 cm^{-1} (νCC) and the disappearance of the 1618 cm^{-1} band in the SERRS spectrum. This may be due to orientation of the macrocycle at the metal surface and/or to environmental effects on the molecule. Electromagnetic enhancement theory attributes the relationship between band intensities and molecular orientation to the coupling of the electric field at the electrode surface with the polarizability tensors of the adsorbed molecule. Bonds that have polarizability tensors perpendicular to the electrode surface are preferentially enhanced.[22,23] The Chl b bands in the SERRS spectrum that are enhanced support edge-wise orientation as was found for Chl a in SERRS studies by Thomas et al.[19] The strong enhancement of the 1663 cm^{-1} (νC_3=O) band in the SERRS spectrum suggests that C_3=O is, not only near the electrode surface, but aligned perpendicular to it, as well.

The thin film samples were prepared by evaporating con-

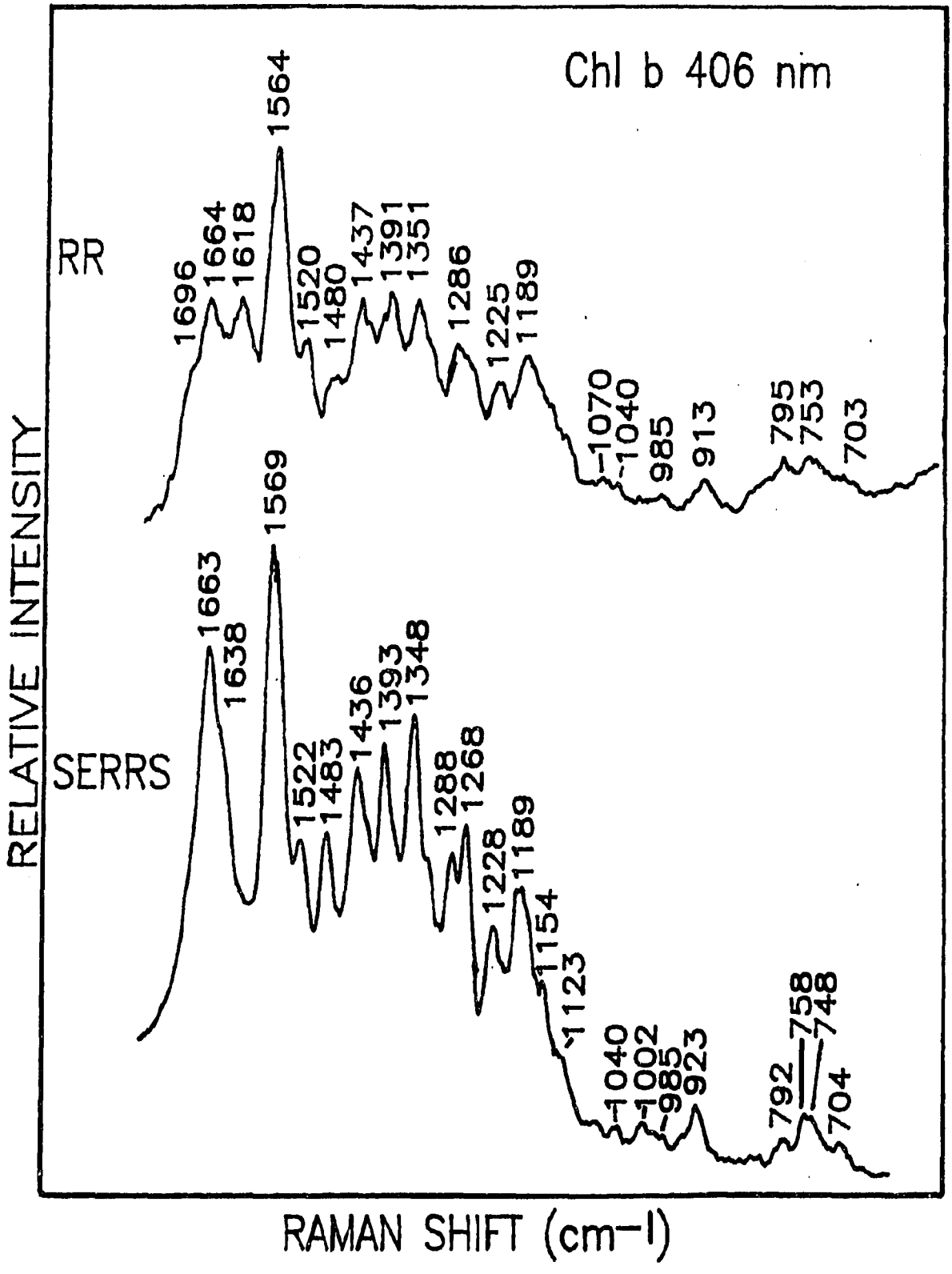

Figure 3-3. RR and SERRS of Chl b at 406 nm excitation.

centrated samples of Chl b in CH_2Cl_2. This could be the reason for the 1618 cm^{-1} band in the RR spectrum. This band has been associated with aggregated species[6,10] and assigned as a bound formyl (υC_3=O) vibration.[6,8] However, the SERRS spectrum arises from dipping the electrode into a dilute unaggregated solution of Chl b. Thus, a change in Chl b intermolecular interactions may account for the presence or absence of the 1618 cm^{-1} band.

457.9 nm excitation (Figure 3-4). As with violet excitation, a comparison of the RR and SERRS spectra shows there are differences and similarities. The carbonyl bands at 1696 and 1664 cm^{-1} in the RR spectrum occur in the SERRS spectrum with about the same intensity. However, the 1620 cm^{-1} band in the RR spectrum disappears in the SERRS spectrum and instead a band at 1638 cm^{-1} appears. Note the 1638 cm^{-1} shoulder in the SERRS spectrum at 406.7 nm excitation. The behavior of the 1620 cm^{-1} band was discussed in the previous section. The 1638 cm^{-1} band has been assigned by Lutz and Breton[6] and Lutz and Robert[6] as a bound formyl (υC_3=O) vibration. Lutz and Robert[8] reported that Chl b dissolved in methanol produced two bands at 1670 and 1647 cm^{-1} which correspond to formyl group stretches, free and hydrogen-bonded, respectively. A solution RR spectrum of Chl b in ACN/MeOH (3:1 v/v) with 457.9 nm excitation (not shown) matches the SERRS spectrum shown in Figure 3-4. Thus, although there are no bound formyl vibrations due to aggregation in the SERRS spectrum (Chl b is not aggregated when dissolved in ACN/MeOH[10]), bound and unbound formyl vibra-

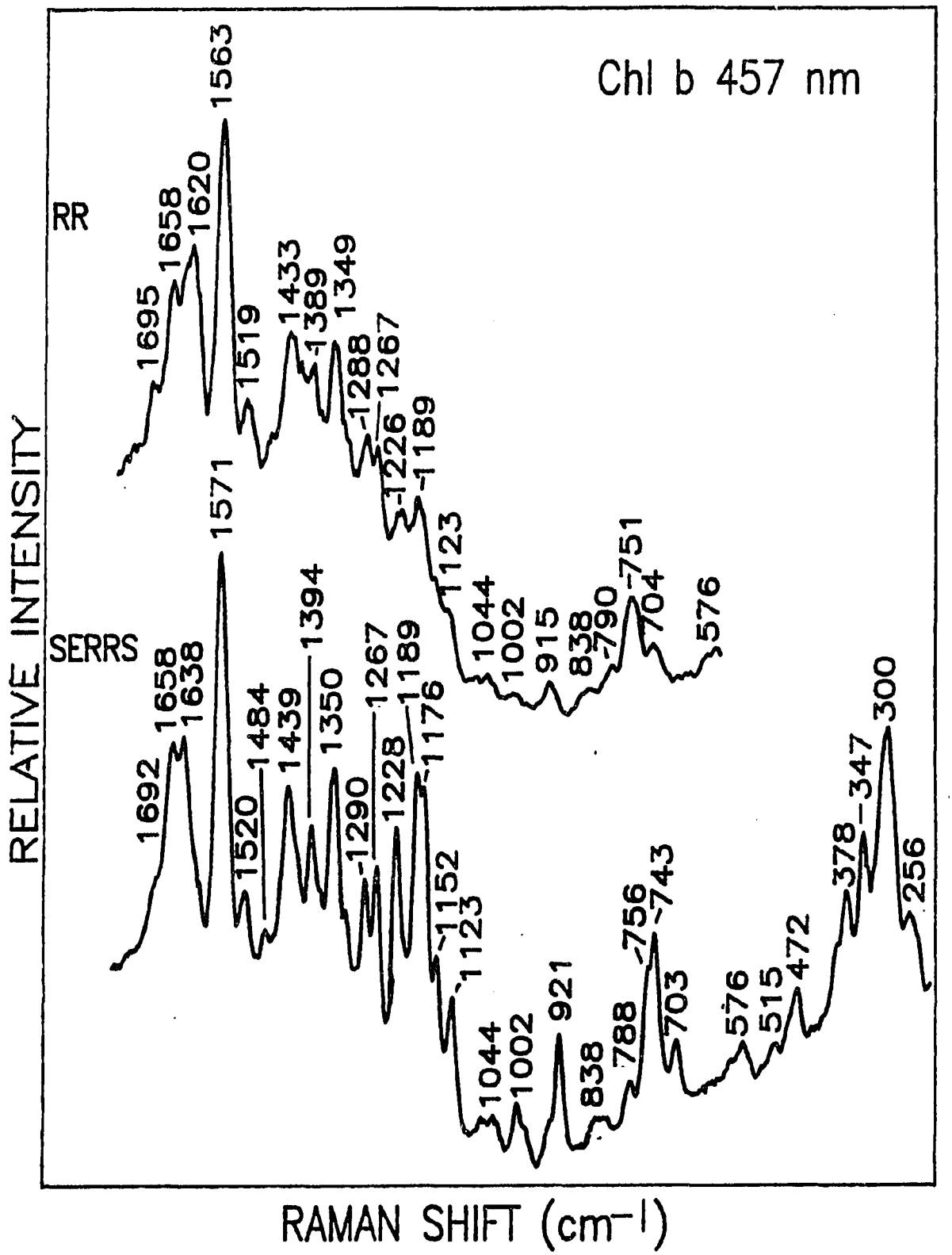

Figure 3-4. RR and SERRS of Chl b at 457.9 nm excitation.

tions exist. Hence, Chl b molecules could be adsorbing randomly edgewise at the electrode surface with some molecules oriented with the formyl group at the surface (1638 cm^{-1}) and some molecules oriented with the formyl group free (1664 cm^{-1}). On the other hand, the Chl b sample was adsorbed onto the SERRS electrode from a solvent containing 25% methanol. Thus, the υC_3=O bands in the SERRS spectrum could be due to free and hydrogen bound formyl groups.

The band wavenumbers in the RR and SERRS spectra are in agreement in the 1600-575 cm^{-1} region, but the bands are sharper and some are more intense in the SERRS spectrum. The bands at 1394, 1290/1267, 1228, 1189, 1002, and 921 cm^{-1} increase in intensity. These bands correspond to pyrrole stretching modes and the intensity changes are probably due to the orientation of Chl b at the electrode surface as discussed previously. In addition, the SERRS spectrum reveals a detailed low frequency region below 575 cm^{-1}.

514.5 nm excitation (Figure 3-5). As with the previously discussed spectra, a comparison of the RR and SERRS spectra excited at 514.5 nm shows a similar intensity pattern, but the SERRS spectrum contains sharper bands and an enhanced low frequency region. The most noticeable feature of the Raman spectra obtained with 514.5 nm excitation is the absence of all carbonyl bands. The RR spectrum has the familiar band at ca. 1619 cm^{-1} band, but, unlike spectra obtained at other excitation wavelengths, this band occurs in the SERRS spec-

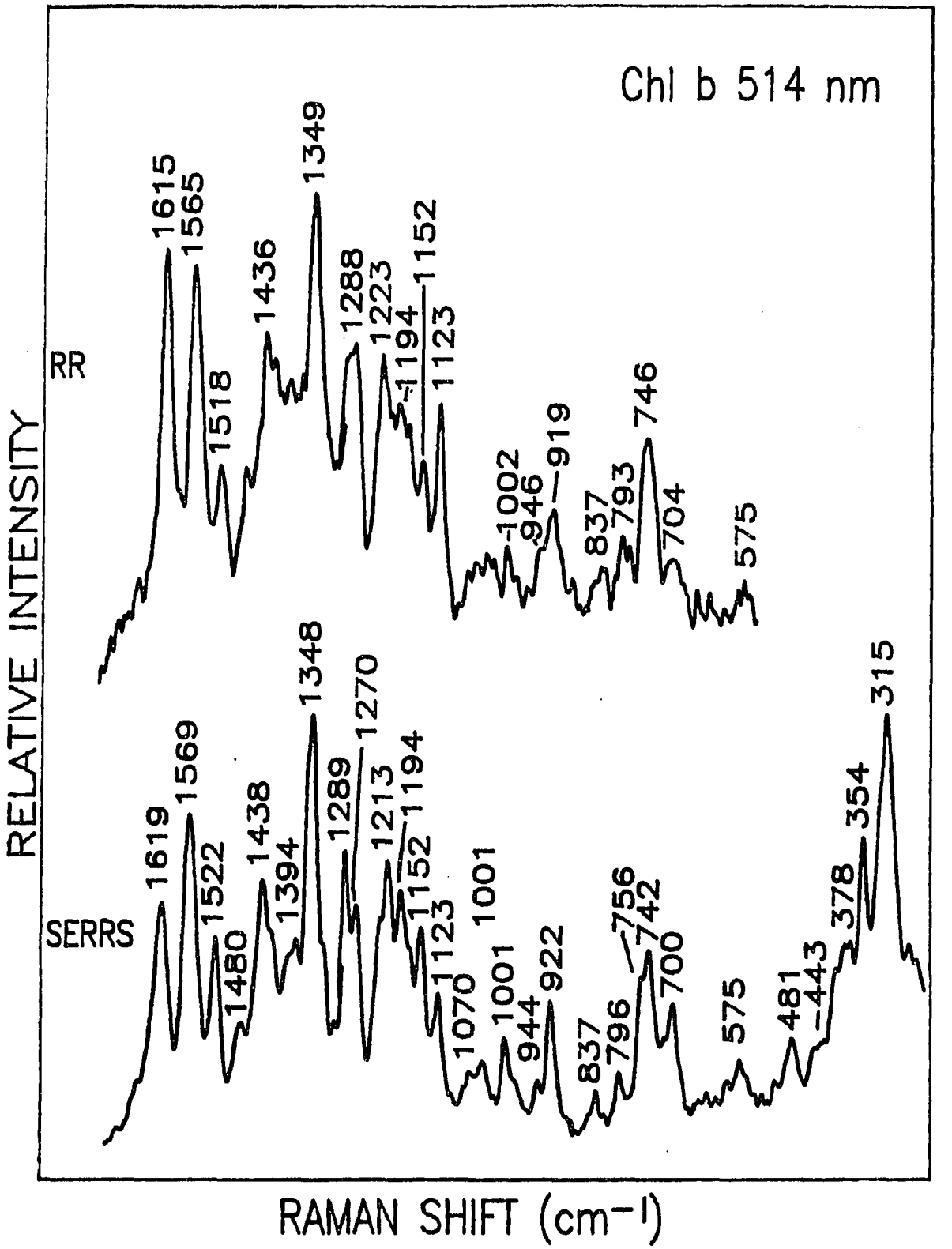

Figure 3-5. RR and SERRS of Chl b at 514.5 nm excitation.

trum, as well. Furthermore, the intensity of the 1615 cm^{-1} band is greater than the intensity; of the 1565 cm^{-1} band in the RR spectrum. In contrast, the 1619 cm^{-1} band is less intense than the 1569 cm^{-1} band in the SERRS spectrum. The band at ca. 1619 cm^{-1} coincides with the 1610 cm^{-1} (νC_aC_m (α,β)) band in the SERRS spectrum of Chl *a*[19] which also is very intense with 514.5 nm excitation. This band may be less intense in the SERRS spectrum of Chl *b* than the RR spectrum because the RR sample is an aggregated sample and, therefore, has a bound $\nu C_3{=}O$ mode contributing to the 1615 cm^{-1} band as well as the νC_aC_m (α,β) mode donation. In contrast, the SERRS sample is not aggregated[10] and does not have the formyl contribution. Consequently, an intensity decrease in the 1619 cm^{-1} band occurs.

Although the SERRS spectrum resembles the RR spectrum some intensity differences do exist. In the SERRS spectrum the bands at 1619 and 1123 cm^{-1} are lower in intensity whereas the 1522, 1438, 1001, and 922 cm^{-1} bands are more intensite when contrasted with the RR spectrum. In addition, the bands at ca. 1288 and 746 cm^{-1} in the RR spectrum split into two bands at 1289/1270 and 757/742 cm^{-1} and increase in intensity in the SERRS spectrum. Futhermore, the 1223 cm^{-1} band in the RR spectrum shifts to 1213 cm^{-1} and increases in intensity. Again, these bands are assigned to pyrrole stretching modes and the intensity changes between the RR and SERRS spectra may reflect the orientation of Chl *b* at the electrode surface as

explained by surface selection rules.

568.2 nm excitation (Figure 3-6). In contrast to violet, blue, and green excitation, yellow excitation provides themost comparable RR and SERRS spectra. The presence of the ester band (νC_{10a}-OR) at 1758 cm^{-1} is present in both the RR and SERRS spectra and is also unique to spectra obtained by excitation at 568.2 nm. However, as with excitation at 514.5 nm, the 1612 cm^{-1} band appears in both the RR and SERRS spectra. Likewise, some bands in the SERRS spectrum increase in intensity as compared to the RR spectrum. The bands at 1215, 1150, 1048, 1000, 919, 836, and 753 cm^{-1} (which splits to 753/746 cm^{-1}) increase in intensity in the SERRS spectrum.

SERRS. Figure 3-7 and 3-8 display the SERRS spectra of Chl b excited from the violet to the red regions of the electromagnetic spectrum. Each spectrum is distinct. This is expected considering the different electronic transitions that occur under B and Q excitation conditions. Previous RR[24] and SERRS[11] studies on chlorins also demonstrated variation in intensity patterns with changes in excitation wavelength. In addition, the SERRS study of Chl a[19] on a roughened Ag electrode reported similar results. The data indicate that the Ag electrode does not significantly perturb the Chl b electronic states.

Excitation at 406 and 457 nm produces spectra that are in resonance with the B_x and B_y absorption bands, respectively. The spectra are dominated by totally symmetric Franck-Condon

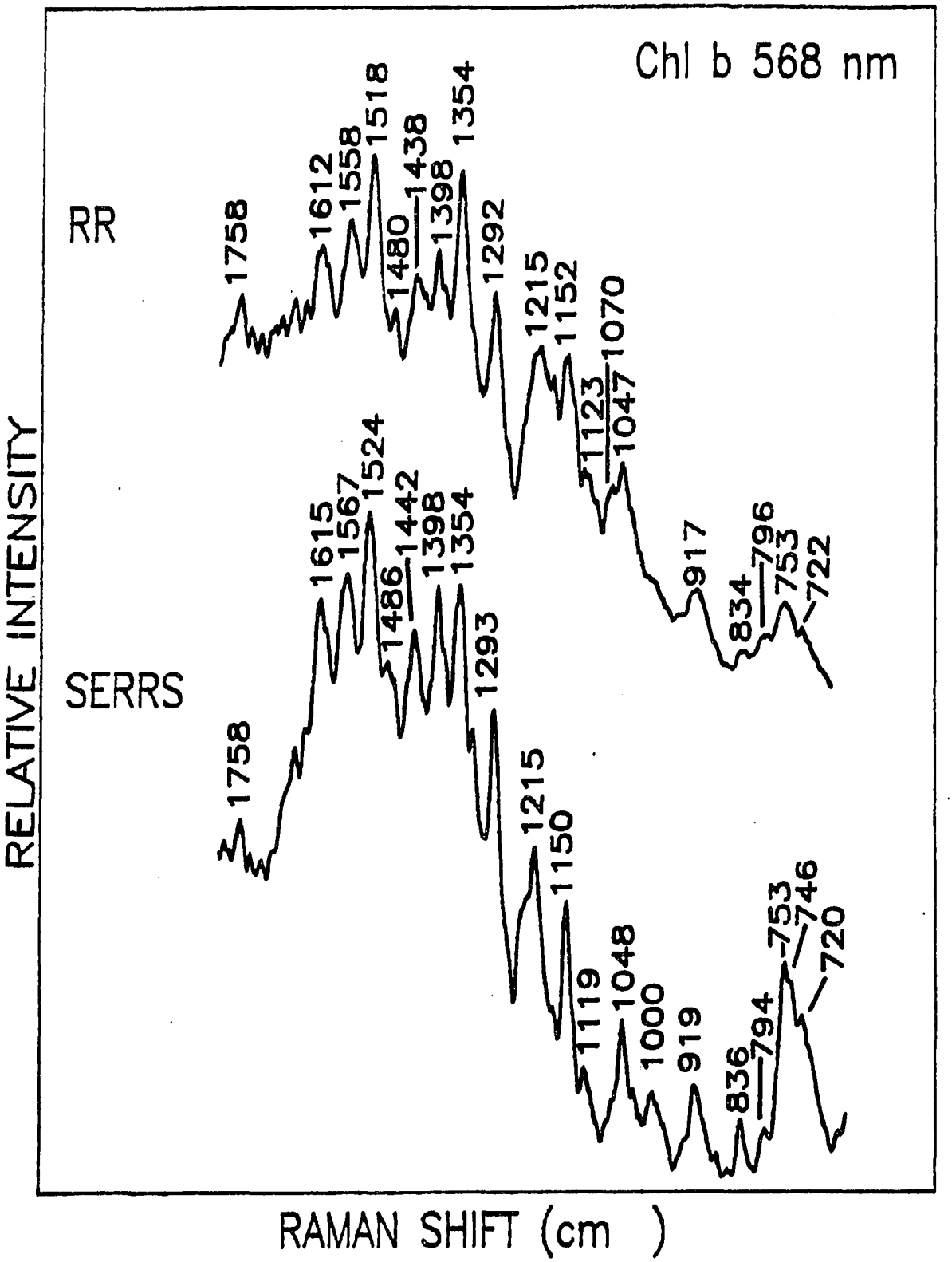

Figure 3-6. RR and SERRS of Chl b at 568.2 nm excitation.

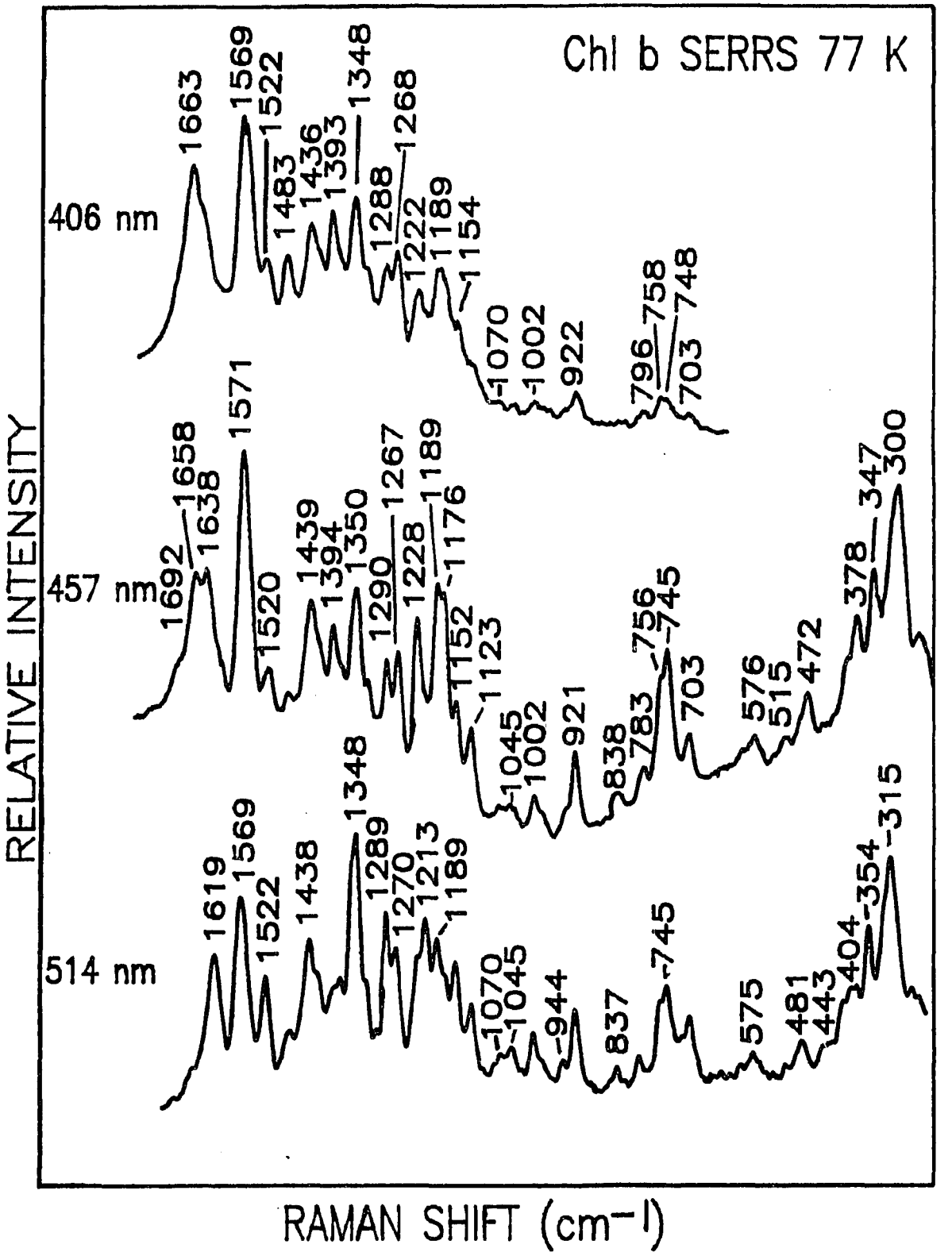

Figure 3-7. SERRS of Chl b at 77 K.

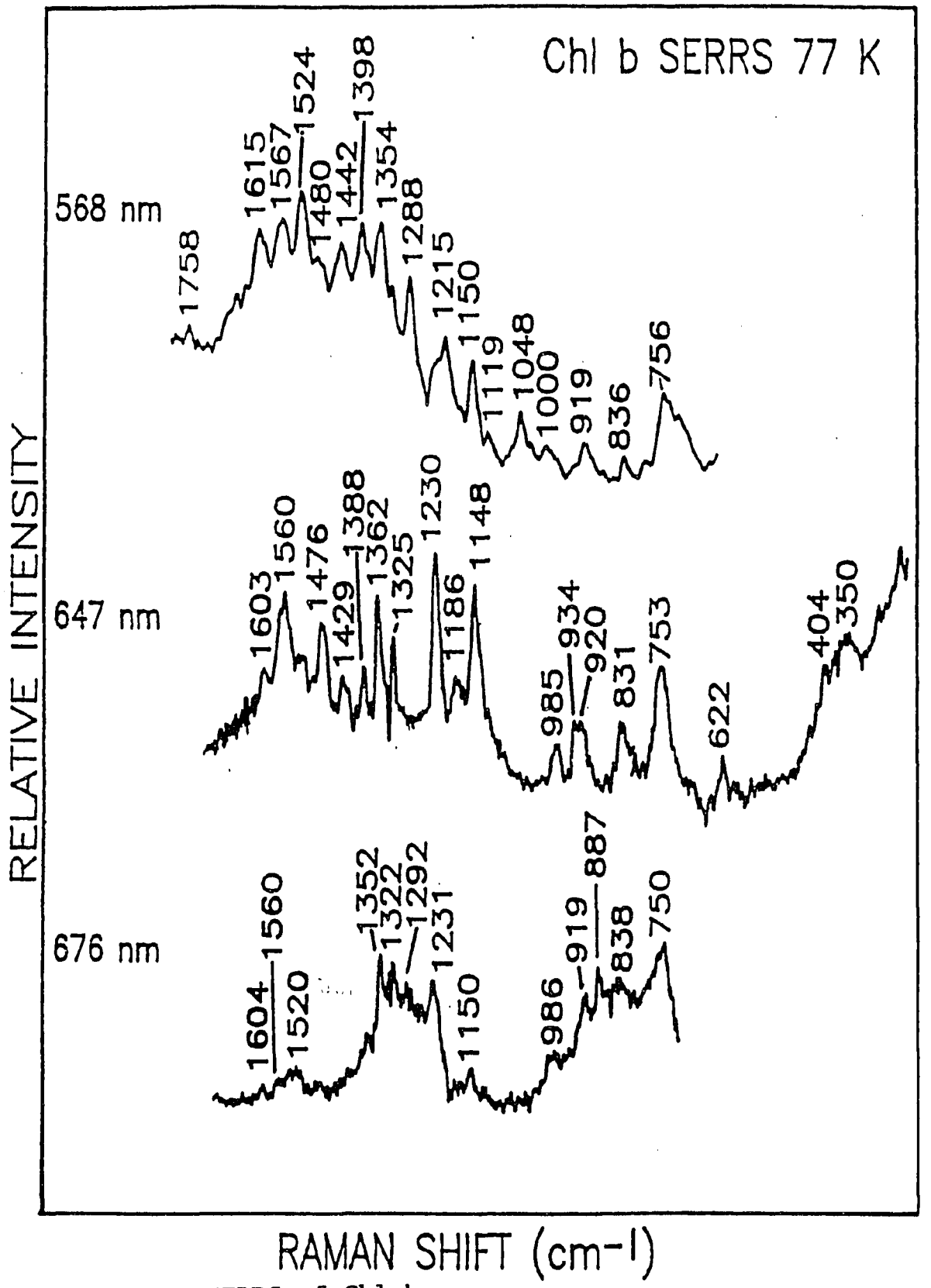

Figure 3-8. SERRS of Chl b.

active modes aligned along the x (406 nm excitation) and y (457 nm excitation) axes. A comparison of the 406 and 457 nm excited spectra shows a similar intensity pattern with some bands preferentially enhanced at one excitation wavelength as compared to the other. The most obvious difference is in the carbonyl region (1700-1600 cm^{-1}). The band at ca. 1696 cm^{-1} is assigned as the υC_9=O which lies along the y axis of the macrocycle. As expected, it is more apparent in the 457 nm excited (B_y) spectrum. In contrast, the υC_3=O stretch (1664 cm^{-1}) is aligned along the x-axis and is anticipated to be stronger with excitation at 406 nm (B_x). Note the intensity of this band in relation to the intensity of the band at ca. 1569 cm^{-1} in both spectra. The 1664 cm^{-1} band is more intense with excitation in resonance within the B_x transition at 406 nm. Due to the intensity of the 1664 cm^{-1} band the 1638 cm^{-1} band appears as a shoulder in the 406 nm excited spectrum, but it is a distinct band (1664/1638 cm^{-1}) in the 457.9 nm excited spectrum. As previously discussed in the context of the RR spectra the 1638 cm^{-1} band is a formyl vibration that is caused by either the interaction with the surface or by hydrogen bonding. Also, in the 1500-1100 cm^{-1} region, the 1483 and 1393 cm^{-1} bands are more intense with 406 nm excitation, but the 1228, 1189, and 1123 cm^{-1} bands are stronger with excitation at 457 nm. Most of these vibrations involve the macrocycle skeletal modes. Thus, varying the excitation wavelength results in differing enhancements for the vibrations of the

various rings. In the 500-200 cm^{-1} region Raman bands from glass interfered with the SERRS signal of Chl b with 406 nm excitation, whereas excitation at 457.9 nm produces strong, well resolved bands from Chl b in this region.

Increasing the excitation wavelength to 514.5 nm produces a spectrum devoid of carbonyl bands. Comparing the 514.5 nm excited spectrum with the Soret excited spectra shows very different enhancement patterns in the 1620-1100 cm^{-1} region. The 1619 cm^{-1} peak in the 514.5 nm excited spectrum does not appear with Soret excitation and has been discussed in the RR section. The bands at ca. 1522, 1438, 1348, and 1289 cm^{-1} bands are also strongest with green excitation. These modes correspond to a different set of macrocycle skeletal vibrations than those enhanced with Soret excitation. It is interesting that the 1228 cm^{-1} (γC_bH (IV); δC_mH (δ)) band disappears and a new band at 1213 cm^{-1} (νC_3C_3; δC_mH) appears. This indicates that 514 nm coincides with an electronic transition that contains an x polarized component. However, in the 1100-200 cm^{-1} range the 514 nm excited spectrum is very similar to the 457 nm excited spectrum. Thus, the lack of carbonyl bands, which is similar to the 568 nm ($Q_{x(0,0)}$) excited SERRS spectrum, and the close resemblance of the 514 nm with the 457nm ($B_{y(0,0)}$) excited 1100-200 cm^{-1} region, suggests a mixing of B_y and Q_x contribution is occurring at 514 nm excitation.

Excitation at 568.2 nm is in resonance with the $Q_{x(0,0)}$ transition. Although the spectrum has some features in common

with the preceding spectra, it also presents unique features. No carbonyl bands occur in the 1700-1620 cm^{-1} region but, the ester band (C_{10a}-OCH_3) appears at 1758 cm^{-1}. Also, the 1615 and 1524 cm^{-1} bands are more intense than the 1567 cm^{-1} band. The 1480-1300 cm^{-1} range resembles the 406 nm excited spectrum. This is not the case in the 1300-800 cm^{-1} region where the 1288 cm^{-1} band has lost its 1270 cm^{-1} shoulder, at 1215 and 1150 cm^{-1} definite bands occur, and bands at 1189 and 1123 cm^{-1} have virtually disappeared. Both green and yellow excitation enhance the νC_3C_3 mode at ca. 1215 cm^{-1} over the 1228 cm^{-1} mode (γC_bH (IV); δC_mH (δ)) found with the other excitation wavelengths. In addition, unlike the previous spectra, the band at 1048 cm^{-1} is stronger than bands at 1000 and 919 cm^{-1}. Furthermore, the 838 cm^{-1} band has grown in intensity.

As with yellow excitation, red excitation provides a SERRS spectrum that has some characteristics that are similar to those found in the other spectra, but it also has characteristics that are unparalleled. In the 1800-1500 cm^{-1} region the SERRS spectrum at 647 nm excitation shows no carbonyl bands but, the 1560 cm^{-1}band, common to all of the Chl <u>b</u> SERRS spectra, is present. The 1603, 1520, 1288, 1186, 1048, and 1002 cm^{-1} bands (C_aC_b, C_bC_b, C_aC_m, and C_aN vibrations) are weak or have disappeared. The νCC modes are strong at 1476, 1362, and 1324 cm^{-1}. The 1324 cm^{-1} (νC_aN (I); δC_mH (δ)) band is unique to red excitation. The bands at 1148 (νC_aN(IV); $\delta C_aC_mC_a$ (α-δ)), 985 (δC_mC_aN (III); νC_9C_{10}), 920 (υCN; υCNC; υC_aC_b), and 831 cm^{-1}

are more intense in the 647 nm excited spectrum. Also, the band at 1230 cm^{-1} reappears with no band found at ca. 1215 cm^{-1}. As with 568.2 nm excitation, the low frequency region (800-200 cm^{-1}) has fewer bands and loses intensity when compared with the Soret and green excited spectra.

Excitation at 647 nm is in resonance with the $Q_{y(0,0)}$ transition. Although excitation at 457 (B_y) and 647 nm should enhance those vibrational modes aligned along the y-axis the most, the modes enhanced are not the same for both spectra. Thus, as was found with Chl *a*[19], it appears the Franck-Condon active modes are different for the B_y and Q_{y0} transitions. Changes in the ground state configurations with respect to the excited state are not the same for B_y and Q_{y0} excitation. Mattioli et al.[26] reported significant (ca. 40%) non-Condon activity within the Q_{y0} excitation region as a result of vibronic coupling to one or more of the B states for nickel pheophytin *a* (Chl *a* with Ni in place of Mg). This transition is not as strong for Chl *b* as for NiPheo *a* and Chl *a*. Thus, non-Condon activity via vibronic coupling to one or more of the B states may be more prevalent for Chl *b*.

Excitation further into the red at 676.2 nm produces a SERRS spectrum with a dramatic intensity decrease in the 1700-1400 cm^{-1} region in which the C-C pyrrole stretches are usually strong. Also, the low frequency region (below 745 cm^{-1}) contains only noise (not shown). The electronic absorption spectrum of Chl *b* (Figure 3-2) shows that 676 nm is near the

baseline of the $Q_{y(0,0)}$ transition. Perhaps the decrease in the Raman signal intensity with excitation at 676 nm is due to the loss of resonance enhancement at this wavelength. At any rate, 676 nm excites a different electronic transition than 647 nm. The two red excitation wavelengths produce very different SERRS spectra. In fact, although bands do occur that are found in the previous spectra, the 676 nm excited spectrum is different from the spectra obtained at other excitation wavelengths. Many bands are absent, but a new band appears at 887 cm^{-1}.

In general, excitation at 406 nm enhances the carbonyl and C_bC_b modes. These modes are also enhanced with excitation at 457 nm along with the 1230-250 cm^{-1} region, as well. With excitation at 514.5 nm the carbonyl bands are not enhanced and the strongest bands correspond to the macrocycle CC modes. Also, as with 568 nm excitation, a new band at 1213 cm^{-1} (νC_3C_3) appears and, as with 457 nm excitation, the 1000-250 cm^{-1} region is enhanced. The ester band at 1758 cm^{-1} and the macrocycle skeletal modes at 1615 and 1524 cm^{-1} are the most notable characteristics of the SERRS spectrum with 568 nm excitation. 647 nm excitation provides an enhanced 1480-830 cm^{-1} region. The bands at 1325 and 985 cm^{-1} were unresolved shoulders at all other excitation wavelengths. Furthermore, the 1230 cm^{-1} band returns to replace the band at ca. 1215 cm^{-1}. Excitation at 676 nm produces a weak spectrum in the 1610-1400 cm^{-1} region, most peaks found at the other excitation wavelengths in the

1200-1000 cm^{-1} region disappear, and the 700-200 cm^{-1} has no bands stronger than the noise. While the remaining regions contain bands similar to the other SERRS spectra at the other excitation wavelengths a new band appears at 887 nm.

A comparison of the SERRS spectra of Chl b with the SERRS spectra of Chl a[19] at the same excitation wavelengths shows many bands are common, but have different intensities. Interestingly, with Soret excitation, the υC_3=O of Chl b is much more intense than the υC_9=O of Chl a. While both Chl b and Chl a exhibit low frequency modes with 457 nm excitation, this region is more detailed and enhanced for Chl b. Also, the 500-200 cm^{-1} region of Chl b is very strong with excitation at 514 nm. This is not true for Chl a.

CONCLUSIONS

This paper is the first detailed comparison of the RR and SERRS spectra of Chl b under various excitation conditions. The RR spectra are in accordance with those recorded previously with Soret and green excitation. The agreement between the RR and SERRS spectra indicate that adsorption of Chl b does not structurally alter it or significantly perturb the electronic states that are found in the 406-568 nm range. The similarity of the RR and SERRS spectra also suggests an electromagnetic mechanism as the major contributor to the surface enhancement.

Although similar, considerable intensity differences occur between the RR and SERRS spectra. In addition, the band at ca. 1619 cm^{-1} in the RR spectra with Soret excitation disappears in the SERRS spectra. The 1619 cm^{-1} band is present also in the 514 and 568 nm excited RR spectra. However, even though it loses intensity at 514 nm excitation, the 1619 cm^{-1} band appears is the SERRS spectra, as well. These differences between the RR and SERRS spectra may reflect aggregation effects for the RR sample, as well as, the orientation of the macrocycle with respect to the electrode surface for the SERRS sample.

Most significantly, the fluorescence-quenching advantage of SERRS allows acquisition of SERRS spectra of Chl b by excitation within the lowest energy transition. The SERRS spectrum provides unique insights regarding the electronic

properties of this state. Excitation at 647 and 676 nm produce quite different SERRS spectra. The bands occurring in the 647 nm excited spectrum support the assignment of the $Q_{y(0,0)}$ transition as the main contributor at this excitation wavelength.

Previous RR studies included isolated chlorophylls and various photosynthetic preparations[8,26]. The results of this paper support SERRS as a viable technique to study intact photosynthetic preparations. Our previous studies of reaction centers[27], chromatophore preparations[28], and Chl *a*[19] have illustrated the potential of SERRS for investigating designated membrane components. The distance sensitivity of SERRS can be used to probe the spatial relationship of the constituents within various photosynthetic complexes with respect to each other and to the membrane surface (e.g., Chl *a* and Chl *b* within the LHC of green plants).

ACKNOWLEDGEMENTS

Ames laboratory is operated for the U.S. Department of Energy by Iowa State University under contract no. W-7405-Eng-82. This article was supported by the Division of Chemical Sciences, Office of Basic Energy Sciences.

REFERENCES

1. Glazer, A. N.; Anastasios, M. Ann. Rev. Plant Physiol. **1987**, 38, 11-45.
2. Mathis, P.; Rutherford, A. W. In Photosynthesis; Amesz, J., Ed.; Elsevier: Amsterdam, 1987; pp. 63-96.
3. Hansson, Ö; Wydrzynski, T. Photosyn. Res. **1990**, 23, 131-162.
4. a) Hall, D. O.; Rao, K. K. In New Studies in Biology Photosynthesis; Edward Arnold: London, 1987; pp. 37-47. b) Ibid. p.26.
5. Eads, D. D.; Castner, E. W., Jr.; Alberte, R. S.; Mets, L.; Fleming, G. R. J. Phys. Chem. **1989**, 93, 8271-8275.
6. Lutz, M.; Breton, J. Biochem. Biophys. Res. Commun. **1973**, 53, 413-418.
7. Lutz, M.; J. Raman Spectrosc. **1974**, 2, 497-516.
8. Lutz, M.; Robert, B. In Biological Applications of Raman Spectroscopy; Spiro, T. G., Ed.; John Wiley & Sons, Inc.: New York, 1988; Vol. 3, pp. 347-411.
9. Lutz, M.; Kleo, J.; Gilet, R.; Henry, M.; Plus, R.; Leickman, J. P. In Proceedings of the 2nd International Conference on Stable Isotopes; Klein, E. R., Klein, P. D., Eds.; U.S. Department of Commerce: Springfield, VA, 1975; pp. 462-469.
10. Fujiwara, M.; Tasumi, M. J. Phys. Chem. **1986**, 90, 250-255.
11. Hildebrandt, P.; Spiro, T. G. J. Phys. Chem. **1988**, 92,

3355-3360.

12. Weitz, D. A.; Garoff, S.; Gersten, J. I.; Nitzan, A. J. Chem. Phys. **1983**, 78, 5324-5338.

13. Cotton, T. M.; Schultz, S. G.; Van Duyne, R. P. J. Am. Chem. Soc. **1980**, 102, 7960-7962.

14. Cotton, T. M. In Spectroscopy of Surfaces; Clark, R. J. H., Hester R. E., Eds.; John Wiley & Sons: New York, 1988; Vol. 16, pp. 91-153.

15. Koglin, E.; Sequaris, J. -M. In Topics in Current Chemistry; Springer-Verlag: Berlin, 1986; Vol. 134, pp. 1-53.

16. Nabiev, I.; Efremov, R. G.; Chumanov, G. D. Sov. Phys. Usp. **1988**, 31, 241-262.

17. Uphaus, R. A.; Cotton, T. M.; Möbius, D. Thin Film Solids, **1986**, 132, 173-185.

18. Andersson, L. A.; Loehr, T. M.; Cotton, T. M.; Simpson, D. J.; Smith, K. M. Biochim. Biophys. Acta **1989**, 974, 163-179.

19. Thomas, L. L.; Kim, J. -H.; Cotton, T. M. J. Am. Chem. Soc. **1990**, 112, 9378-9386.

20. a) Strain, H. H.; Svec, W. A. In The Chlorophylls; Vernon, L. P., Seely, G. R., Eds.; Academic: New York, 1966; pp. 163-179. b) Strain, H. H.; Svec, W. A. In The Chlorophylls; Vernon, L. P., Seely, G. R., Eds.; Academic: New York, 1966; pp. 30-35.

21. Boldt, N. J.; Donohoe, R. J.; Birge, R. R.; Bocian, D. F. J. Am. Chem. Soc. **1987**, 109, 2284-2298.

22. Van Duyne, R. P. In Chemical and Biochemical Applications of Lasers; Moore, C. B., Ed.; Academic Press: New York,1979; Vol. IV, p. 101.

23. Moskovits, M. J. Chem. Phys. **1982**, 77, 4408-4416.

24. Thomas, L. L. Application of surface-enhanced resonance Raman spectroscopy to chlorophyll and chlorophyll derivatives; Ph.D. thesis, Iowa State University, Ames, IA, 1991, Chapter 1.

25. Andersson, L. A.; Loehr, T. M.; Cotton, T. M.; Simpson, D. J.; Smith, K. M. Biochim. Biophys. Acta **1989**, 974, 163-179.

26. Mattioli, T. A.; Haley, L. V.; Koningstein, J. A. Chem. Phys. **1990**, 140, 317-329.

27. Fonda, H. N.; Babcock, G. T. In Progress in Photosynthesis Research; Biggens, J., Ed.; Martinus Nijhoff Publishers: The Netherlands, 1987; Vol. I, pp. 1.4.449-452.

28. Cotton, T. M.; Van Duyne, R. P. FEBS Lett. **1982**, 147, 81-84.

29. a) Picorel, R.; Holt, R. E.; Cotton, T. M.; Seibert, M. In Progress in Photosynthesis Research; Biggins, J., Ed.; Martinus Nijhoff Publishers: The Netherlands, 1987; pp. 1.4.423-426. b) Picorel, R.; Holt, R. E.; Cotton, T. M.; Seibert, M. J. Biol. Chem. **1988**, 263, 4327-4380. c) Seibert, M.; Cotton, T. M.; Metz, J. G. Biochim. Biophys. Acta **1988**, 934, 235-246.

d) Picorel, R.; Lu, T.; Holt, R. E.; Cotton, T. M.; Seibert, M. Biochemistry **1990**, 29, 707-712.

SECTION 4. A ROUGHENED GOLD ELECTRODE AS A SURFACE-ENHANCED RESONANCE RAMAN SCATTERING SUBSTRATE FOR CHLOROPHYLL *a*, PHEOPHYTIN *a*, AND CHLOROPHYLL *b* WITH RED EXCITATION

ABSTRACT

Surface-enhanced resonance Raman scattering (SERRS) spectra are reported for chlorophyll b, chlorophyll a, and pheophytin a adsorbed at roughened silver and gold electrodes at 77 K with 647.1 and 676.4 nm excitation. A comparison of the SERRS spectra on Ag versus Au indicates a different molecular orientation and/or interaction at each surface. The Ag SERRS substrate produces better spectra with 647.1 nm excitation and the Au surface provides better enhancement at 676.4 nm excitation for all three pigments. Selective monitoring of chlorophyll a can be accomplished with excitation at 676.4 nm excitation because this wavelength produces a strong SERRS spectrum for chlorophyll a and weak spectra for chlorophyll b and pheophytin a. In contrast, chlorophyll b is is more strongly enhanced at 647.1 nm excitation than observed for chlorophyll a and pheophytin a. Also, excitation at 647.1 nm produces a SERRS spectrum with a distinct low frequency region which is unique to pheophytin a. These results show that SERRS obtained with red excitation offers considerable promise for selectively monitoring these photosynthetic pigments.

INTRODUCTION

Chlorophyll *a* (Chl *a*), pheophytin *a* (Pheo *a*), and chlorophyll *b* (Chl *b*) are involved in the harvesting, trapping, and the photoinduced conversion of light energy into chemical energy in green plants. It is accepted that Chl *a* and Chl *b* play important roles in harvesting light energy within the light harvesting complexes (LHC) of photosystems I and II (PS I and PS II, respectively). Much more is known about PS II because of its structural and functional similarities with the thoroughly studied bacterial reaction center (RC). Within the RC of PS II a specialized Chl *a* and Pheo *a* are the primary electron donor and acceptor, respectively. A Chl *a* dimer is generally considered as the primary electron donor and a specialized Chl *a* as the primary electron acceptor within the RC of PS I.

The involvement of these pigments in photosynthesis has generated a great deal of interest in identifying and determining their structural organization within the LHC and the RC. The structural information can provide insight regarding the mechanism by which light energy is transferred to and photoinduced charge separation occurs in the RC. A first step in resolving the nature of the interaction of these pigments *in vivo* is to study their properties individually *in vitro*. Absorption, fluorescence, NMR, CD, and MCD spectroscopies are techniques that have been used to study Chl *a*, Pheo *a*, and Chl *b*.[1-3] In addition, electronic absorption spectroscopy and ESR

have been employed to study the Chl a cation and Pheo a anion radicals.[4-10] Although these methods provide valuable information on the individual pigments, many of these techniques produce unresolved data in vivo. Infrared (IR) and Raman spectroscopy supply vibrational "fingerprints" that can identify a specific molecule. IR investigations of chlorophylls have provided information on hydrogen-bonding, ligation, and aggregation interactions.[12-17] Nabedryk et al. have reported FTIR difference spectra for the Chl a cation and Pheo a anion radicals.[17]

However, water absorbs strongly in the IR region which presents a problem for most biomolecules. Raman spectroscopy is free of this problem, but it is not a very sensitive technique. The sensitivity can be increased by exciting within an electronic transition of a molecule which is known as resonance Raman (RR) spectroscopy. RR also offers selectivity by preferrentially selecting an excitation wavelength that corresponds to an electronic transition for one molecule and not another. Several RR studies have appeared in the literature for Chl a, Pheo a, and Chl b.[18-28] In addition, RR spectroscopy has been employed to investigate electrochemically generated Chl a cation [29,30] and Pheo a anion [31] radicals.

On the other hand, fluorescence can overwhelm the RR signal of biomolecules. In fact intense fluorescence occurs when exciting into the lowest energy π^1-π^* transition of chlorophylls and pheophytins. Thus, the RR studies cited above

employed excitation wavelengths within 400-540 nm of the electronic absorption spectrum. Other methods have been employed in order to overcome the fluorescence interference. Höxtermann et al.[32] reported resonance CARS spectra of Chl *a* excited with 694.3 nm light. Recent studies by Andersson et al.[33] and Mattioli et al.[34] used chlorophyll derivatives which do not fluoresce from the Q_y transition as model compounds for Chl *a*.

Surface-enhanced resonance Raman scattering (SERRS) spectroscopy has proven to be a viable tool for obtaining spectra of highly fluorescent molecules. Adsorption of molecules on a SERS-active metal surface results in fluorescence quenching and can increase Raman scattering intensity by 10^3-10^6-fold.[35] Although the origin of this effect is not completely understood, it is generally accepted that there are two major classes of enhancement mechanisms. Electromagnetic mechanisms attribute the SERS enhancement to increased local electric field strengths at the metal surface. The increased field strength is due to excitation of the collective oscillations of the conduction electrons (surface plasmons) at the metal surface.[36-38] Molecular or chemical mechanisms attribute the enhanced scattering to the formation of new excited states via charge transfer (adatom) or to the formation of a molecule-metal complex.[39,40] Regardless of the origins of the enhancement, SERRS has been used to gain vibrational information for many biologically significant molecules.[44-46] Further-

more, SERRS spectra have been reported for chlorophylls and chlorophyll derivatives. Uphaus et al.[44] obtained SERRS spectra with 457.9 nm excitation for Chl _a_, bacteriochlorophyll _a_, and bacteriopheophytin _a_ monolayers on silver island films. Andersson et al.[33] reported a Q_y-excited SERRS spectrum of Chl _a_ multilayers on a silver film. Hildebrandt and Spiro[45] reported SERRS spectra of copper chlorophyllin _a_ which was adsorbed on colloidal silver or gold and excited within the blue and red regions of the electronic absorption spectrum. However, metal electrodes are preferable for SERRS studies of photosynthetic systems because electrogenerated radical species can be created and monitored with minimal sample manipulation and chemical interference. Heald[31] obtained the SERRS spectra of Pheo _a_ and the electrochemically generated Pheo _a_ anion radical using a silver electrode with Soret excitation. Also, Thomas et al.[46,47] obtained SERRS spectra of Chl _a_, Pheo _a_, and Chl _b_ with roughened Ag electrodes at 77 K using Soret through red excitation.

The SERRS spectra of the chlorophylls and Pheo _a_ demonstrate that the Ag electrode is a viable approach for obtaining spectra from the lowest energy electronic transition. In the past, Ag electrodes have been used extensively because it is possible to consistently roughen the electrode surface and obtain a SERS active substrate. Nevertheless, Ag is not stable within the electrochemical range needed to study electron transfer reactions involving Chl _a_, the electron donor of

Pheo a in the photoinduced charge separation process during photosynthesis. Fortunately, Au and Cu are also SERS active with red excitation and the former has a greater electrochemical range. However, until recently, it was difficult to obtain a roughened Au surface that was SERS active. Gao et al.[48] developed a computer controlled electrochemical roughening procedure for Au electrodes which consistently produces a SERS signal. Many of the early experiments performed with a roughened Ag electrode are now being repeated with the Au electrode. Improved methods for obtaining SERS from Cu electrodes are also being developed. Cu was not chosen for this study due to its increased reactivity and its limited electrochemical range. The Au electrode has the electrochemical and spectral range required for electron transfer SERRS studies of the photosynthetic pigments within their lowest energy π^1-π^* transitions.

This investigation presents the SERRS spectra of Chl a, Pheo a, and Chl b with excitation at 647.1 and 676.4 nm on roughened Ag and Au electrodes at 77K. A comparison of the SERRS spectra on Ag vs Au indicates a different molecular orientation and/or interaction at each surface. Also, the Ag electrode produces better enhancement with 647.1 nm excitation and the Au electrode provides a stronger SERRS spectrum, especially for Chl a, with excitation at 676.4 nm. In addition, 647.1 nm excitation produces a SERRS spectrum with a distinct high frequency region for Chl b which distinguishes

it from Chl *a* and Pheo *a*. Similarly, 647.1 nm excitation produces a Pheo *a* SERRS spectrum with a unique low frequency region not observed in the SERRS spectra of Chl *a* or Chl *b*.

EXPERIMENTAL

Sample Preparation. Chl *a* and Chl *b* (Figure 4-1.) were isolated from spinach according to an established procedure.[49] Pheo *a* (Figure 4-1.) was prepared by acidification of Chl *a* with HCl. All samples were purified by reverse phase high performance liquid chromatography (rp-HPLC).[46]

For SERRS experiments, after roughening, the electrode was rinsed with MeOH and then immersed in the chosen chlorophyll or pheophytin *a* fraction that had been separated by HPLC. The Chl *a*, Chl *b*, and Pheo *a* were adsorbed onto the electrochemically roughened electrode by dipping the electrode into the solution of purified compound (ca. 1 X 10^{-4} M in acetonitrile/methanol 3:1 v/v) for 25 minutes. The electrode was transferred to a quartz Dewar flask containing liquid nitrogen. The Dewar flask was constructed with a transparent body to allow direct acquisition of a SERRS spectrum during electrode immersion in liquid nitrogen. All sample manipulation and experimental operations were performed in subdued light.

The purity of the samples were monitored and confirmed before and after the Raman experiments by analytical rp-HPLC[46] and UV/VIS spectroscopy. Electronic absorption spectra were measured using a 1 mm pathlength cuvette and a Perkin Elmer Lambda 6 UV/VIS spectrophotometer.

Electrode Preparation. The Ag electrode preparation has been described previously.[46] A gold electrode was used as the

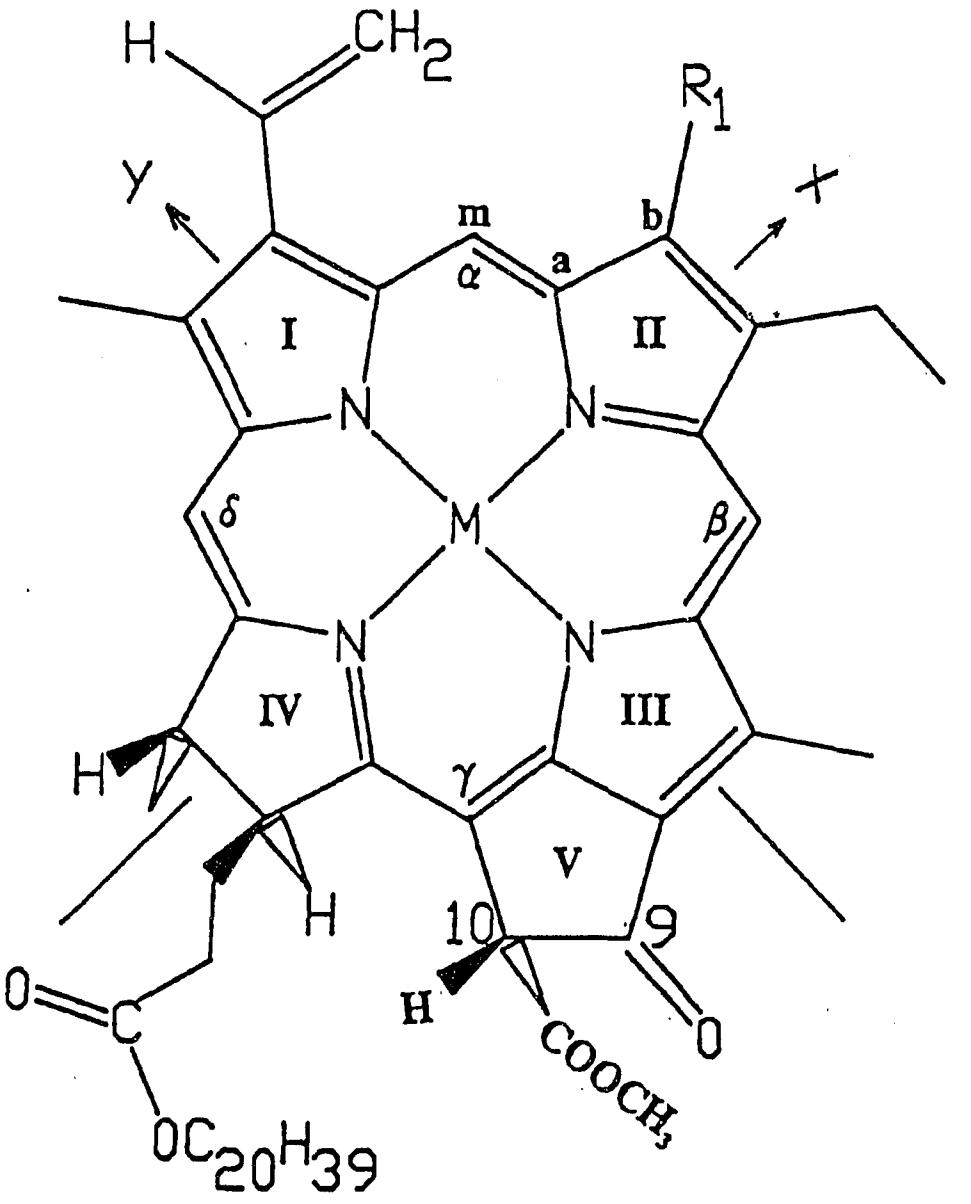

Compound	M	R_1
Chl b	Mg	HC=O
Chl a	Mg	CH_3
Pheo a	2 H	CH_3

Figure 4-1. Structures of Chl b, Chl a, and Pheo a.

second SERRS substrate. It was constructed by sealing a flattened gold wire into a glass tube with Torr Seal. The exposed surface was rectangular with dimensions ca. 4 X 6 mm. The electrode was polished with use of successive finer grades of alumina (0.3 to 0.05 um). The electrode was rinsed and sonicated between polishing steps. Following the polishing procedure the electrode was cleaned by cathodization at -2.2 V for ca. 5 seconds and roughened by successive computer-controlled oxidation reduction cycles.[48] A SSCE (silver/silver chloride electrode) was used as the reference electrode and a Pt wire served as the auxiliary electrode. The electrode potential was varied from -300 to +1200 mV for 25 cycles. It was held at positive potential for 3.0 seconds during each cycle. The roughening procedure was followed by a methanol rinse and transfer of the electrode to the sample.

SERRS Spectroscopy. Laser excitation was provided by a Coherent Innova 100 Kr^+ laser (647.1 and 676.4 nm). The laser power was 10 mW for all the spectra reported here. Raman scattered light was collected in a back-scattering geometry. Spectra were recorded with a Spex Triplemate spectrometer coupled to a Princeton Applied Research Corporation (PARC) Model 1421-R-1024HD intensified SiPD detector cooled to -40°C. The spectra were collected and processed with an OMA-3 (PARC) optical multichannel analyzer. The reported spectra are composites of 15 scans with a 5 second integration period per scan.

RESULTS

Electronic Absorption Spectra (Figure 4-2). The red regions of the electronic absorption spectra of Chl a, Pheo a, and Chl b are shown in Figure 4-2 (a,b,c). These bands are assigned as vibronic bands belonging to the Q_y and Q_x transitions.[49,50] According to the linear dichroism and fluorescence polarization studies of Fragata et al.[50], the 618 nm band in the absorption spectrum of Chl a (Figure 4-2a) belongs to the $Q_{x(0,0)}$ and the 663 nm band to the $Q_{y(0,0)}$. For Pheo a (Figure 4-2b), the same study determined that the 605 nm band includes a major contribution from the Q_x transition. Also, the band at 665 nm includes overlapping contributions from both the $Q_{x(0,0)}$ and $Q_{y(0,0)}$ with the $Q_{x(0,0)}$ contribution occurring near 660 nm. In Chl b (Figure 4-2c), the x and y polarized components of the Q transition are closer in energy than those in Chl a and Pheo a. Thus, the fluorescence polarization data provided the assignment of only the 647 nm band in the red region and this band has a major contribution from the $Q_{y(0,0)}$ transition.[51] Excitation wavelengths of 647.1 and 676.4 nm were used in the Raman experiments. These laser lines fall within the $Q_{y(0,0)}$ transition for all three pigments.

SERRS. Figure 4-3 compares the SERRS (77 K) of Chl b using a roughened Ag electrode versus a roughened Au electrode with excitation at 647.1 and 676.4 nm. The same is shown for Chl a and Pheo a in Figures 4-4 and 4-5, respectively. Figures 4-6 and 4-7 are comparisons of the SERRS spectra of Chl

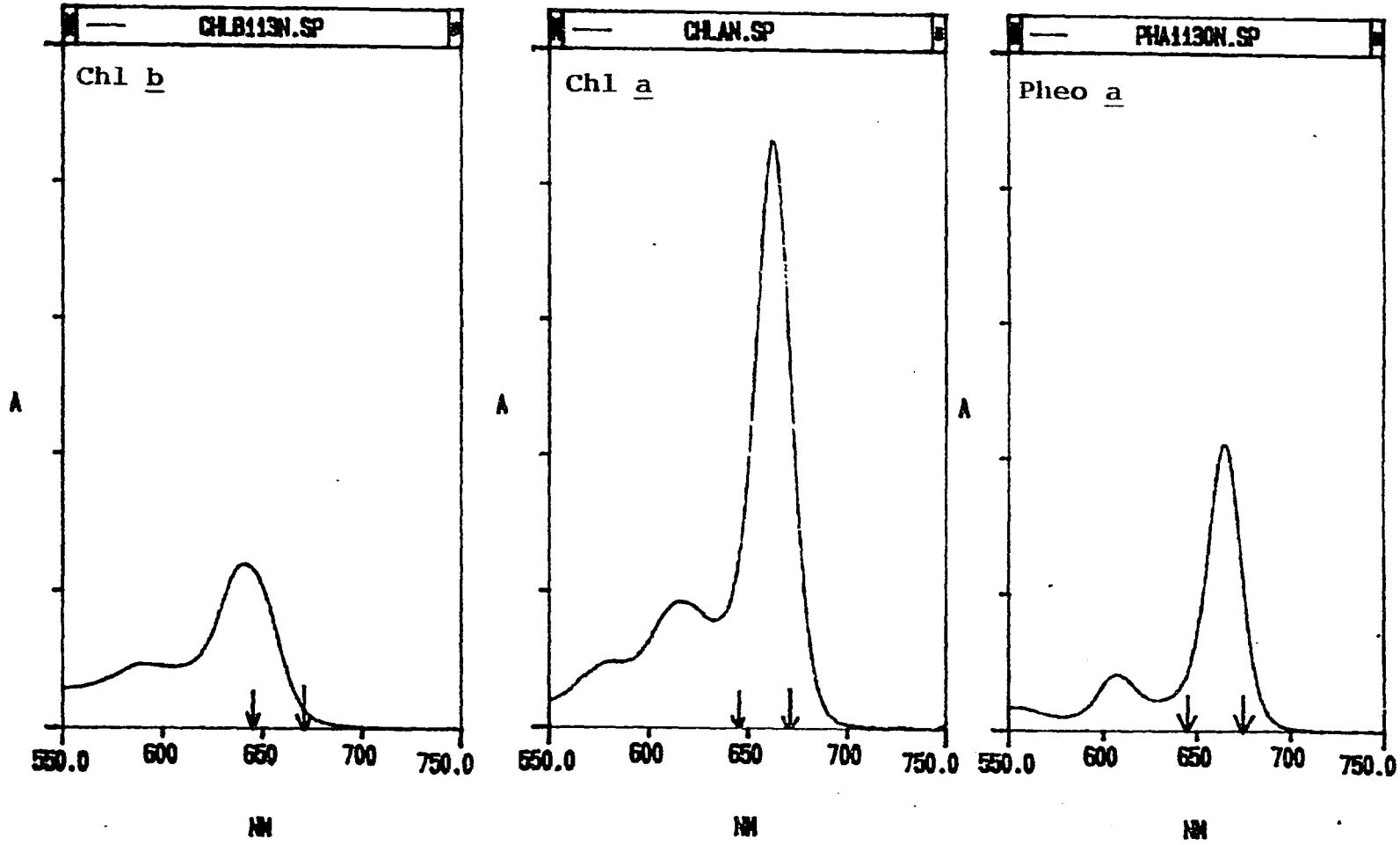

Figure 4-2. Red regions of the absorption spectra of Chl b, Chl a, and Pheo a.

b, Chl a, and Pheo a on Au with excitation at 647.1 and 676.4 nm, respectively. The uncertainty in frequency assignments is ±5 cm^{-1}. Table 4-1 lists the major bands that occur with red excitation for Chl b, Chl a, and Pheo a. The assignments are based on those proposed by Lutz,[18,27] Boldt et al.,[52] and Fonda et al.[53]

Table 4-1. Average Value of the Major SERRS (Ag, Au) Frequencies (cm^{-1}) with excitation at 647.1 and 676.4 nm.

Chl b	Chl a	Pheo a	Assignment[a]
1612			
1603	1604	1607	$\nu C_aC_m(\alpha,\beta)$
		1582	$\nu C_bC_b(I);\nu C_aC_b(III)$
1565	1550		$\nu C_aC_b(III);\nu C_bC_b(I)$
1520	1535	1535	$\nu C_bC_b(I);\nu C_aC_b(III)$
1480	1488	1490	$\nu C_aC_m(\delta);\nu C_aC_b(I)$
	1437	1448	$\nu C_aC_m(\gamma,\delta);\nu C_aC_b(I\text{-}III)$
1428		1408	
1392	1384		$\nu C_aC_b(II);\nu C_aC_m(\alpha,\delta)$
1361		1366	$\nu C_aN(I);\delta C_mH(\alpha)$
1352	1350	1350	$\nu C_aN(IV);\nu C_aN(I,III)$
1323	1327		$\nu C_aN(I);\delta C_mH(\alpha)$
1290	1282		$\delta C_mH(\alpha,\beta);\nu C_aN(II,IV)$
1228	1228	1225	$\gamma C_mH(IV);\delta C_mH(\delta)$
1186	1185		$\nu C_mC_{10}(V);\nu C_bH(IV)$
1148	1146	1152	$\nu C_aN(II);\nu C_aNC_a(I)$
		1134	$\nu C_aC_b(IV);\nu C_aC_mC_a(\alpha,\beta,\gamma)$
	1110	1125	$\nu C_aC_b(IV);\nu C_bS$
		1090	$\nu C_aC_b(III,IV);\nu C_aN(I,III)$
	1071		$\nu C_aC_m(\alpha);\nu C_aN(I,IV)$
	1052		$\nu C_aN(II);\delta C_mC_aN(II);\nu C_bS$
		1037	$\nu C_aN(III);\nu C_bS$

[a]Assignments based on those reported by Lutz[18,27], Boldt et al.[52], and Fonda et al.[53] Mode descriptions are ν = stretch, δ = in-plane deformation, and γ = out-of-plane deformation. C_a, C_b, C_m and the other characters in parentheses refer to the macrocycle position shown in Figure 4-1.

Table 4-1. Continued

Chl b	Chl a	Pheo a	Assignment[a]
985	988	980	$\delta C_m C_a N(III); \nu C_9 C_{10}$
930	935	935	$\delta \nu C_a C_b S$
920	918		$\delta \nu C_a C_b S$
887	889	887	
838	838	835	
	790		
	753	772	
750	745	745	$\delta \nu C_a C_b S$
		730	
690	690	675	$\delta \nu C_a C_b S$
620		618	
		602	
	592	592	
	569	565	
553			
531			
	519		
	507	512	
	473		
404	402	397	
350	353	345	
	262	250	

DISCUSSION

Ag vs. Au. Chl b (Figure 4-3). Both the roughened Ag and Au electrodes produce highly detailed SERRS spectra of Chl b. However, the Ag electrode appears to produce the spectrum with the best S/N ratio in the high frequency region. In the low frequency region the S/N is about the same for both electrodes at both excitation wavelengths. While similar bands appear with both SERRS substrates, the intensity patterns differ, especially in the 1400-1100 cm^{-1} region. With 647.1 nm excitation the bands at ca. 1324, and 1152 cm^{-1} bands are weaker with the Au electrode. In contrast, the 1264 cm^{-1} band, which is not observed in the Ag electrode spectrum, is a medium intensity band. Also, the 930/920 cm^{-1} doublet in the Ag SERRS spectrum is a strong band at 930 cm^{-1} with a 920 cm^{-1} shoulder.

A comparison of Ag vs. Au with 676.4 nm excitation also reveals similar bands in both spectra that differ in relative intensity in the 1400-1100 cm^{-1} region. The band at ca. 1228 cm^{-1} band is less intense in the Au spectrum, but the 1186, 1152, 985, and 748 cm^{-1} bands are stronger.

Thus, for Chl b Ag produces stronger surface-enhanced Raman signals than Au with 647.1 nm excitation, but the reverse is true for excitation at 676.4 nm. Also, a comparison of the SERRS spectra obtained on Ag and Au at both excitation wavelengths shows that some bands differ in relative intensity in the 1400-1100 cm^{-1} region. These differences may indicate a

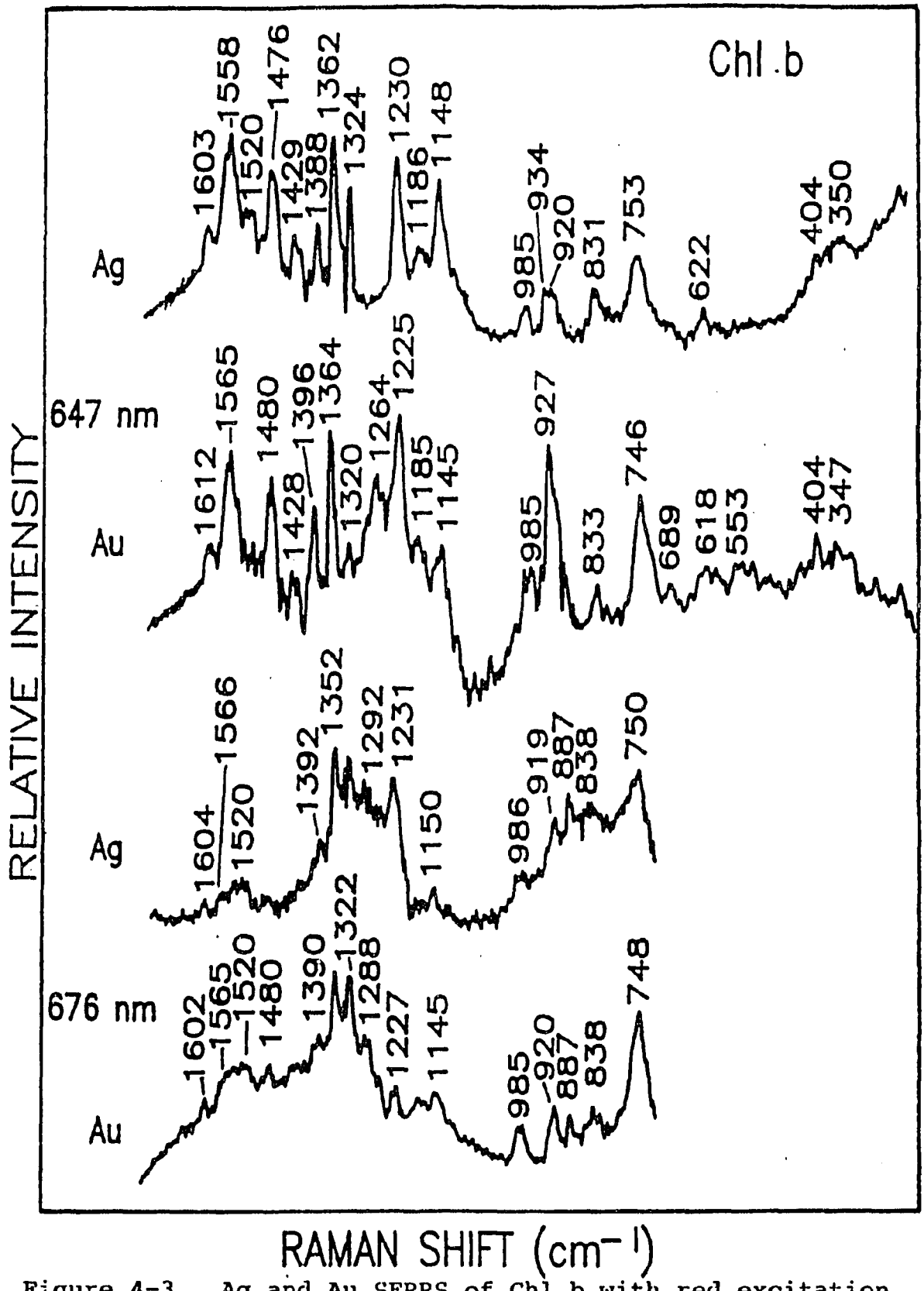

Figure 4-3. Ag and Au SERRS of Chl b with red excitation.

different interaction and/or orientation at the Ag surface as compared to the Au surface. These bands correspond to C_aN stretching and C-H bending modes. It appears that the C_aN stretching modes (1324 and 1148 cm^{-1}) are more strongly enhanced on the Ag surface. On the other hand, the Au surface enhances the C-H and C_aC_bS bending modes (1264, 1225, 930/920 cm^{-1}). Results by Thomas et al.[47] suggest a slanted edgewise orientation of the macrocycle with respect to the Ag electrode surface. The edge and angle of orientation cannot be determined from this data. Future LB monolayer studies may provide this information. Perhaps, at the Au surface, the molecule is adsorbed at the edge of a single pyrrole ring rather than on the edge of two pyrrole rings. This would bring the C_aN stretches to a more parallel orientation with respect to the electrode surface. According to SERS theory, those modes whose polarizability tensors are aligned perpendicular to the surface are most enhanced.[54,55] Thus, the C_aN vibrations would not be as strongly enhanced as is the case with the Ag surface. If indeed the macrocycle is oriented at the edge of a single pyrole ring this would align the C-H(1264 and 1225 cm^{-1}) and C_aC_bS in-plane bending modes perpendicular to the Au surface and enhance these bands.

The manner in which the molecule orients and/or interacts at the electrode surface depends on the physical properties of the molecule and the electrode surface. Several SERS studies have reported the presence of metal salts at the roughened

Ag[56-60] and Au[61,62] electrodes. In accordance with these findings, Ag_2SO_4(s) forms on the Ag electrode surface during roughening conditions and $AuCl_3$(s) is formed on the Au electrode surface. Ag_2SO_4(s) is ionic with a rhombic structure that is insoluble in alcohol and only slightly soluble in water. $AuCl_3$(s) exists as Au_2Cl_6 in solid form and has a planar configuration. In contrast to Ag_2SO_4(s), Au_2Cl_6(s) is very soluble in water and is also soluble in alcohol and ether. $AuCl_4^-$ is the species found in aqueous solutions. After the roughening process, all electrodes were rinsed with MeOH to remove as much of the electrolyte as possible before dipping them into the samples (ca. 1 X 10^{-4} M in ACN/MeOH 3:1 v/v). Nevertheless, the differences between the Ag and Au SERRS spectra may be due to the interaction of the molecule with the as ions salt at the electrode surface.

In previous SERRS studies of Chl *b*, Chl *a*, and Pheo *a*[47] adsorbed on roughened Ag electrodes it was concluded that an electromagnetic mechanism is the major source of the surface enhancement rather than a chemical mechanism (e.g,. a charge-transfer complex between the pigment and the metal). Although some discrepancies occur when comparing the Ag and Au SERRS spectra, the overall similarity in the intensity pattern indicate that, as with the Ag electrode, an electromagnetic mechanism appears to be the major source of surface enhancement at the roughened Au electrode.

A comparison of the SERRS spectra of Chl *b* at 647 and 676

nm excitation shows that the spectra excited at 647 nm are more enhanced than at 676 nm excitation. The electronic absorption spectrum of Chl b (Figure 4-2a) shows that 647 nm corresponds to the maximum of the $Q_{y(0,0)}$ transition. In contrast, 676 nm is near the red edge of the absorption band. Perhaps the decrease in the Raman signal intensity with excitation at 676 nm is due to the loss of resonance enhancement at this wavelength. In general, when using 676 versus 647 nm excitation there is a dramatic decrease in intensity for the 1700-1400 cm^{-1} region in which the the C-C pyrole stretches are usually strong. Furthermore, the low frequency region (below 745 cm^{-1}) contains no bands. It is interesting to note that at 676 nm excitation the 1362 cm^{-1} band found in the 647 nm excited spectrum disappears and is replaced with a band at 1352 cm^{-1}. Also, a new band appears at 887 cm^{-1} with 676 nm excitation. Boldt et al.[52] assigned the band at 1362 cm^{-1} to νC_aN (I)/δC_mH (α) and the 1352 cm^{-1} band to νC_aN (IV)/νC_aN (I,III). C_aN (I) is aligned along the y axis of the chlorophyll macrocycle (Figure 4-1) and C_aN (IV) along the x axis. Modes containing bands that are parallel to the electronic transition dipole moment and that are distorted in the excited state are expected to undergo the strongest enhancement.[63] Thus, the mode involved at 676 nm excitation must contain an x-polarized component that dominates the y-polarized component and, therefore, the 1352 cm^{-1} band appears.

Chl a (Figure 4-4). As with Chl b, when comparing the

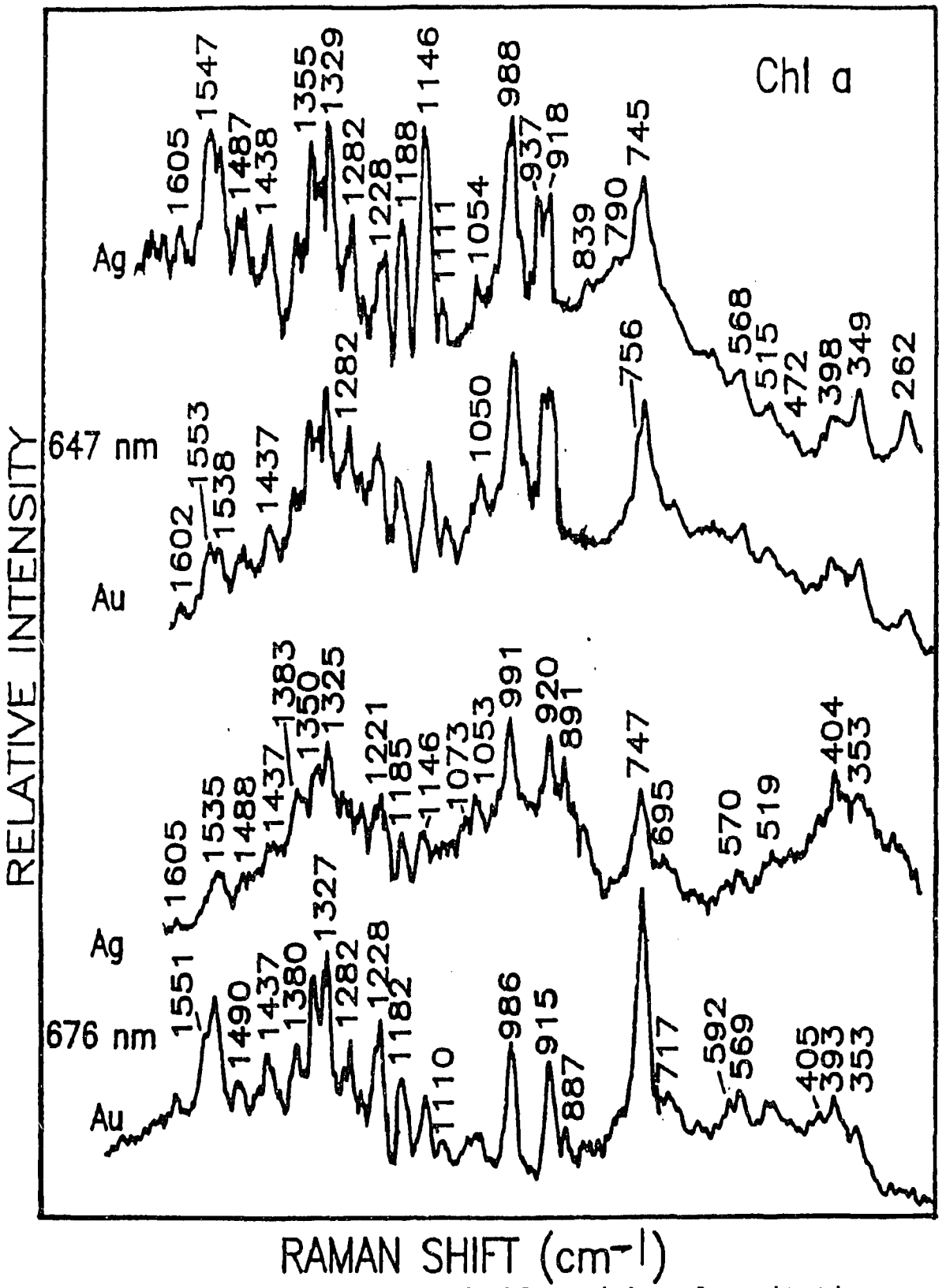

Figure 4-4. Ag and Au SERRS of Chl a with red excitation.

SERRS spectra of Chl a obtained with 647 nm excitation using Ag versus Au electrodes some relative intensity differences occur. The spectrum produced with the Au electrode has a medium intensity band at 1553/1538 cm^{-1} (νC_aC_b (III); νC_bC_b (I)). This band is twice as strong with Ag as the SERRS substrate. The bands at 1188 (νC_mC_{10} (V); νC_bH (IV)) and 1146 cm^{-1} (νC_aN (II); νC_aNC_a (I)) also decrease in intensity when using the Au electrode. On the other hand, bands at 1054 (νC_aN (III)), 988 (νC_mC_aN (III); νC_9C_{10} (V)) and 937/918 (δC_aC_bS) increase in intensity on the Au electrode.

Excitation at 676 nm also produces Chl a SERRS spectra in which some bands differ in relative intensity on a Ag versus a Au surface. The Au electrode provides a spectrum with a higher S/N ratio and the bands at 1551/1532 (νC_aC_b (III); νC_bC_b (I)), 1228 (γC_bH (IV); δC_mH (δ)) and 743 (δC_aC_bS) cm^{-1} are more intense than in the Ag SERRS spectrum. Again, as mentioned above with Chl b, these relative intensity differences may result from the interaction and/or orientation of the molecule at the electrode surface. The orientation of Chl a at the Ag and Au electrode surface depends on the physical properties of both Chl a and the metal electrode surfaces as discussed in the previous section.

A comparison of the Au SERRS spectra at the two excitation wavelengths reveals that 676 nm excitation produces a SERRS spectrum that, although similar, is distinct from the 647 nm excited spectrum. The bands at 1553/1538 (νC_aC_b (III);

νC_bC_b (I)), 1228 (γC_bH (IV); δC_mH (δ)) and 748 (δC_aC_bS) cm^{-1} are stronger with 676 nm excitation. The bands at 1282 (δC_mH (α,β); νC_aN (II,IV)), 1143 (νC_aN (II); νC_aNC_a (I)) and 1110 cm^{-1} (νC_aC_b (IV); νC_bS) are more intense with 647 nm excitation. Note also the absence of the 262 cm^{-1} band and the appearance of the 887 cm^{-1} band in the 676 nm excited spectrum. In addition, bands that have shoulders or are doublets with 647 nm excitation (i.e., 986 (δC_mC_aN (III); νC_9C_{10}), 932/918 (δC_aC_bS), and 756/748 cm-1 (δC_aC_bS)) are sharp bands at 986, 915, and 743 cm^{-1} with excitation at 676 nm. In fact, the 743 cm^{-1} band is the most intense band in the 676 nm excited spectrum.

The excitation lines at 647 and 676 nm fall on opposite sides of the 663 nm band in the electronic absorption spectrum of Chl a (Figure 4-2b). From the above comparison it appears that excitation with 647 nm may involve overlapping transitions that are oppositely polarized (i.e. one is aligned along the x axis and the other is aligned along the y axis). Thus, the C_aN (II,IV) and C_aC_b (IV) stretches, which lie along the x axis, are enhanced and appear as the 1282, 1143, and 1110 cm^{-1} bands. In contrast, excitation at 676 nm appears to fall within the $Q_{y(0,0)}$ transition. Consequently, the C-C (I,III) and C-N (I,III) pyrrole modes (1553/1538, 1350, 1327 cm^{-1}) which are aligned parallel to the y axis of the Chl a macrocycle are enhanced and appear as strong bands.

These results support the linear dichroism and fluorescence polarization study on Chl a by Fragata et al.[50] in which

it is reported that at 670 nm 100% of the fluorescence intensity is due to the $Q_{y(0,0)}$ transition. However, at 649 nm 14% is due to the $Q_{y(0,0)}$ and at 635 nm 9% is due to the $Q_{x(0,0)}$ transition. Clearly, 647nm radiation excites both the $Q_{x(0,0)}$ and $Q_{y(0,0)}$ electronic transitions. Perhaps excitation of both the x and y polarized components by 647 nm excitation explains the presence of the doublets found in the 1000-700 cm^{-1} region which do not occur with 676 nm excitation. This also suggests that the bands at ca. 918 and 745 cm^{-1} are due to δC_aC_bS modes on rings I and III and the bands at 932 and 756 cm^{-1} are due to δC_aC_bS modes on rings II and IV.

Pheo a (Figure 4-5). Attempts to obtain a SERRS spectrum of Pheo a using a roughened Ag electrode at 676 nm excitation were unsuccessful due to overwhelming fluorescence. Therefore, excitation at 647 nm will be used to compare the Pheo a SERRS spectra using Ag versus Au electrodes. Overall, Pheo a on both surfaces shows fluorescence interference in the high frequency region and the C-C pyrole stretches which are strong at other excitation wavelengths are weak with red excitation. The roughened Au electrode provides much better S/N in the 1300-900 cm^{-1} region compared with the Ag electrode. This region includes C_aN, C_mC_aN stretching and $C_aC_mC_a$, C_mH, and C_bH deformation modes (III,IV). In the low frequency region (below 900 cm^{-1}) the Pheo a SERRS spectra obtained with both surfaces are identical at 647 nm excitation.

A comparison of the 647 excited Pheo a Au SERRS spectrum

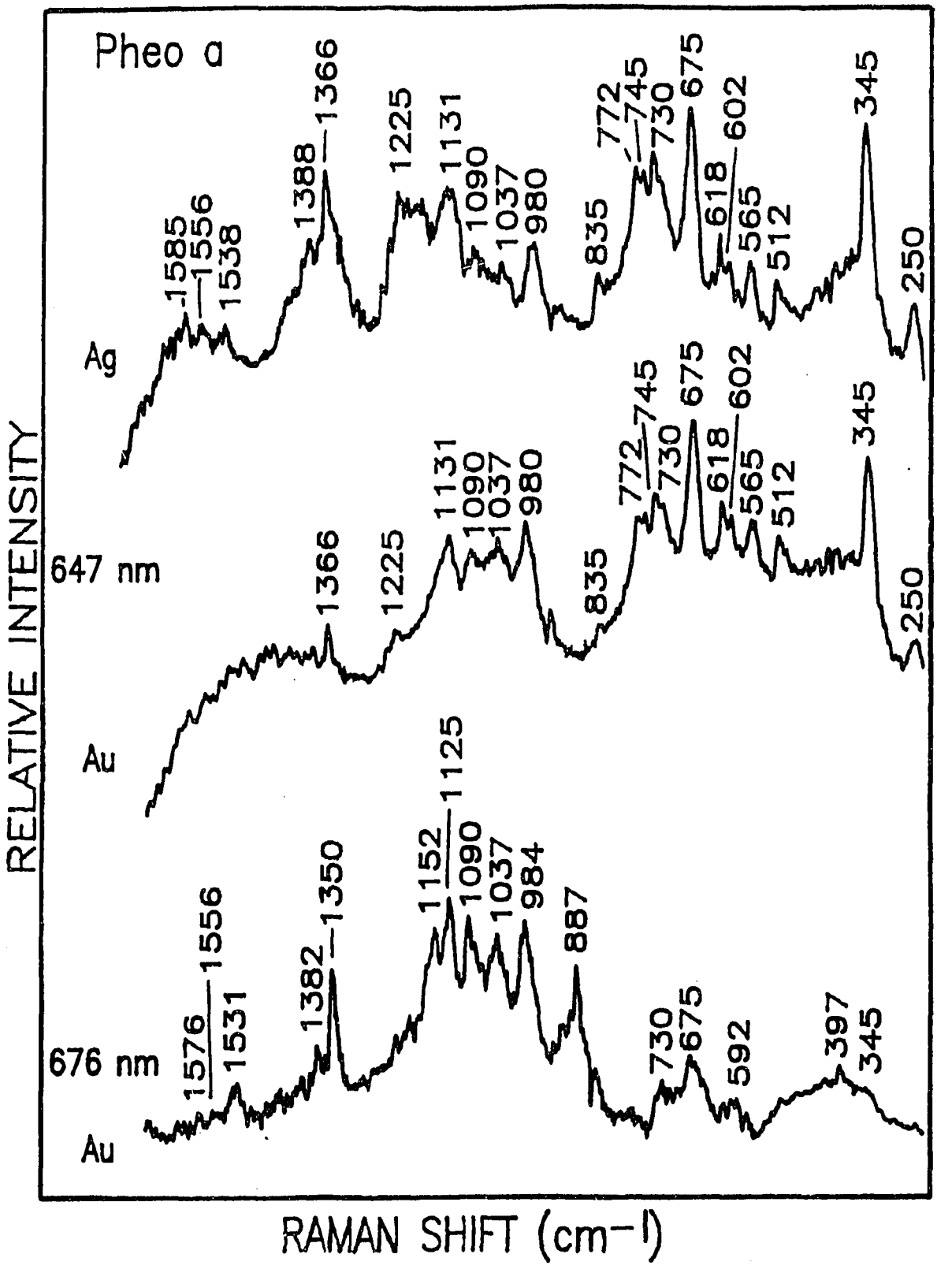

Figure 4-5. Ag and Au SERRS of Pheo a with red excitation.

versus the 676 nm spectrum shows that the high frequency region at both excitation wavelengths suffers from fluorescence interference and contains weak Raman peaks. Also, it is interesting to note that, as with Chl b, 647 nm excitation produces a 1366 cm^{-1} band that disappears and is replaced with a band at 1350 cm^{-1} with excitation at 676 nm. In general, excitation at 676 nm provides stronger Raman signals than 647 nm excitation in the 1160- 800 region, but the opposite is true for the 800-200 cm^{-1} region. The two red excitation wavelengths produce quite different intensity patterns in the 1300-800 cm^{-1} region. At 647 nm excitation weak bands at 1265, 1225 (δC_bH (IV); δC_mH (δ), 935, and 835 cm^{-1} appear. These bands do not occur with 676 nm excitation and new bands appear at 1152 (νC_aN (IV); $\delta C_aC_mC_a$ ($\alpha,\beta,\gamma,\delta$)), 1125 ($\nu C_aC_b$ (IV); νC_bS), and 887 cm^{-1}. The 1090 (νC_aC_b (III,IV);νC_aN (I,III)), 1037 (νC_aN (III); νC_bS), and 984 cm^{-1} (νC_mC_aN (III); νC_9C_{10} (V)) bands are common to both excitation wavelengths.

The relative intensity pattern also differs between the two red excitation wavelengths in the low frequency region (below 800 cm^{-1}). Excitation at 647 nm gives the strongest Raman signal. The 675 cm^{-1} band has the greatest intensity in this region for both wavelengths. However, with 676 nm excitation a loss of the 835, 565, 345, and 250 cm^{-1} bands occurs. Also, the 772/745 cm^{-1} shoulders disappear to leave only the 730 cm^{-1} band. Likewise, the 618/602 cm^{-1} doublet in the 647 nm excited spectrum is replaced by a weak 592 cm^{-1} band in the 676

nm excited spectrum. The lower frequency bands have not yet been assigned.

The vibrations aligned along the y-axis of the Pheo a macrocycle (Figure 4-1), i.e., in rings I and III, yield the strongest Raman signal with 676 nm excitation. However, these bands are fairly intense with 647 nm excitation as well. Also, the new bands that appear with 676 nm excitation are modes aligned along the y-axis (ring IV). This indicates that, as with Chl a and in agreement with Fragata et al.[50], the 665 nm band in the electronic absorption spectrum of Pheo a is a mixture of the Q_x and Q_y transitions.

Chl b, Chl a, Pheo a at a Au Electrode. Excitation at 647 nm (Figure 4-6). Although the Au SERRS spectra of Chl b, Chl a, and Pheo a obtained at 647 nm excitation have similar bands, each spectrum is unique with respect to relative intensities. The SERRS spectrum of Chl b is strong in the high frequency region (1700-1150 cm^{-1}) whereas the SERRS spectrum of Chl a is fairly strong only in the 1350-1150 cm^{-1} regio. Pheo a is very weak between 1700-1150 cm^{-1} and will not be discussed. Chl b and Chl a can be distinguished within the 1700-1150 cm^{-1} region of the SERRS spectra by the presence of the 1560, 1480, 1428 and 1392 cm^{-1} bands in the Chl b spectrum versus the 1553/1538, 1490, 1437, and 1385 cm^{-1} bands of Chl a. The remaining portions of the high frequency region are similar with bands of differing relative intensities. In the Chl b SERRS spectrum the bands at 1349 and 1226 cm^{-1} are strongest,

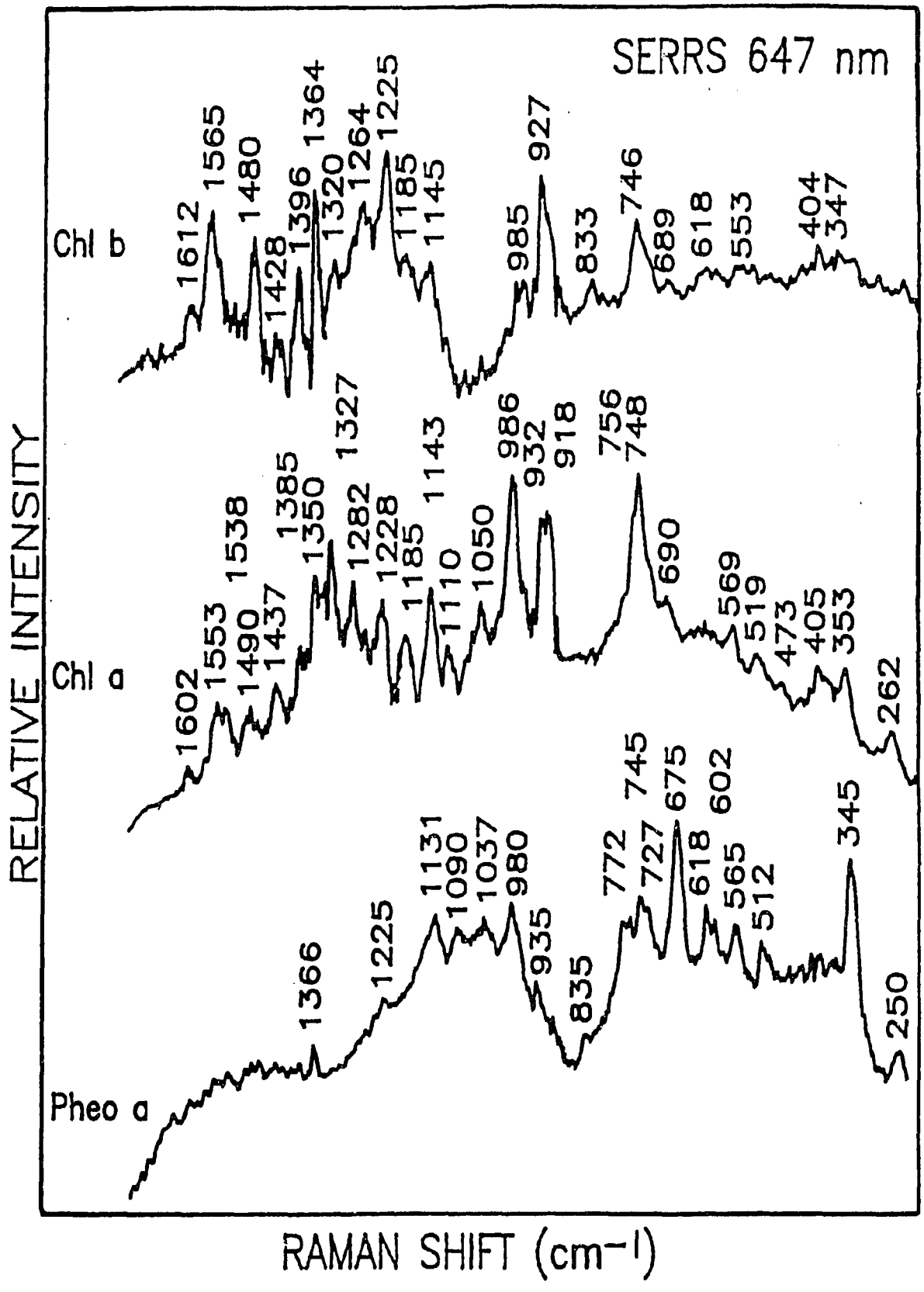

Figure 4-6. Au SERRS of Chl b, Chl a, and Pheo a (647 nm).

whereas in the Chl a SERRS spectrum the band at 1327 cm^{-1} is strongest with medium intensity bands at 1282, 1228, and 1185cm^{-1}. Also, Chl b has no bands between 1150 and 1000 cm^{-1}. Unlike Chl b, Chl a and Pheo a have bands within the 1150-1000 cm^{-1} region and each are distinct. Chl a has bands at 1143, 1110, and 1050 cm^{-1} in contrast to the bands at 1131, 1090, and 1037 cm^{-1} in the Pheo a SERRS spectrum.

In the 1000-800 cm^{-1} region all three pigments have several bands in common. The weak 985 cm^{-1} band in the Chl b SERRS spectrum appears as a strong band at 986 cm^{-1} in the Chl a spectrum and a medium band at 980 cm^{-1} in the Pheo a spectrum. In contrast, a very strong band occurs in the Chl b SERRS spectrum at 922 cm^{-1} which is a fairly strong doublet for Chl a and a weak 935 cm^{-1} band for Pheo a. Also noteworthy is the 838 cm^{-1} band that appears in the Chl b spectrum, but occurs only as very weak shoulders in the Chl a and Pheo a spectra.

The low frequency region (800-200 cm^{-1}) for Chl b and Chl a are very similar. Both have very strong bands at ca. 745 cm^{-1} with the remaining bands weak-medium in intensity. On the other hand, the Pheo a SERRS spectrum in this region is unique and very distinct from Chl b and Chl a. In the Pheo a SERRS spectrum a medium-weak triplet at 772/745/727 cm^{-1} occurs with a strong band at 675 cm^{-1}. Furthermore, a strong band appears at 345 cm^{-1} which is weak for Chl b and Chl a. Pheo a has a band at 250 cm^{-1} which corresponds to the 262 cm^{-1} band for Chl a.

The results at 647 nm indicate that, if monitoring a system with all three pigments present, Chl b can be distinguished from Chl a by the presence of the 1565 cm^{-1} band versus the 1553/1538 cm^{-1} band of Chl a (Pheo a has no strong bands in this region) and also by the lack of bands in the 1150-1000 cm^{-1} region for Chl b. Pheo a can be distinguished from both Chl a and Chl b by its distinct 800-200 cm^{-1} region. Thus, using a roughened Au electrode to observe these individual pigments *in vivo* at 647 nm excitation should be possible.

Excitation at 676 nm (Figure 4-7). In general, the entire Chl a SERRS spectrum is much more intense with a larger S/N than Chl b or Pheo a. In contrast to the SERRS spectra at 647 nm excitation, Chl b and Pheo a are much weaker with a lower S/N.

It is clear that Chl a could be monitored selectively over Chl b and Pheo a *in vivo* using a roughened Au electrode with 676 nm excitation. This wavelength produces a Chl a SERRS spectrum that overwhelms the Raman signals from Chl b and the fluorescence interference from Pheo a.

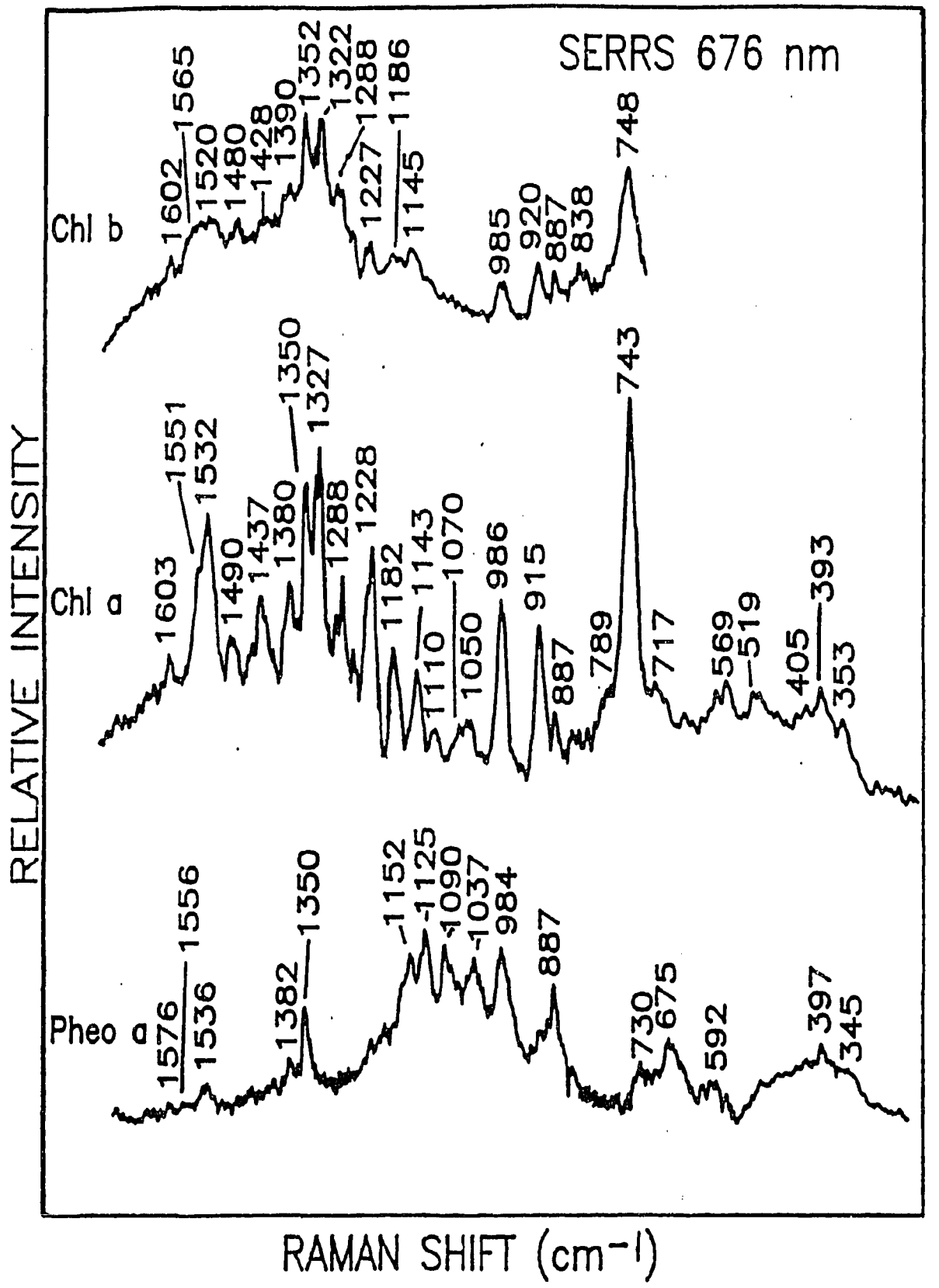

Figure 4-7. Au SERRS of Chl b, Chl a, and Pheo a (676 nm).

CONCLUSIONS

This report presents the first SERRS spectra of Chl b, Chl a, and Pheo a with excitation at 647 and 676 nm using a roughened Au electrode as the SERS substrate. Distinct SERRS spectra were observed for each pigment at both excitation wavelengths. A comparison of the Ag versus Au SERRS spectra show some relative intensity differences for a few bands. These differences may be due to the differences of the physical properties of the metal salt formed during the roughening process at each electrode and the interaction of the molecule at these surfaces. In any case, the SERRS intensity frequencies are similar enough to suggest that surface enhancement at the Au electrode, as with the Ag electrode, results primarily from an electromagnetic mechanism.

A comparison of the Au SERRS spectra at 647 versus 676 nm excitation reveals an enhanced Chl b spectrum with 647 nm excitation, in contrast to, a strong Chl a spectrum with excitation at 676 nm. Pheo a displays a very weak high frequency region with both excitation wavelengths, but produces a low frequency region distinct from Chl a and Chl b with 647 nm excitation.

Several intact photosynthetic complexes have been studied using RR spectroscopy.[64-67] Nevertheless, it has not been possible to observe RR scattering from these systems or their isolated pigments with excitation wavelengths in resonance with Q_y because of intense fluorescence emission. SERRS has

also been used to investigate reaction centers[68] and chromatophore preparations[69] using Soret excitation. SERRS offers a viable approach for the study of intact photosynthetic preparations with excitation within the Q_y because of the fluorescence quenching advantage. In addition, employing Ag and Au electrodes as SERRS substrates provides the ability to control the potential at an electrode surface. Therefore, SERRS may be valuable for obtaining spectra at fixed redox states of the reaction center.

ACKNOWLEDGEMENT

Ames laboratory is operated for the U.S. Department of Energy by Iowa State University under contract no. W-7405-Eng-82. This article was supported by the Division of Chemical Sciences, Office of Basic Energy Sciences.

A special thanks to Joe Franek for his technical assistance with the computer program that controls the ORC for Au roughening.

REFERENCES

1. The Chlorophylls; Vernon, L. P., Seely, G. R., Eds.; Academic: New York, 1966.
2. Katz, J. J.; Shipman, L. C.; Cotton, T. M.; Janson T. R. In The Porphyrins; Dolphin, D., Ed.; Academic: New York, 1978; Vol. V, Part C, pp 401-458.
3. Loach, P. A. In Progress in Bioorganic Chemistry; Kaiser, E. T., Ed.; John Wiley: New York, 1978; pp 91ff.
4. Davis, M. S.; Forman, A.; Fajer, J. Proc. Natl. Acad. Sci. U.S.A. **1979**, 76, 4170-4174.
5. Horning, T. L.; Fujita, E.; Fajer, J. J. Am. Chem. Soc. **1986**, 108, 323-325.
6. Fajer, J.; Forman, a.; Davis, M. S.; Spaulding, L. D.; Brune, D. C.; Felton, R. H. J. Am. Chem. Soc. **1977**, 99, 4134-4140.
7. Borg, D. C.; Forman, A.; Fajer, J. J. Am. Chem. Soc. **1976**, 98, 6889-6893.
8. Fajer, J.; Fujita, I.; Forman, A.; Hanson L. K.; Craig, G. W.; Goff, D. A.; Keheres, L. A.; Smith, K. M. J. Am. Chem. Soc. **1983**, 105, 3837-3843.
9. Fajer, J.; Borg, D. C.; Forman, A.; Dolphin, D.; Felton, R. H. J. Am. Chem. Soc. **1973**, 95, 2739-2741.
10. Fujita, I.; Davis, M. S.; Fajer, J. J. Am. Chem. Soc. **1978**, 100, 6280-6282.
11. Fajer, J.; Davis, M. S. In The Porphyrins; Dolphin, D., Ed.; Academic: New York, 1979; Vol. IV, Part B, pp 197-

353.

12. Katz, J. J.; Dougherty, R. C.; Boucher, L. J. In The Chlorophylls; Vernon, L. P., Seely, G. R., Eds.; Academic: New York, 1966; pp 185-252.

13. Cotton, T. M.; Loach, P. A.; Katz, J. J.; Ballschmitter, K. Photochem. Photobiol. **1978**, 27, 735-749.

14. Chapados, C.; Germain, D.; Leblanc, R. M. Biophys. Chem. **1980**, 12, 189-198.

15. Chapados, C.; Leblanc, R. M. Biophys. Chem. **1983**, 17, 211-244.

16. Chapados, C. Photochem. Photobiol. **1988**, 47, 115-132.

17. Nabedryk, E.; Leonard, M.; Mantele, W.; Breton, J. Biochemistry **1990**, 29, 3242-3247.

18. Lutz, M. In Advances in Infrared and Raman Spectroscopy; Clark, R. J. H., Hester, R. E., Eds.; Wiley-Heyden: Chichester, UK, 1984; Vol. 11, pp 211-300.

19. Lutz, M. J. Raman Spectrosc. **1974**, 2, 497-516.

20. de Wilton, A.; Haley, L. V.; Koningstein, J. A. Chem. Phys. Lett. **1983**, 97, 538-540.

21. Lutz, M.; Kléo, J.; Gilet, R.; Henry, M.; Plus, R.; Leickman, J. P. In Proc. 2nd Internat. Conf. on Stable Isotopes; Klein, E. R., Klein, P. D., Eds.; U.S. Department of Commerce: Springfield, VA, 1975; pp 462-469.

22. Lutz, M. Biochim. Biophys. Acta **1977**, 460, 408-430.

23. Fujiwara, M.; Tasumi, M. J. Phys. Chem. **1986**, 90, 250-255.

24. Fujiwara, M.; Tasumi, M. J. Phys. Chem. **1986**, 90, 5646-5650.

25. Binnie, N. E.; Haley, L. V.; Mattioli, T. A.; Thibodeau, D. L.; Koningstein, J. A.; Wang, W. Can. J. Chem. **1988**, 66, 1728-1733.

26. Schick, G. A.; Bocian, D. F.; Biochim. Biophys. Acta **1987**, 895, 127-154.

27. Lutz, M.; Robert, B. In Biological Applications of Raman Spectroscopy; Spiro, T. G., Ed.; John Wiley & Sons: New York, 1988; Vol. 3, pp 347-411.

28. Fonda, H. N.; Babcock, G. T. In Progress in Photosynthesis Research; Biggens, J., Ed.; Martinus Nijhoff: Boston, 1987; Vol. I., pp 449-452.

29. Heald, R. L.; Callahan, P. M.; Cotton, T. M. J. Phys. Chem. **1988**, 92, 4820-4824.

30. Heald, R. L.; Cotton, T. M. J. Phys. Chem. **1990**, 94, 3968-3975.

31. Heald, R. L. Resonance Raman and Electrochemical Investigations of Primary Electron-Transfer Species in Photosynthesis; Ph.D thesis, University of Nebraska, Lincoln, NE, 1989.

32. Höxtermann, B.; Werncke, W.; Tscho, J. T.; Hoffmann, P. Studia Biophys. **1986**, 115, 85-94.

33. Andersson, L. A.; Loehr, T. M.; Cotton, T. M.; Simpson, D. J.; Smith, K. M. Biochim. Biophys. Acta **1989**, 974, 163-179.

43. Mattioli, T. A.; Haley, L. V.; Koningstein, J. A. Chem. Phys. **1990**, 140, 317-329.

35. Weitz, D. A.; Garoff, S.; Gersten, J. I.; Nitzan, A. J. Chem. Phys. **1983**, 78, 5324-5338.

36. Gersten, J. I.; Nitzan, A. J. Chem. Phys. **1980**, 73, 3023-3037.

37. Kerker, M.; Wang, D. S.; Chew, H. Appl. Opt. **1980**, 19, 4159-4174.

38. Ferrell, T. L. Phys. Rev. B: Condens. Matter **1982**, 25, 2930-2932.

39. Furtak, T. E. J. Electroanal. Chem. Interfacial Electrochem. **1983**, 150, 375-388.

40. Otto, A. In Light Scattering in Solids; Cardona, M., Gunthrodt, G., Eds.; Springer-Verlag: Berlin, 1984; Vol. IV, pp 289-461.

41. Cotton, T. M. In Spectroscopy of Surfaces; Clark, R. J. H., Hester, R. E., Eds.; John Wiley & Sons: New York, 1988; Vol. 16, pp 91-153.

42. Koglin, E.; Sequaris, J. -M. In Topics in Current Chemistry; Springer-Verlag: Berlin, 1986; Vol. 134, pp 1-53.

43. Nabiev, I.; Efremov, R. G.; Chumanov, G. D. Soviet Phys. Uspekhi **1988**, 31, 241-262.

44. Uphaus, R. A.; Cotton, T. M.; Möbius, D. Thin Solid Films **1986**, 132, 173-185.

45. Hildebrandt, P.; Spiro, T. G. J. Phys. Chem. **1988**, 92, 3355-3360.

46. Thomas, L. L.; Kim, J. -H.; Cotton, T. M. J. Am. Chem. Soc. **1990**, 112, 9378-9386.

47. Thomas, L. L. Application of Surface-Enhanced Resonance Raman Spectroscopy to Chlorophyll and Chlorophyll Derivatives; Ph.D. thesis, Iowa State University, Ames, IA, 1991.

48. Gao, P.; Patterson, M. L.; Tadayyoni, M. A.; Weaver, M. J. Langmuir **1985**, 1, 173-176.

49. Strain, H. H.; Svec, W. A. In The Chlorophylls; Vernon, L. P., Seely, G. R., Eds.; Academic: New York, 1966; pp 21-66.

50. Fragata, M.; Norden, B.; Durucsev, T. Photochem. Photobiol. **1988**, 47, 133-143.

51. Hall, D. O.; Rao, K. K. In New Studies in Biology Photosynthesis; Edward Arnold: London, 1987; p. 26.

52. Boldt, N. J.; Donohoe, R. J.; Birge, R. R.; Bocian, D. F. J. Am. Chem. Soc. **1987**, 109, 2284-2298.

53. Fonda, H. N.; Oertling, W. A.; Salehi, A.; Chang, C. K.; Babcock, G. T. J. Am. Chem. Soc. **1990**, 112, 9497-9507.

54. Moskovits, M. J. Chem. Phys. **1982**, 77, 4408-4416.

55. Creighton, J. A. In Spectroscopy of Surfaces Advances in Spectroscopy; Clark, R. J. H., Hester, R. E., Eds.; John Wiley & Sons: New York, 1988; Vol. 16, pp 37-90.

56. Evans, J. F.; Albrecht, M. G.; Ullevig, D. M.; Hexter, R. M. J. Electroanal. Chem. **1980**, 106, 209-234.

57. Wetzel, H.; Gerischer, H.; Pettinger, B. Chem. Phys.

Lett. **1981**, 78, 392-397.

58. Fleischman, M.; Hendra, R. J.; Hill, I. R.; Pemble, M. E. J. Electroanal. Chem. **1981**, 117, 243-255.

59. Owen, J. F.; Chen, T. T.; Chang, R. K.; Laube, B. L. Surf. Sci. **1983**, 125, 679-698.

60. Weaver, M. J.; Hupp, J. T.; Barz, F.; Gordon, J. G.; Philpott, M. R. J. Electroanal. Chem. **1984**, 160, 321-333.

61. Gao, P.; Weaver, M. J. J. Phys. Chem. **1986**, 90, 4057-4063.

62. Holze, R. Surf. Sci. **1988**, 202, L612-L620.

63. Hirakawa, A. Y.; Tsuboi, M. Science **1975**, 188, 359-361.

64. Lutz, M.; Breton, J. Biochem. Biophys. Res. Commun. **1973**, 53, 413-418.

65. Lutz, M.; Robert, B. In Spectroscopy of Biological Molecules; Alix, A. J. P., Bernard, L., Manfait, M., Eds.; Wiley: New York, 1985; pp. 310-318.

66. Fonda, H. N.; Babcock, G. T. In Progress in Photosynthesis Research; Biggens, J., Ed.; Martinus Nijhoff: Netherlands, 1987; Vol. I, 1.4.449-1.4.452.

67. Moënne-Loccoz, P.; Robert, B.; Lutz, M. Biochemistry **1989**, 28, 3641-3645.

68. Cotton, T. M.; Van Duyne, R. P. FEBS Lett. **1982**, 147, 81-84.

69. a) Picorel, R.; Holt, R. E.; Cotton, T. M.; Seibert, M. In Progress in Photosynthesis Research; Biggens, J., Ed.; Martinus Nijhoff: Netherlands, 1987; Vol. I, 1.4.423-

1.4.426. b) Picorel, R.; Holt, R. E.; Cotton, T. M. Seibert, M. J. J. Biol. Chem. **1988**, 263, 4374-4380. c) Seibert, M. J.; Cotton, T. M.; Metz, J. G. Biochim. Biophys. Acta **1988**, 934, 235-246. d) Picorel, R.; Lu, T.; Holt, R. E.; Cotton, T. M.; Seibert, M. Biochemistry **1990**, 29, 707-712.

CONCLUSIONS

The results presented herein demonstrate the promise of SERRS for obtaining complete excitation spectra of the chlorophylls and pheophytins. In the past, high fluorescence has inhibited RR studies with excitation in resonance with the Q_y transition. The fluorescence-quenching advantage of SERRS makes it ideally suited for obtaining spectra of the lowest energy $^1\pi$-π^* state of Chl *a*, Chl *b*, and Pheo *a*.

Also, SERRS surface selection rules provide information that can determine the molecular orientation at the electrode surface. Future studies will include the characterization of Langmuir-Blodgett monolayers of Chl *a*, Chl *b*, and Pheo *a* at Ag and Au electrodes using SERRS. This technique will allow better experimental control over the macrocycle orientation. Electrode surface composition also effects molecular orientation at the surface. Ag_2SO_4, an insoluble salt, forms on the electrode surface when roughening Ag electrodes in the presence of 0.1 M Na_2SO_4. Likewise, Au_2Cl_6, a salt that is soluble in water and alcohol, forms on the electrode surface when roughening Au electrodes with 0.1 M KCl as the electrolyte. A comparison of the Ag versus Au SERRS spectra at red excitation shows differences in intensity occur for several bands in the 1400-1100 cm^{-1} region. Thus, the salt coverage on the electrode surface appears to effect molecular orientation at the surface. Roughening the Ag and the Au electrodes in 0.1 M $NaClO_4$ will produce $AgClO_4$ and $Au(ClO_4)$, respectively, on

the electrode surfaces. Both of these salts are soluble in water and alcohol. Obtaining SERRS spectra of the chlorophylls and pheophytin a with these electrodes will provide a more direct comparison between the two surfaces.

Ag and Au electrodes provide the electrochemical range needed to perform SERRS electron transfer studies on photosynthetic pigments. Indeed, the next step in this research is to undertake the SERRS electrochemical experiments of Chl a and Pheo a, which will produce SERRS spectra of the respective radical ions, using various excitation wavelengths, especially red excitation.

Furthermore, the results of these studies indicate that SERRS offers a viable approach for the study of intact photosynthetic preparations. The distance sensitivity can be used to obtain information concerning the spatial relationship of various components relative to the membrane surface. Finally, the ability to control the potential at an electrode surface suggests that SERRS may also be valuable for determining spectra at fixed redox states of the RC.

ACKNOWLEDGEMENT

To say that my graduate career has been a mental awakening, a spiritual enlightenment, and an emotional journey would be an understatement. The knowledge I have gained has blessed me with an invaluable maturity that only graduate school can provide. Although I will not elaborate on my experiences, I do wish to thank the people who assisted me on this endeavor.

To Dr. Cotton, words cannot express my gratitude for your guidance throughout my graduate school years. You are not only my advisor, but also my role model of a sincere scientist, a compassionate parent, and a friend of highest integrity. I will cherish these gifts you have passed on to me always.

To Dr. Johnson, thank-you for "smoothing" my transition from Nebraska to Iowa State. I appreciated your patience and sincerity with my never-ending questions. Thanks, for making me feel welcomed.

To Jae-Ho Kim, a special thanks for showing me the ins and outs of SERRS, for our long talks and your insightful advice, and most of all for the lifelong friendship we will share.

To the Vickster, thanks for the "short" chats we shared. It truely is amazing how two people who appear to totally opposites have such similar beliefs and values (i.e., on men, marriage, families, teenagers, spirituality...). I'm looking forward to these endless discussions in the future.

To the rest of the group, thanks for your support and tolerance, especially in the last few months. To Joe, I hold a deep appreciation for you because I know your sense of humor is as warped as mine (no more gun fights?). To Jeanne, thanks not only for your technical and spiritual assistance, but also for your ability to make me (and everyone else) smile and laugh.

To my family and friends, without you I would not have accomplished this goal. To mom, thanks for expressing your belief in me and being there when I needed you. To Diana, thanks for giving of yourself. You came to visit often, you always called, you showed you cared. To Hinch, my cohort in graduate school, thanks for being with me every step of the way. To Patti and Peggy, we've been close through the years, but the comfort and support you have supplied the last few months will warm my heart for the rest of my life. Thank you.

Above all, endless thanks to Nado, you are a living testament of a true friend. You will never know how much I appreciate all that you have taught me.